Appendix A

Supplemental Photographs of Cast Stainless Steel Specimens

Appendix A

Supplemental Photographs of Cast Stainless Steel Specimens

All rulers shown in the Appendix A figures are in units of inches (25.4 mm).

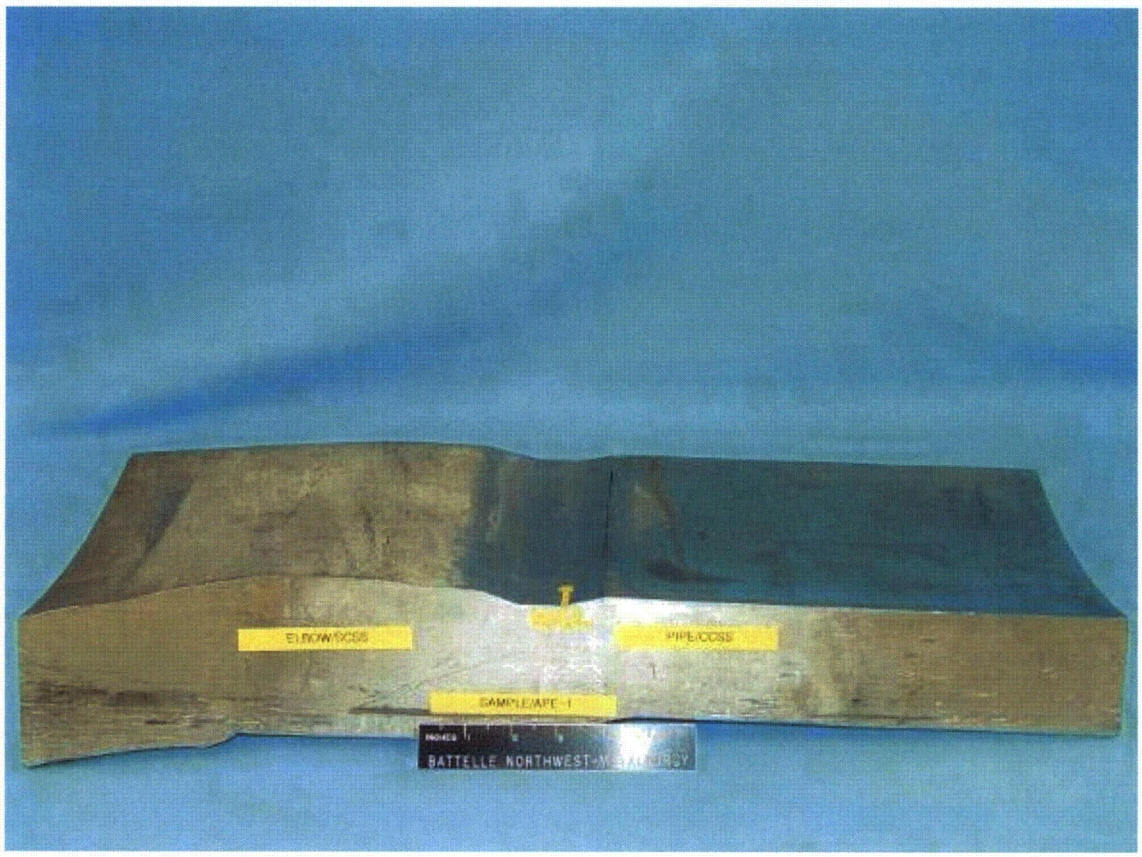

Figure A.1 WOG Specimen APE-1

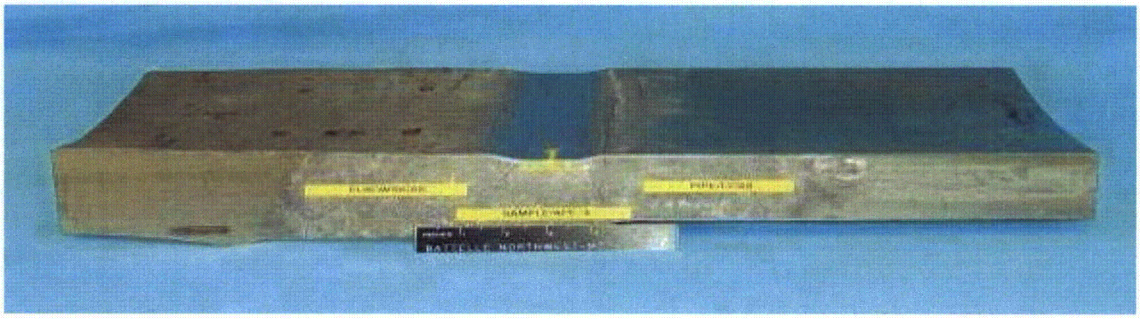

Figure A.2 WOG Specimen APE-4

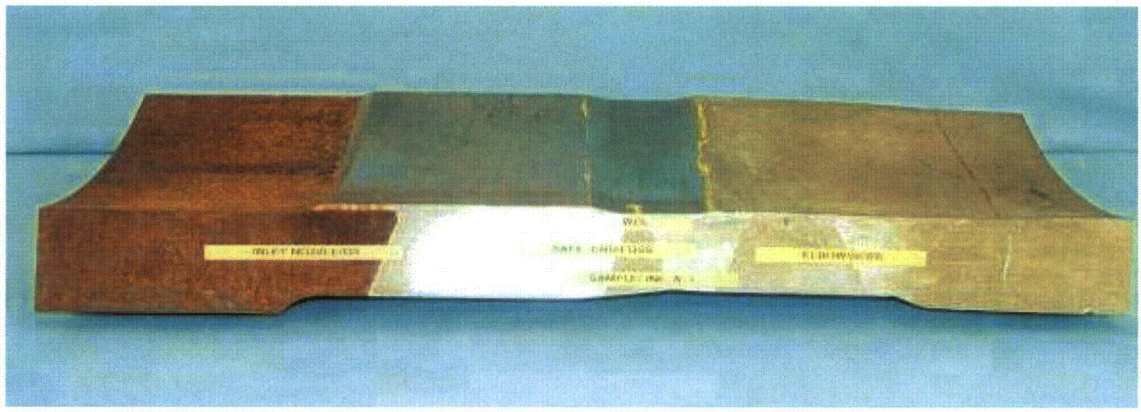

Figure A.3 WOG Specimen INE-A-1

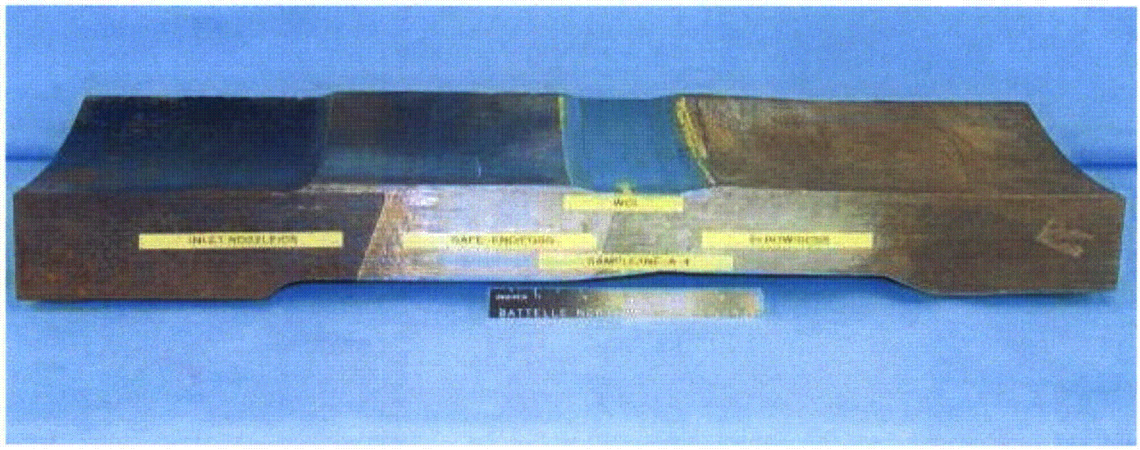

Figure A.4 WOG Specimen INE-A-4

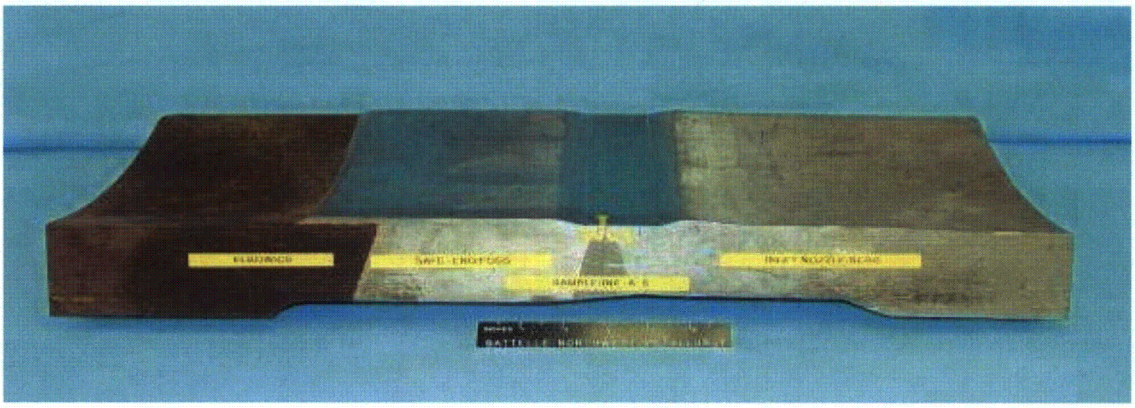

Figure A.5 WOG Specimen INE-A-5

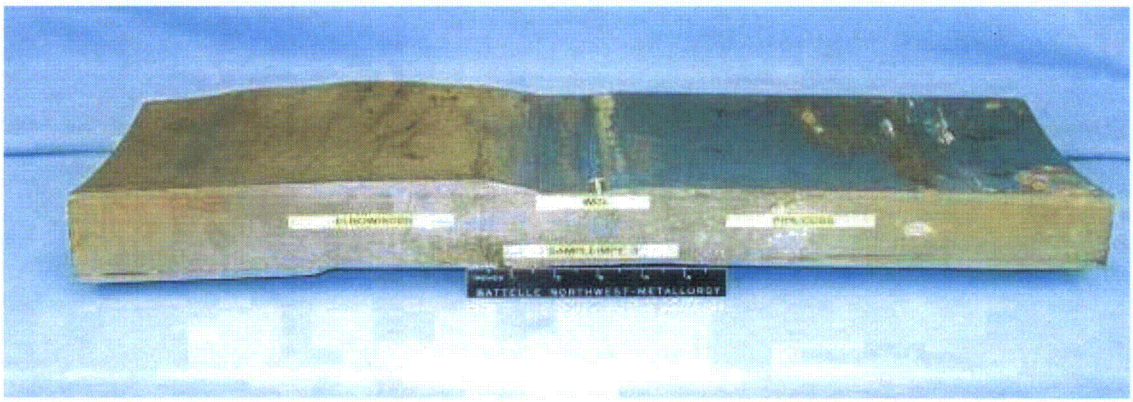

Figure A.6 WOG Specimen MPE-3

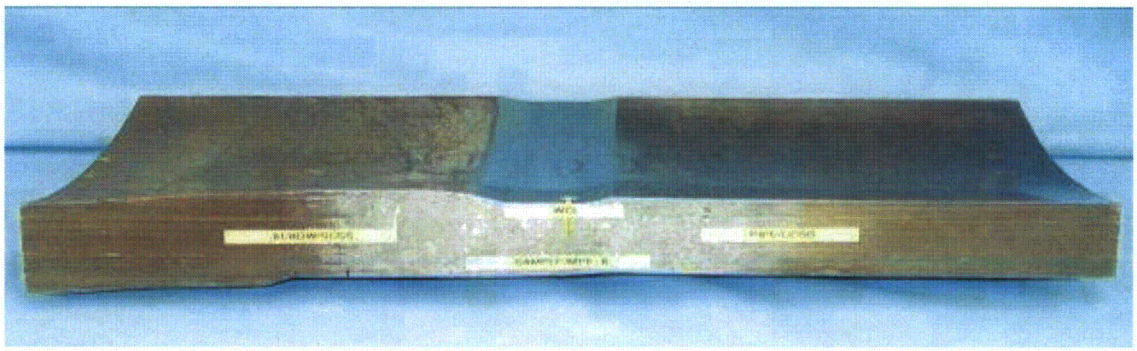

Figure A.7 WOG Specimen MPE-6

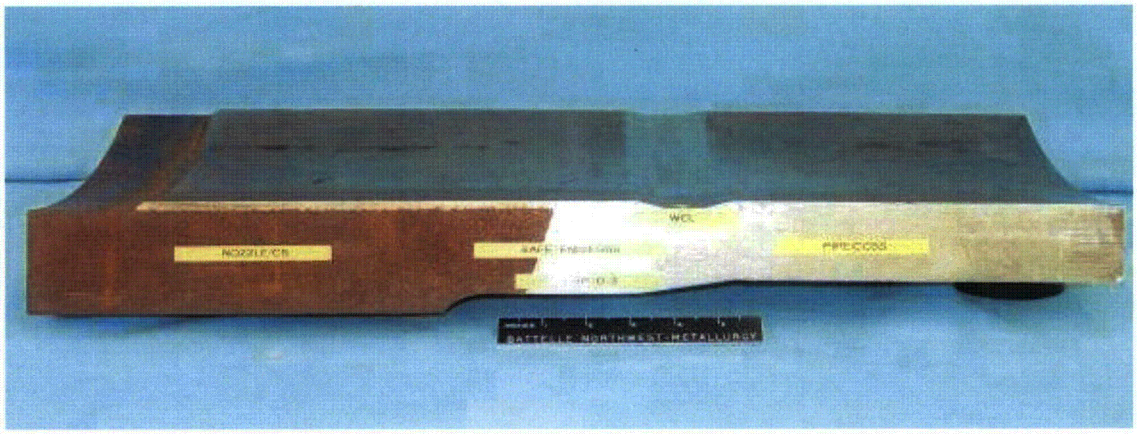

Figure A.8 WOG Specimen ONP-D-2

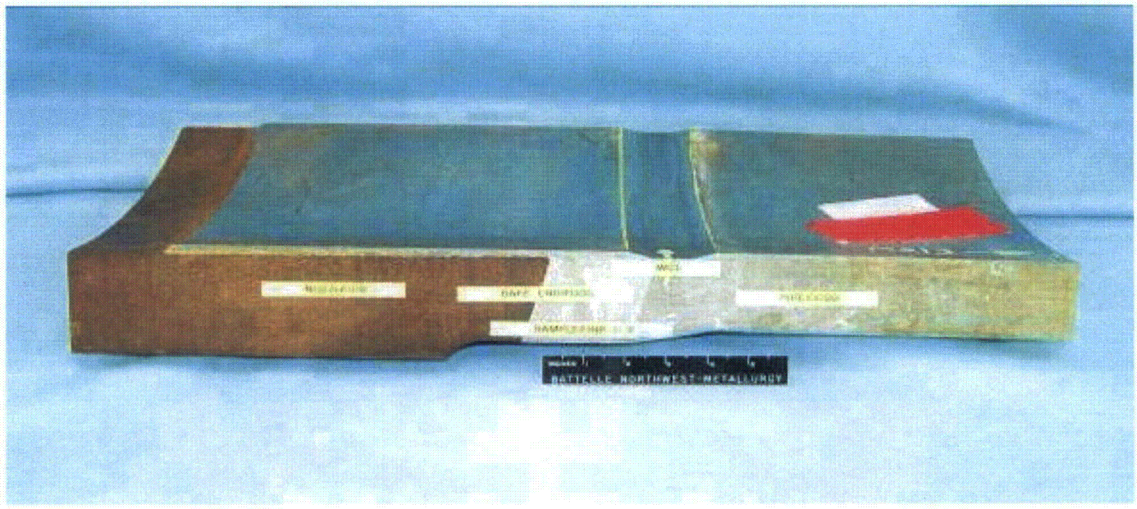

Figure A.9 WOG Specimen ONP-D-5

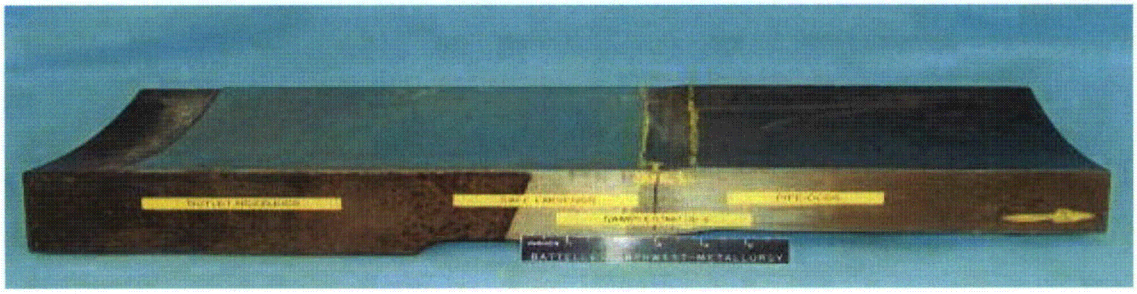

Figure A.10 WOG Specimen ONP-3-5

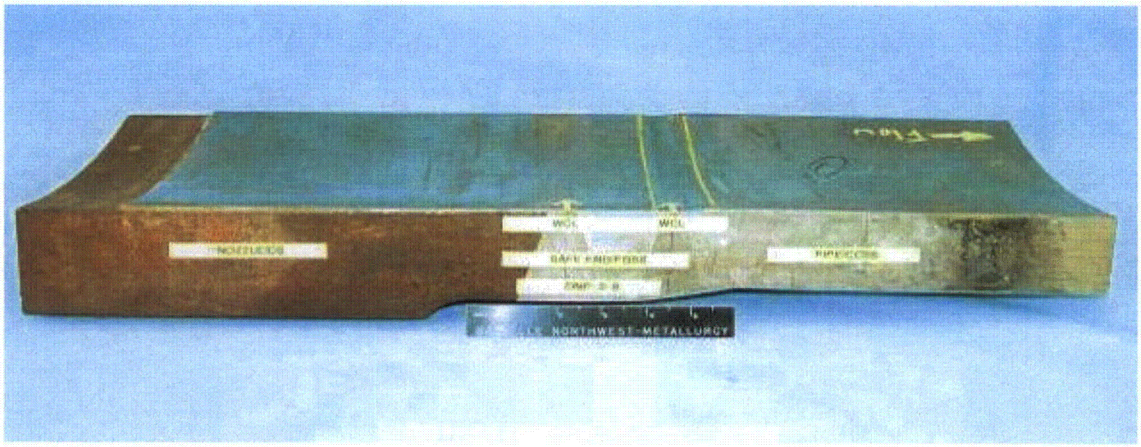

Figure A.11 WOG Specimen ONP-3-8

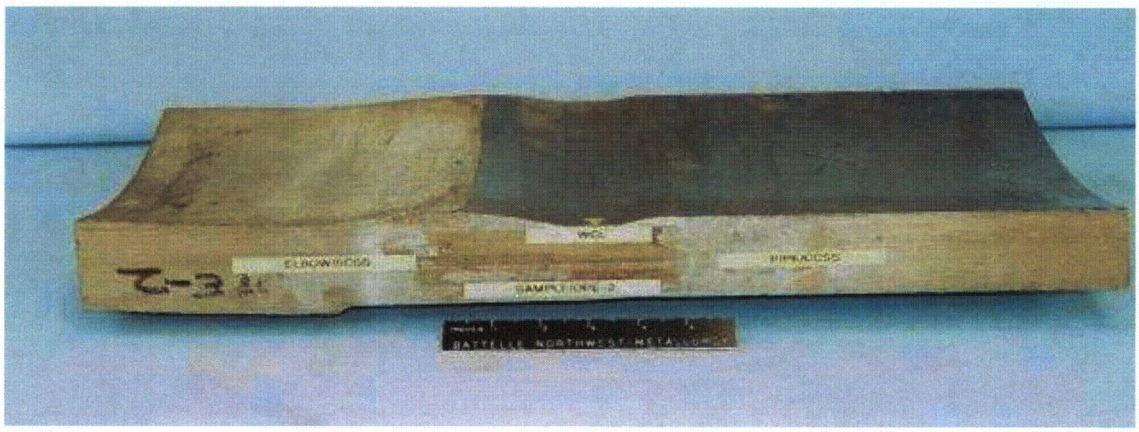

Figure A.12 WOG Specimen OPE-2

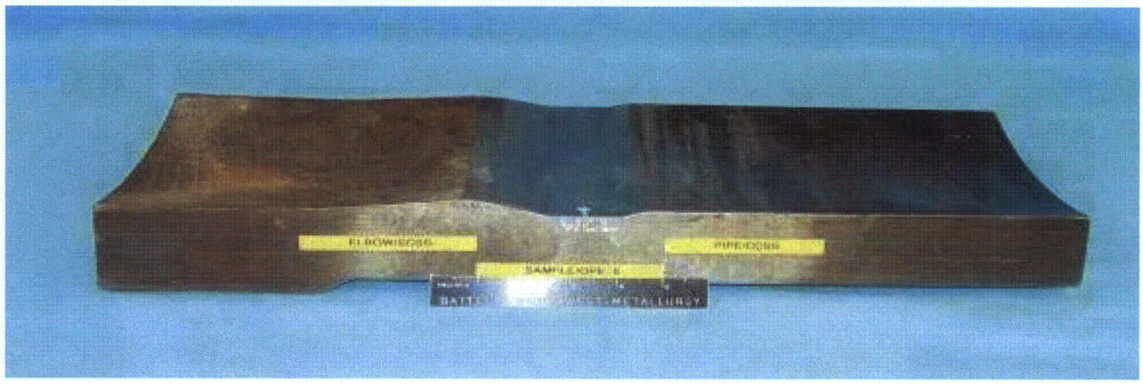

Figure A.13 WOG Specimen OPE-5

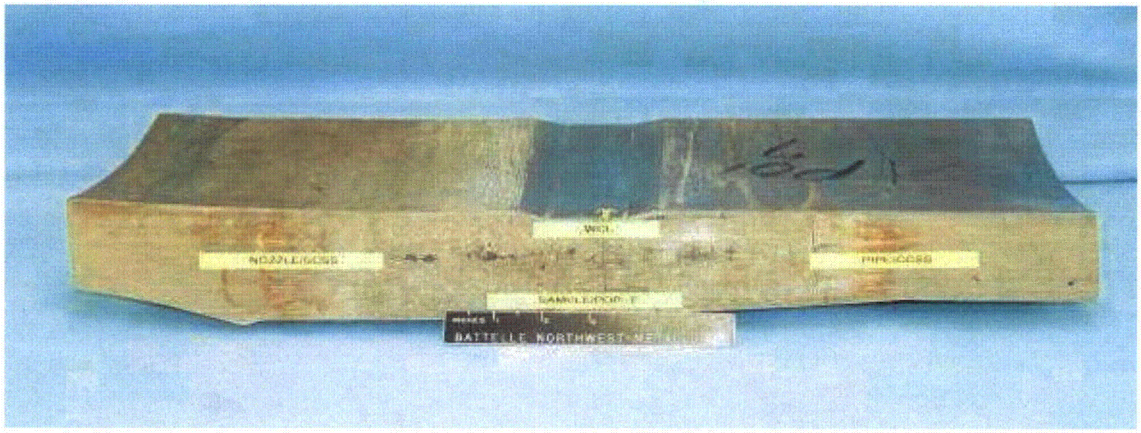

Figure A.14 WOG Specimen POP-7

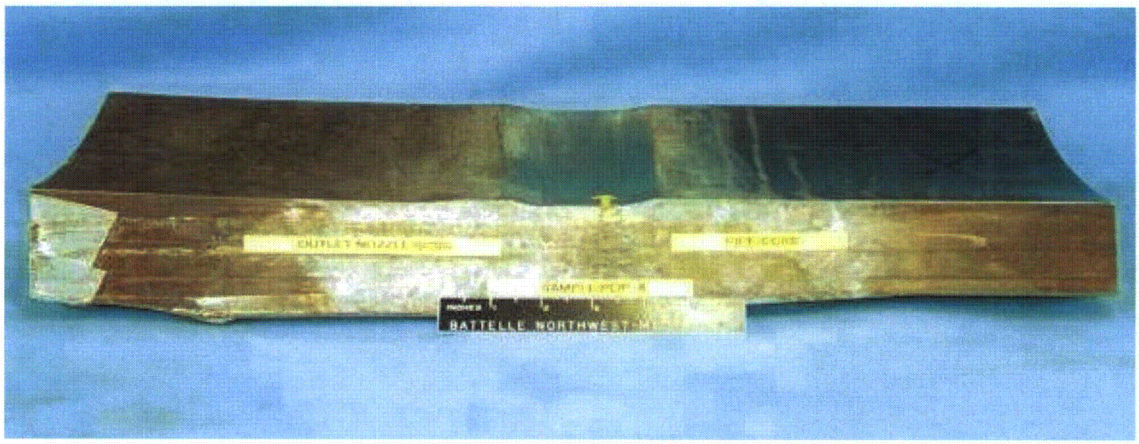

Figure A.15 WOG Specimen POP-8

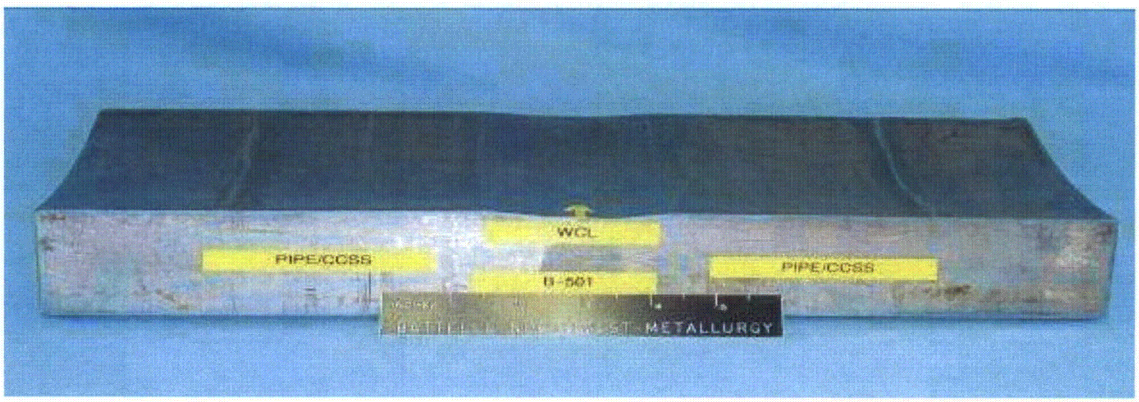

Figure A.16 PNNL Specimen B-501

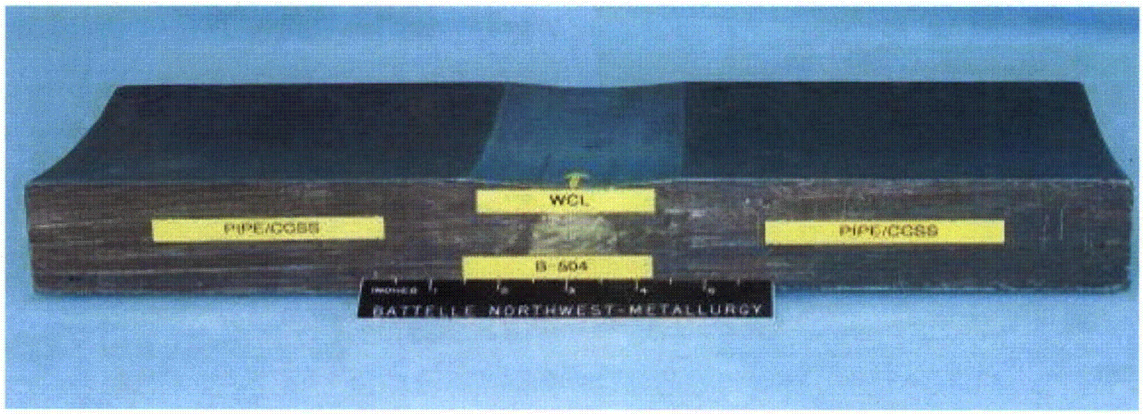

Figure A.17 PNNL Specimen B-504

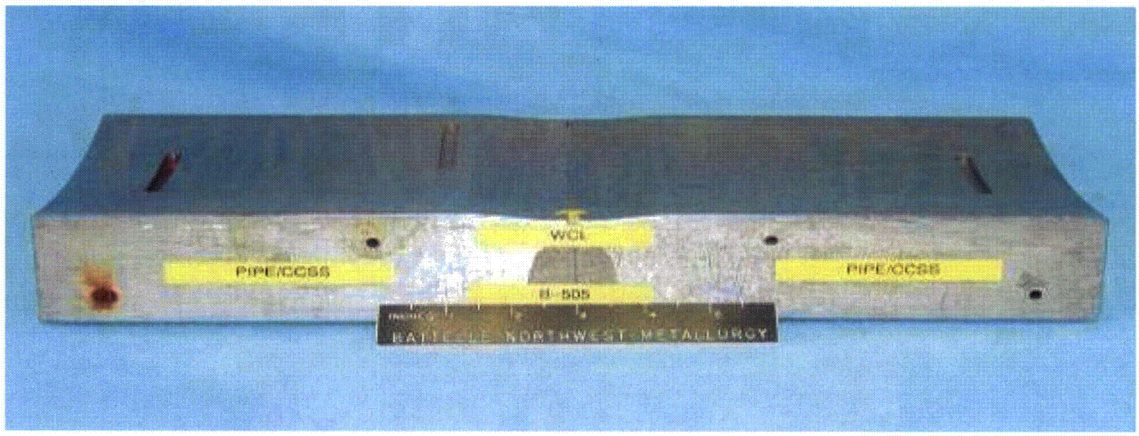

Figure A.18 PNNL Specimen B-505

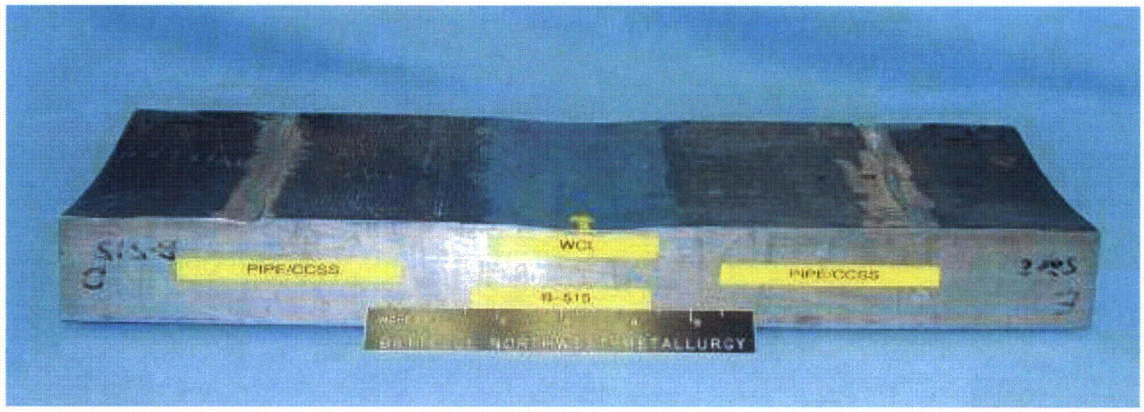

Figure A.19 PNNL Specimen B-515

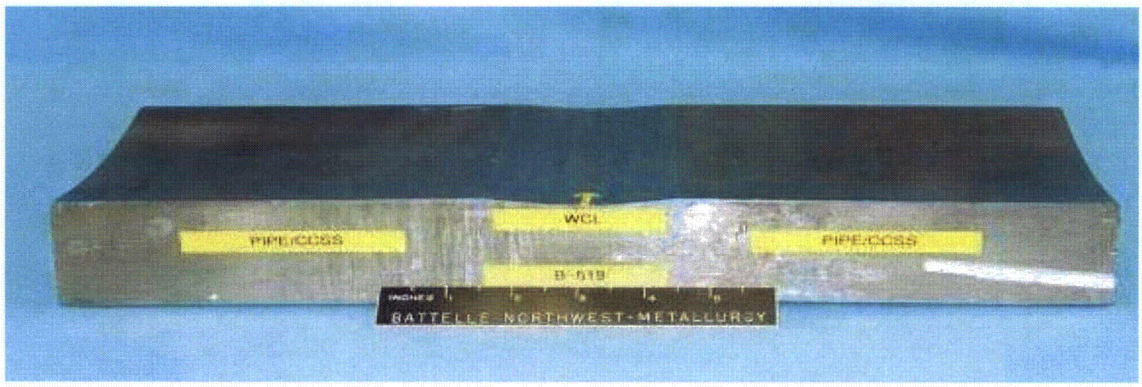

Figure A.20 PNNL Specimen B-519

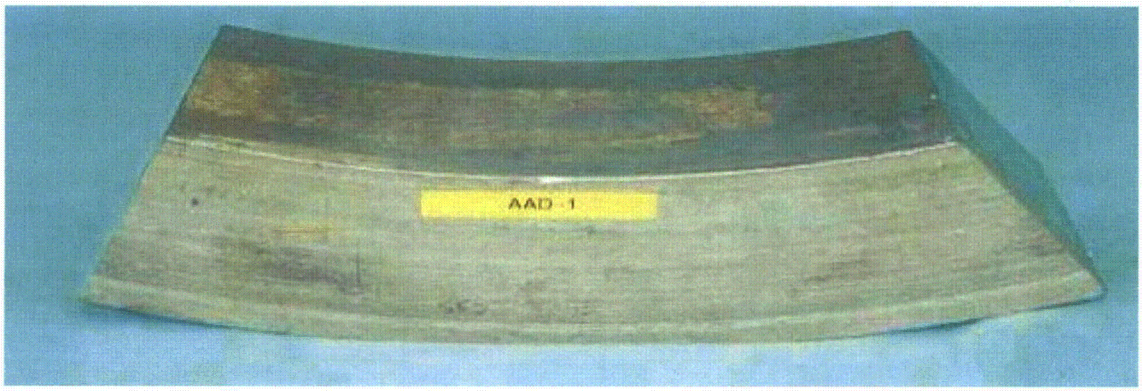

Figure A.21 Southwest Research Institute Specimen AAD#1

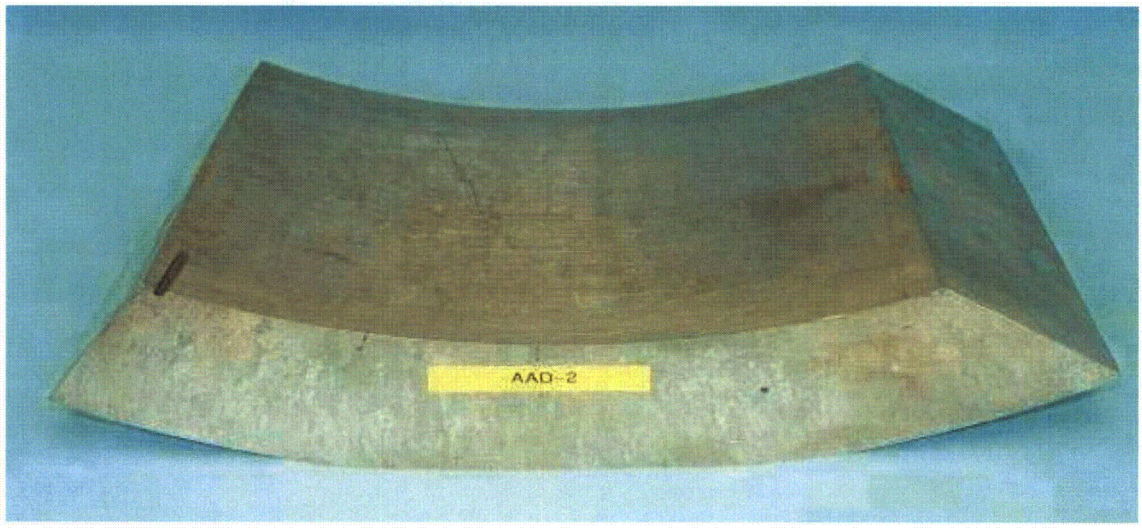

Figure A.22 Southwest Research Institute Specimen AAD#2

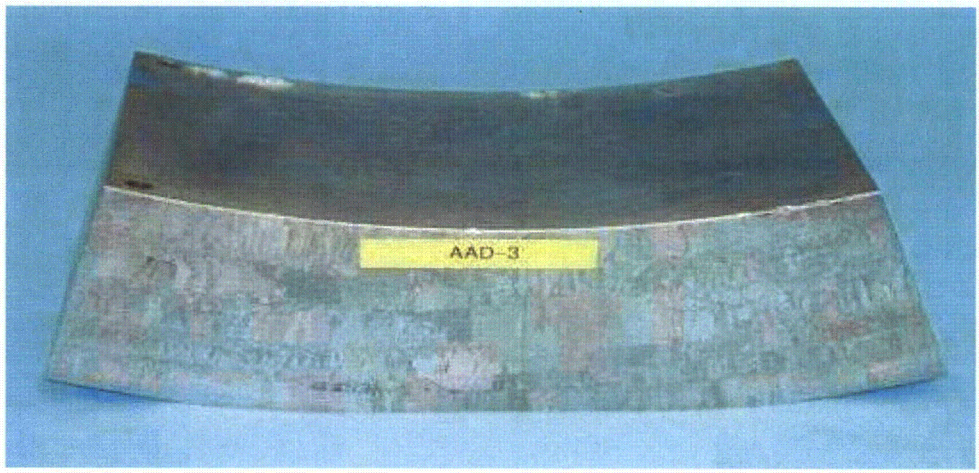

Figure A.23 Southwest Research Institute Specimen AAD#3

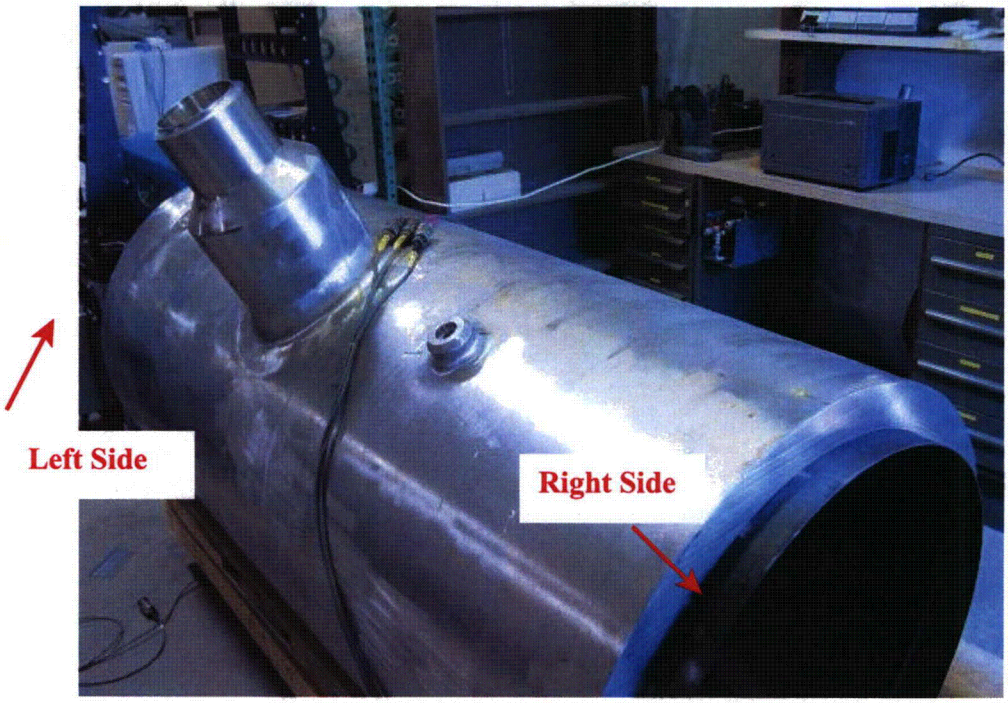

Figure A.24 EPRI NDE Center, Spanish Spool Piece Specimen

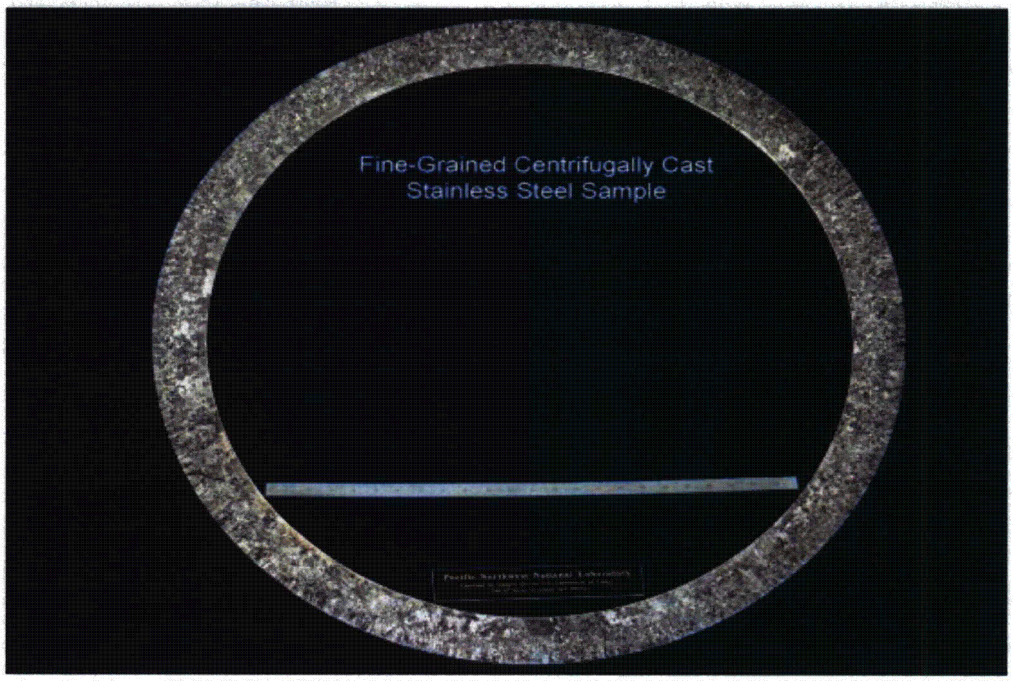

Figure A.25 EPRI NDE Center, Spanish Spool Piece Specimen, Polished and Etched Ring

Figure A.26 Westinghouse Spool Piece Specimen

Figure A.27 IHI Southwest Technologies Inc. Spool Piece Specimen

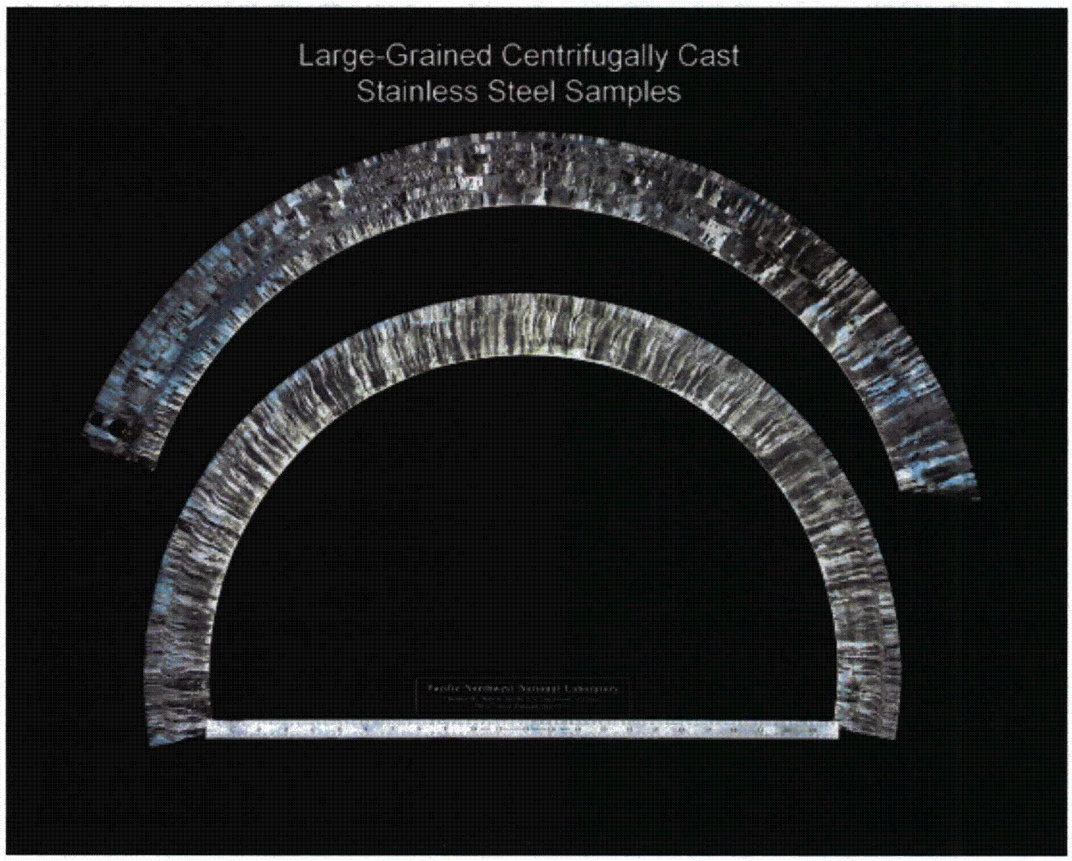

Figure A.28 Westinghouse and IHI Southwest Technologies Inc. Spool Pieces after Polishing and Etching

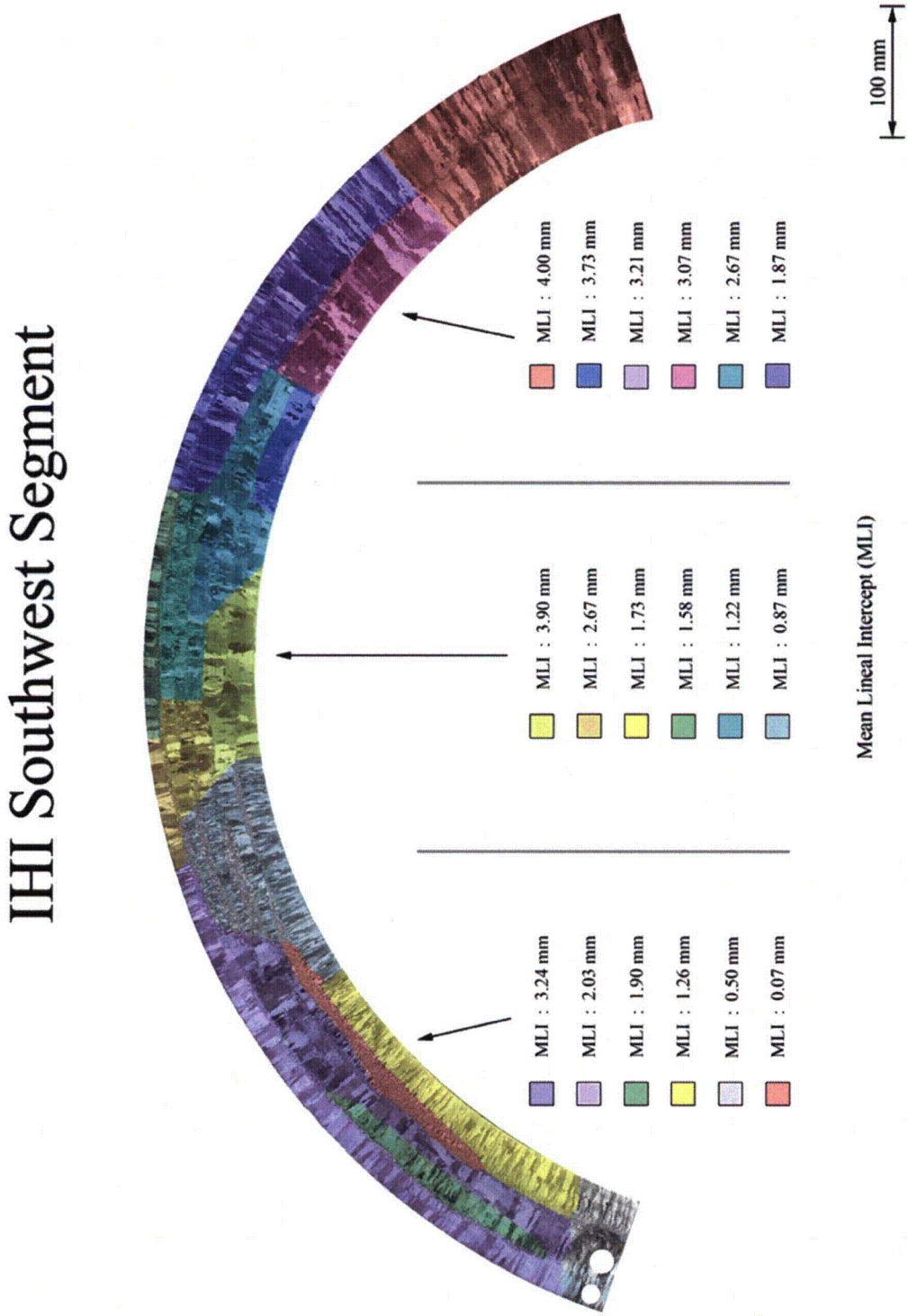

Figure A.29 False-Color Map Depicting Variation of Grains in CCSS Piping from IHI Southwest Technologies, Inc.

Westinghouse Segment

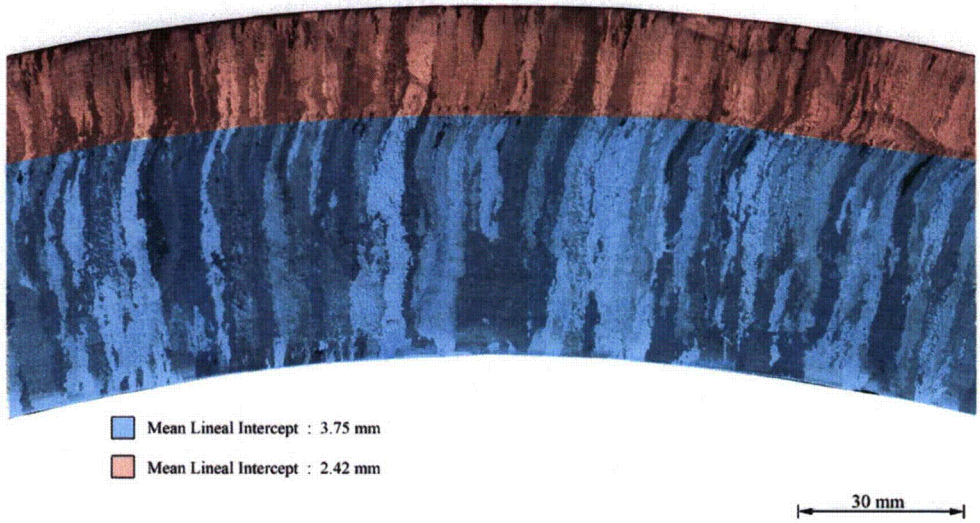

Figure A.30 Portion of CCSS Piping Specimen from Westinghouse, Inc., Showing Dendritic Grain Structure Observed to be Consistent Throughout Circumference

EPRI Ring Segment

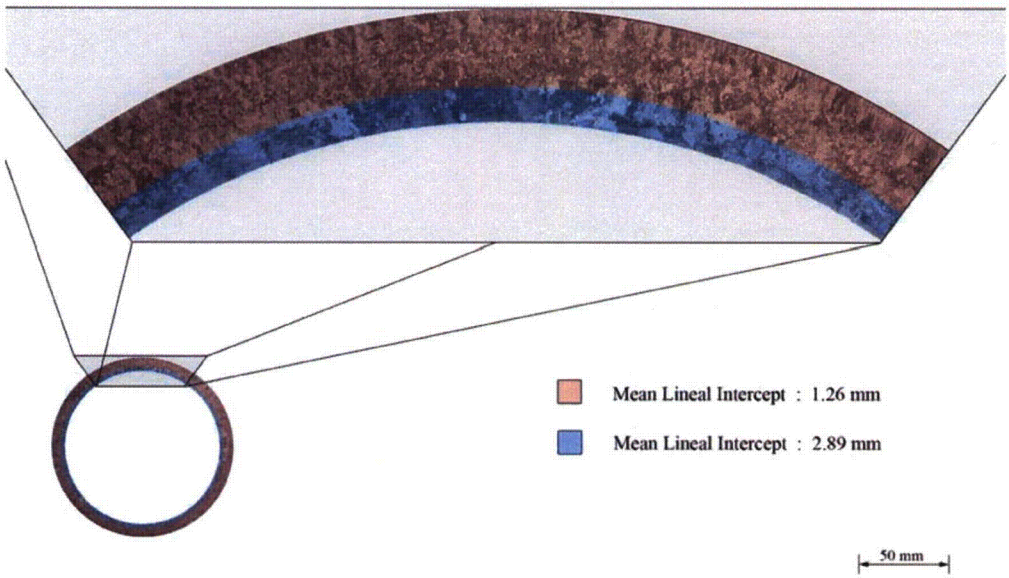

Figure A.31 Portion of Westinghouse, Inc. CCSS Piping Segment Showing Dendritic Grain Structure Observed To Be Consistent Throughout Circumference

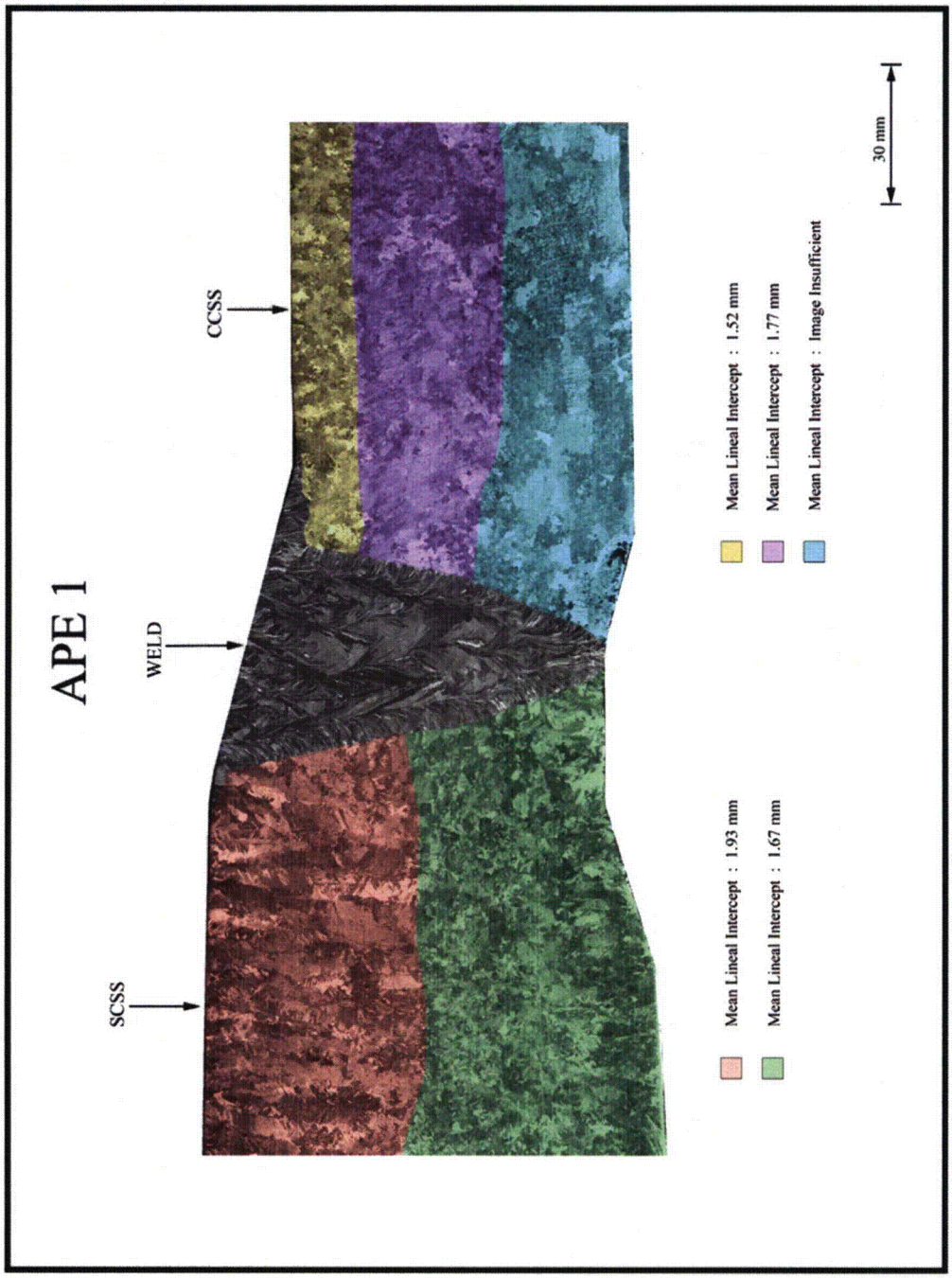

Figure A.32 Axial-Radial Cross Section of WOG Specimen APE-1, Showing Outside and Inside Diameter Geometry, and Grain Size, Typical of APE Configuration

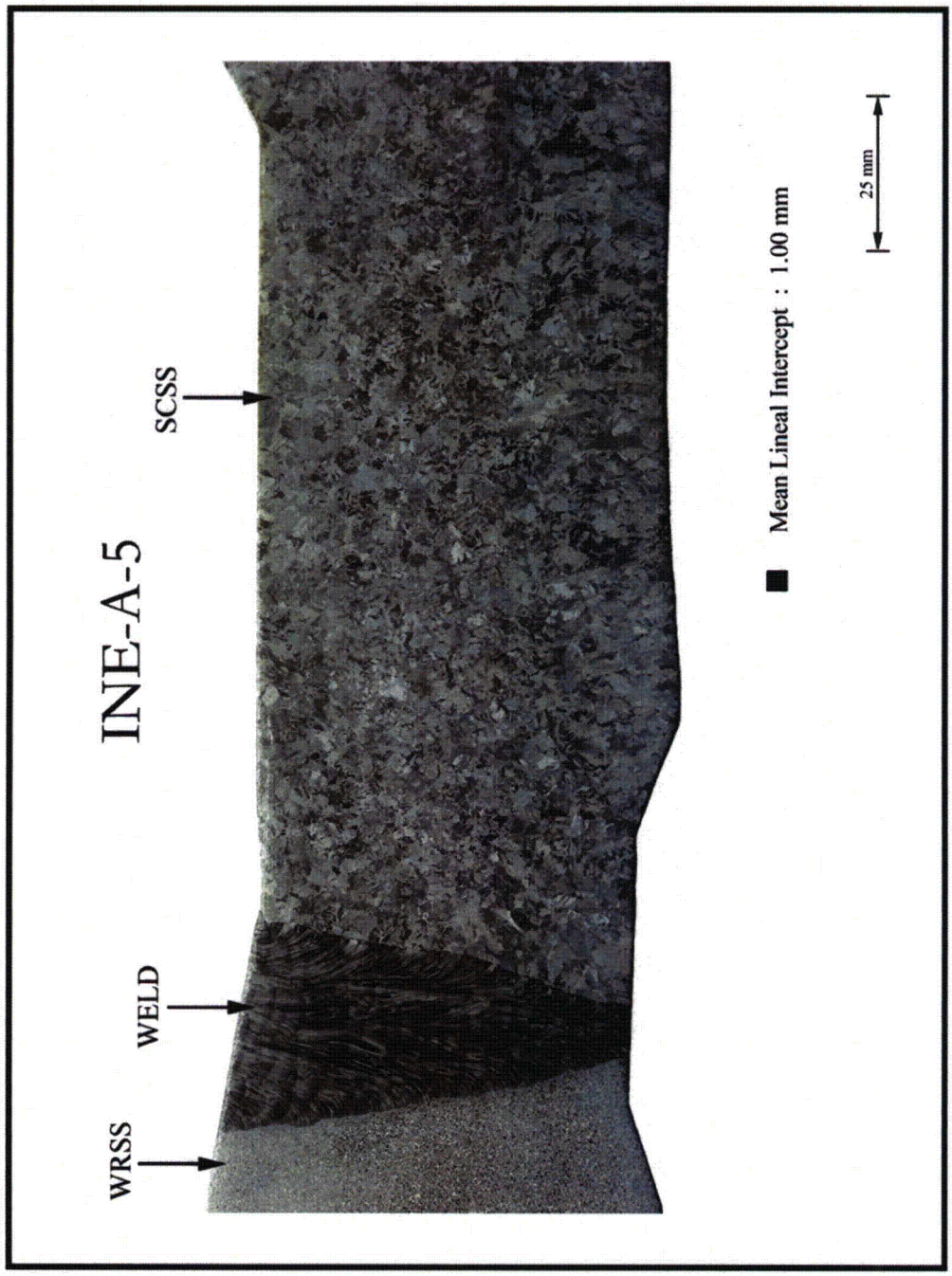

Figure A.33 Axial-Radial Cross Section of WOG Specimen INE-A-5, Showing Outside and Inside Diameter Geometry, and Grain Size, Typical of INE-A Configuration

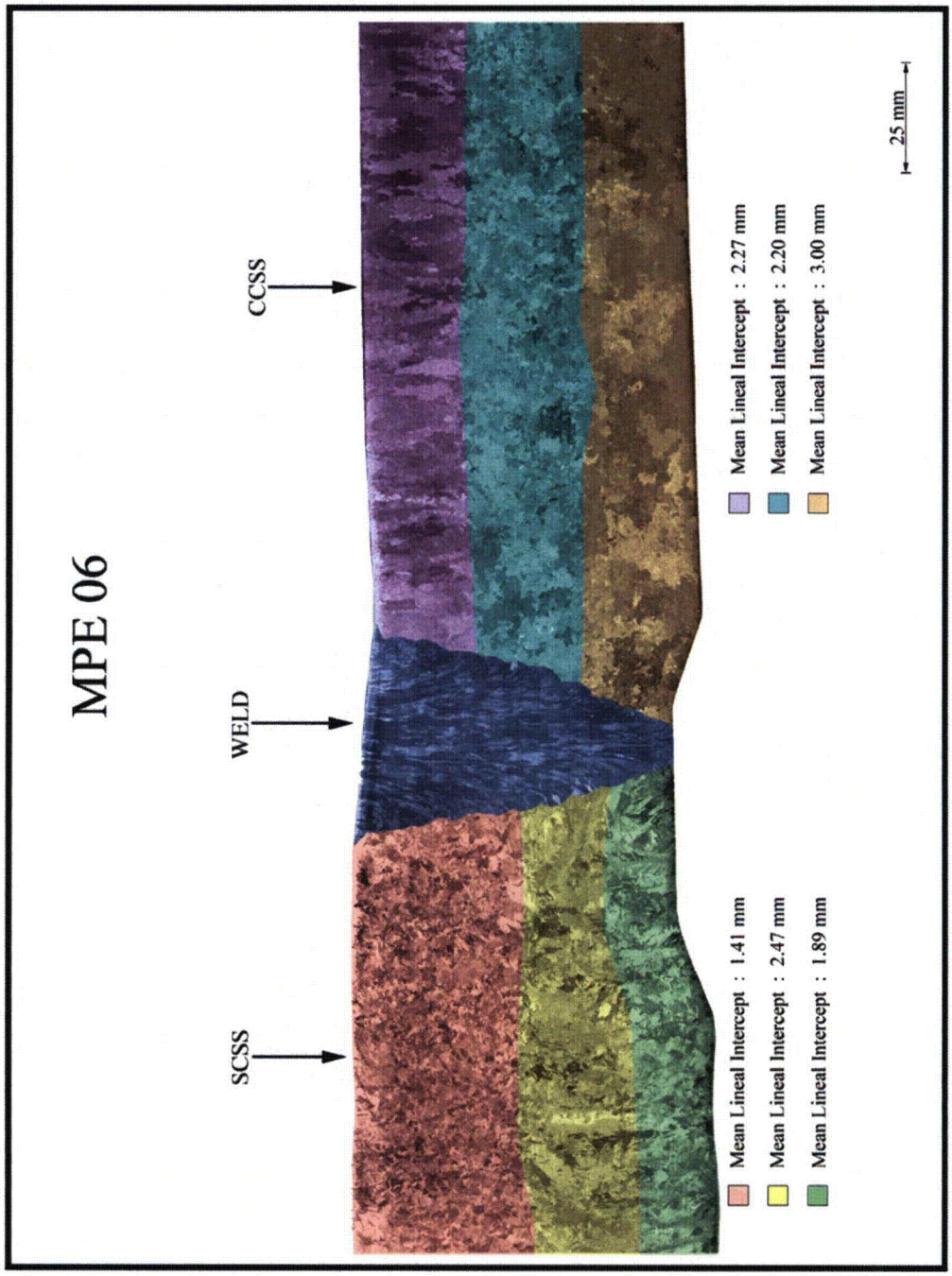

Figure A.34 Axial-Radial Cross Section of WOG Specimen MPE-06, Showing Outside and Inside Diameter Geometry, and Grain Size, Typical of MPE Configuration

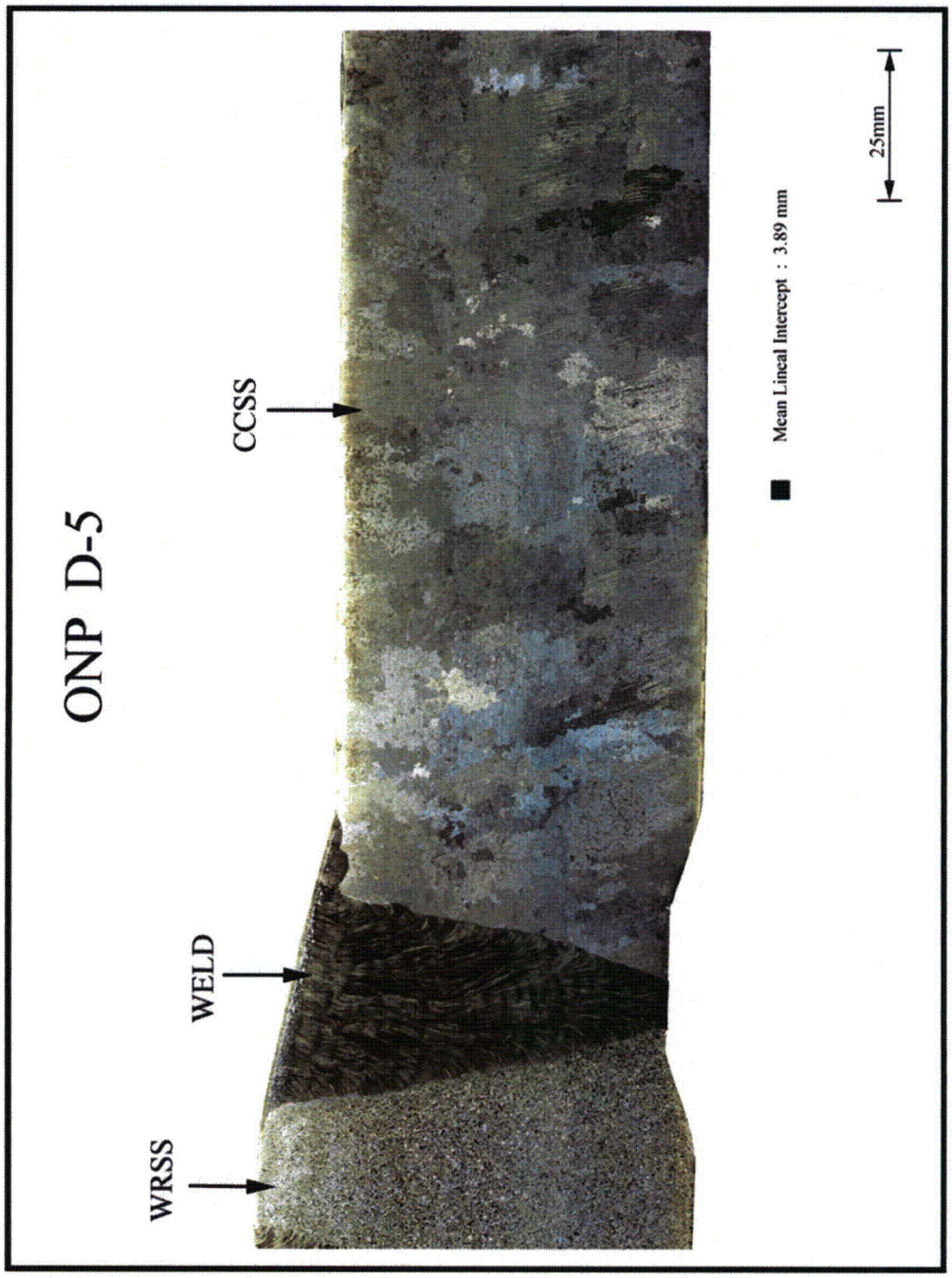

Figure A.35 Axial-Radial Cross Section of WOG Specimen ONP-D-5, Showing Outside and Inside Diameter Geometry, and Grain Size, Typical of ONP-D Configuration

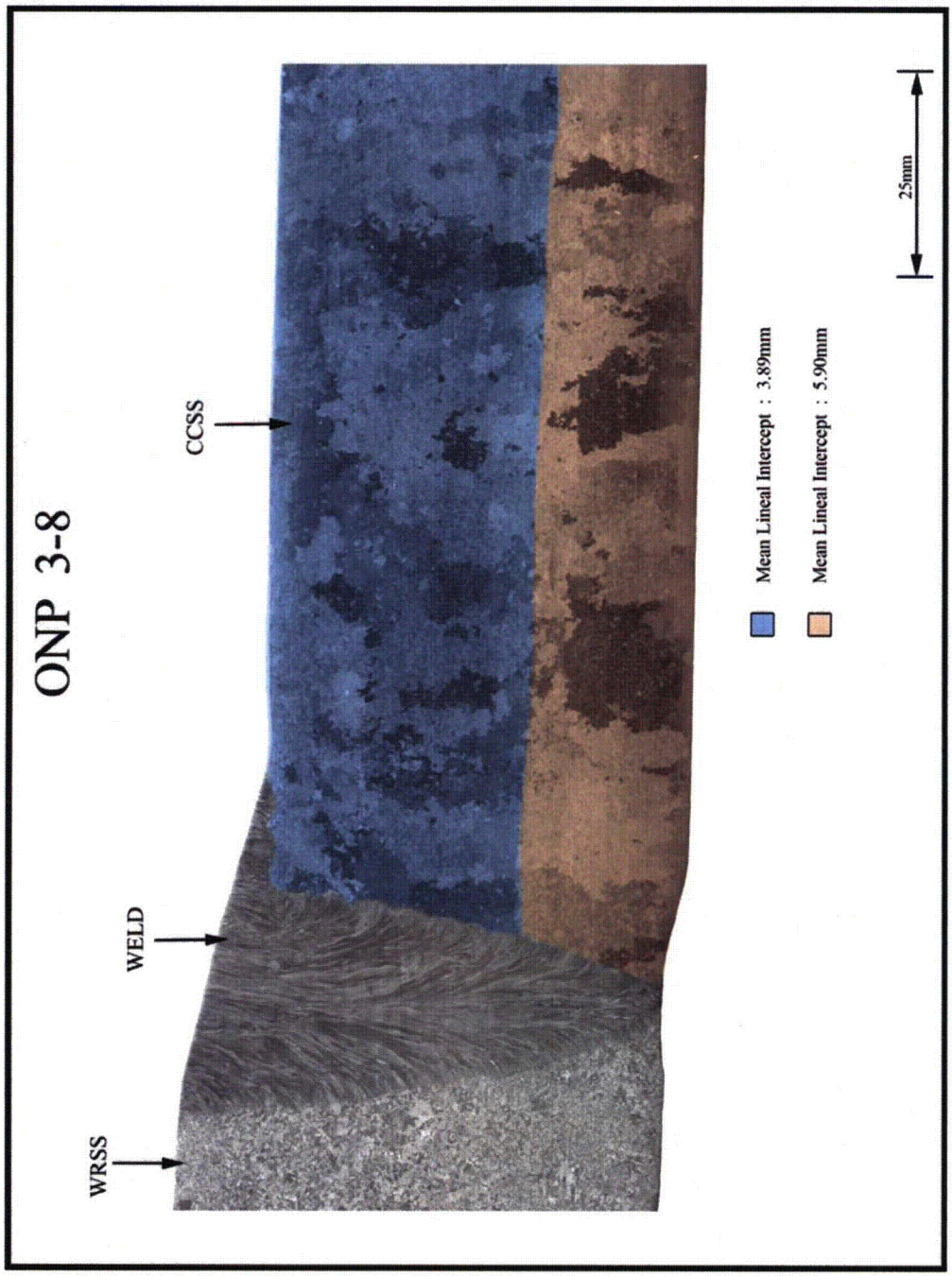

Figure A.36 Axial-Radial Cross Section of WOG Specimen ONP-3-8, Showing Outside and Inside Diameter Geometry, and Grain Size, Typical of ONP Configuration

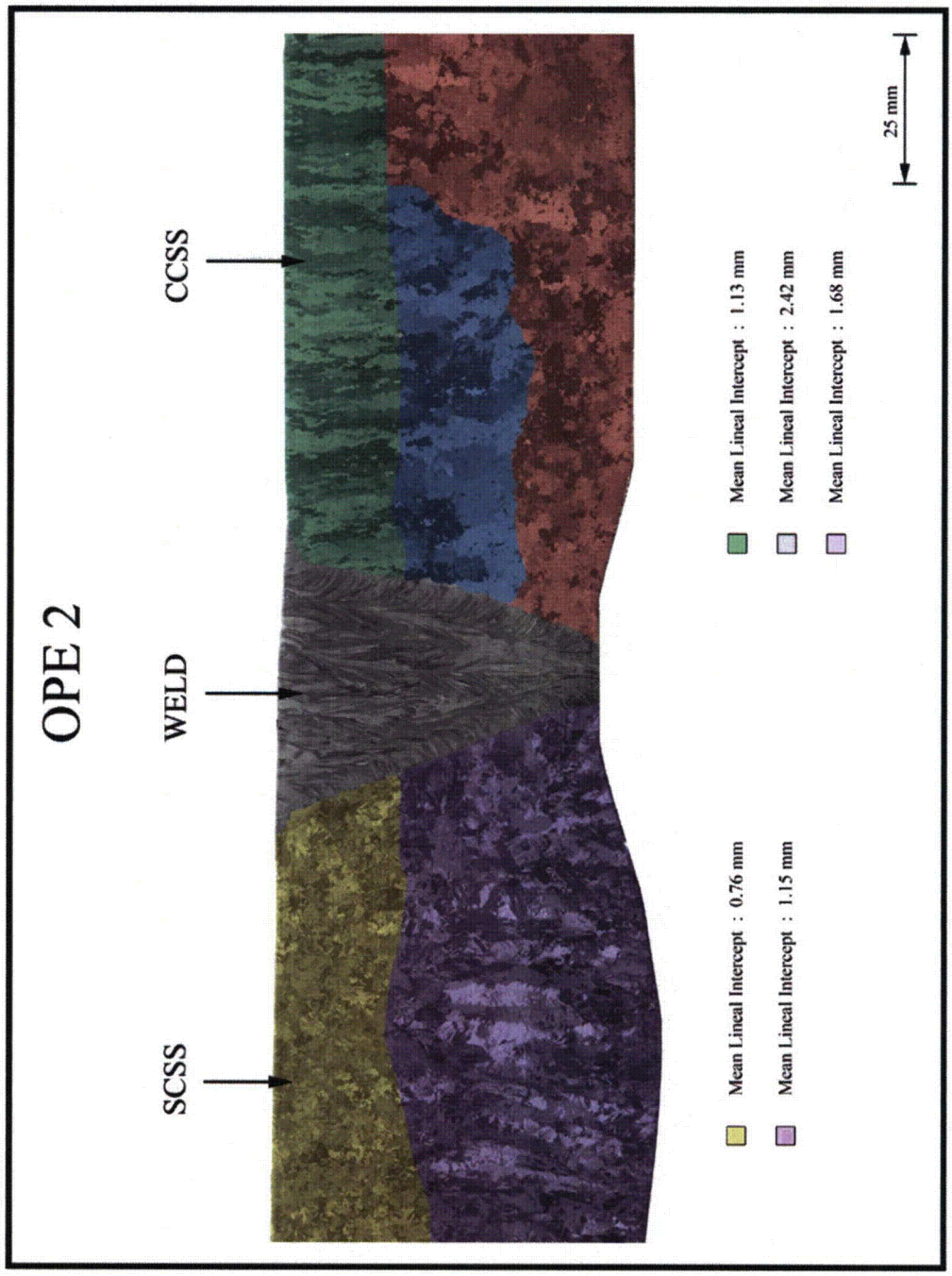

Figure A.37 Axial-Radial Cross Section of WOG Specimen OPE-2, Showing Outside and Inside Diameter Geometry, and Grain Size, Typical of OPE Configuration

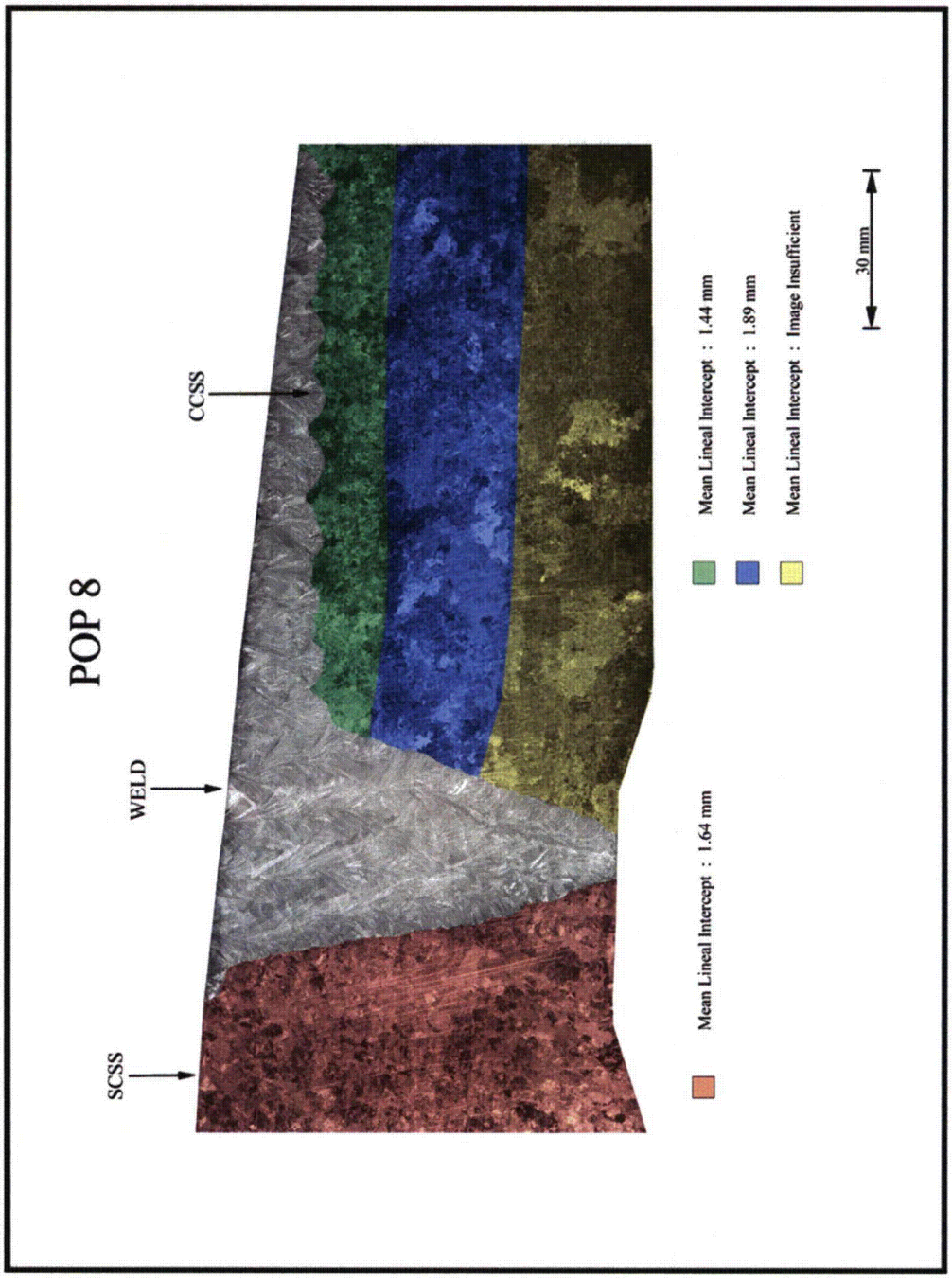

Figure A.38 Axial-Radial Cross Section of WOG Specimen POP-8, Showing Outside and Inside Diameter Geometry, and Grain Size, Typical of POP Configuration

Appendix B

Magnitude Plots from Eddy Current Data

Appendix B

Magnitude Plots from Eddy Current Data

All vertical and horizontal axes shown in these Appendix B plots are in units of inches (25.4 mm).

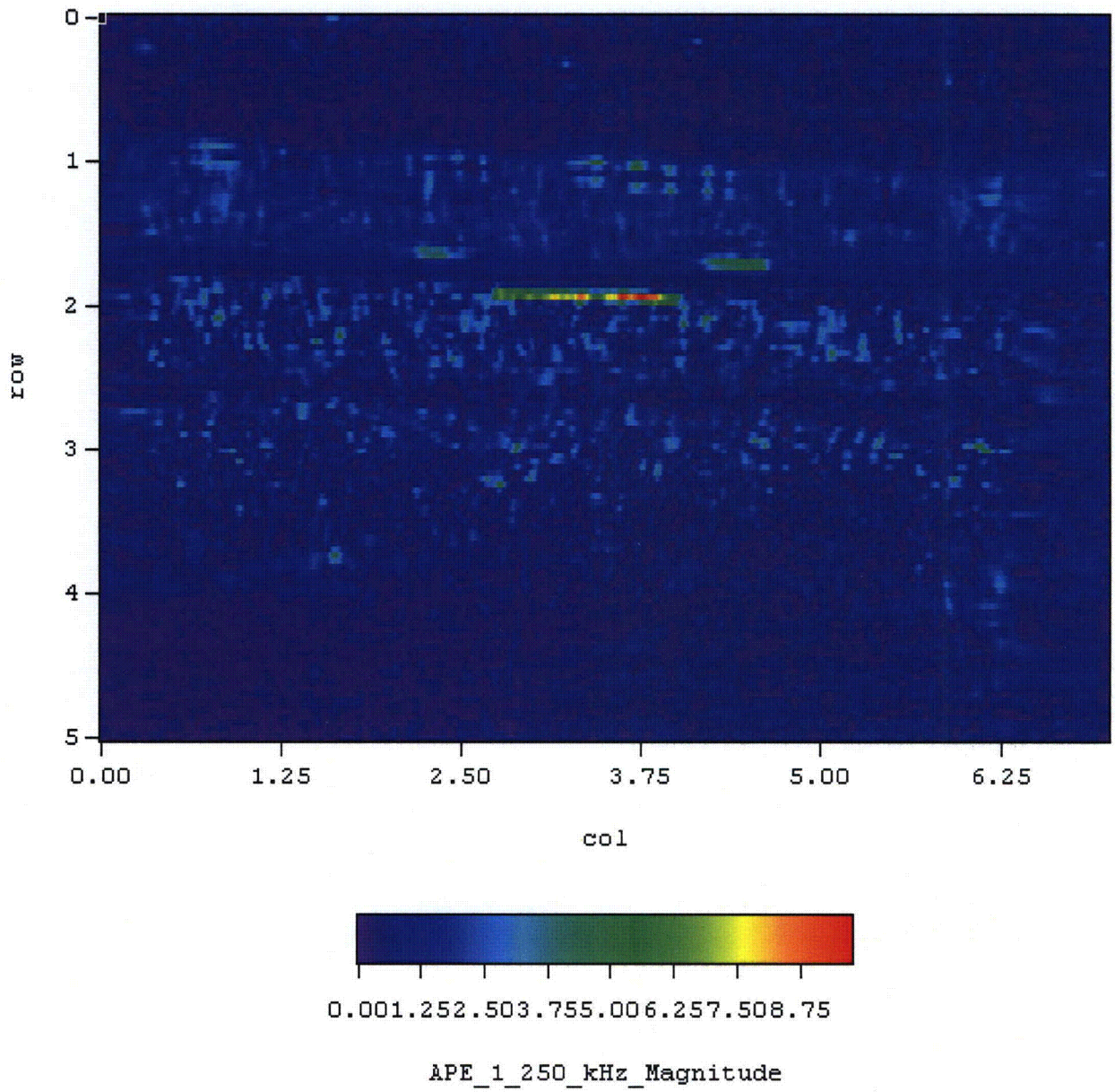

Figure B.1 Magnitude Plot of WOG Specimen APE-1

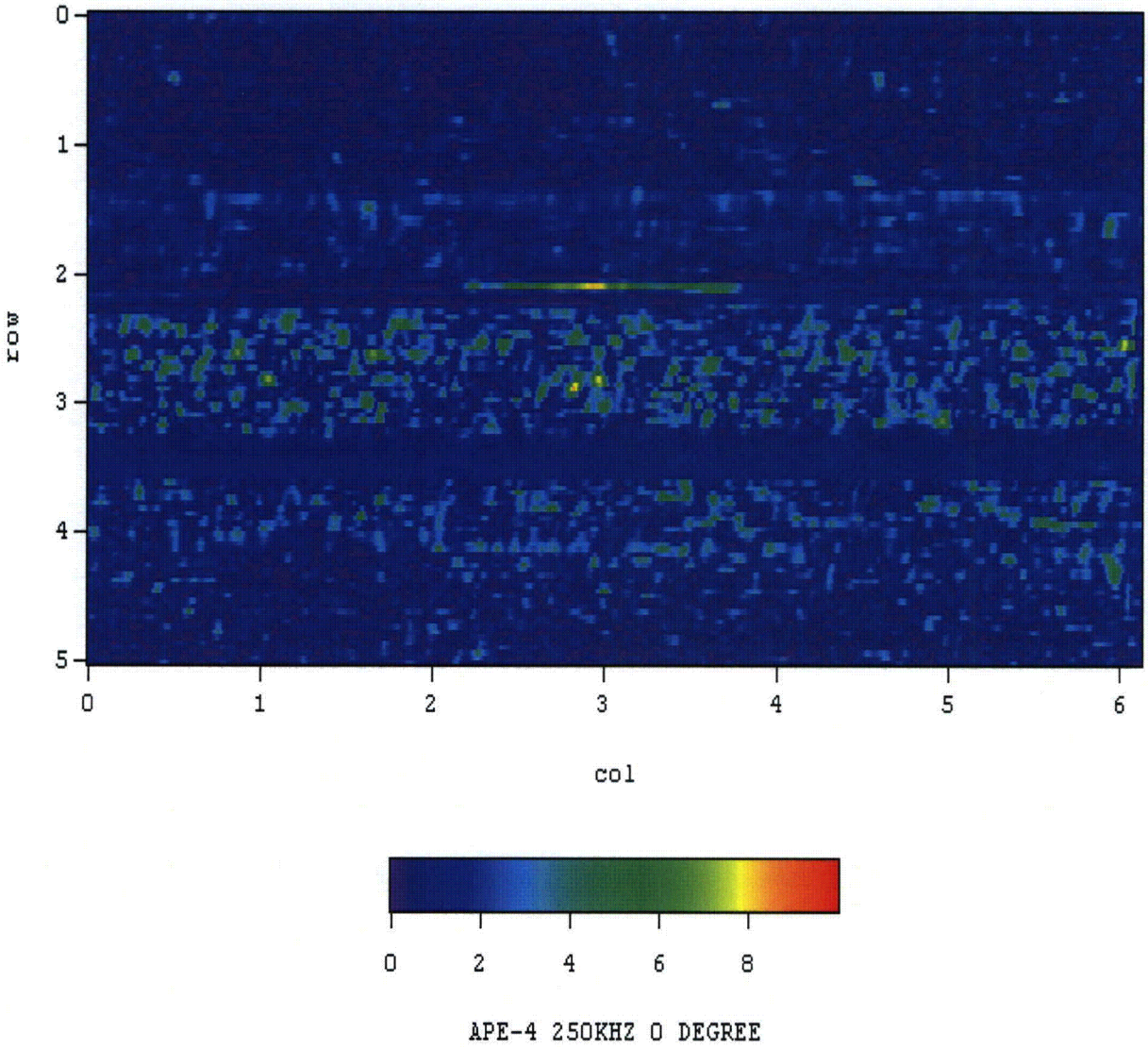

Figure B.2 Magnitude Plot of WOG Specimen APE-4

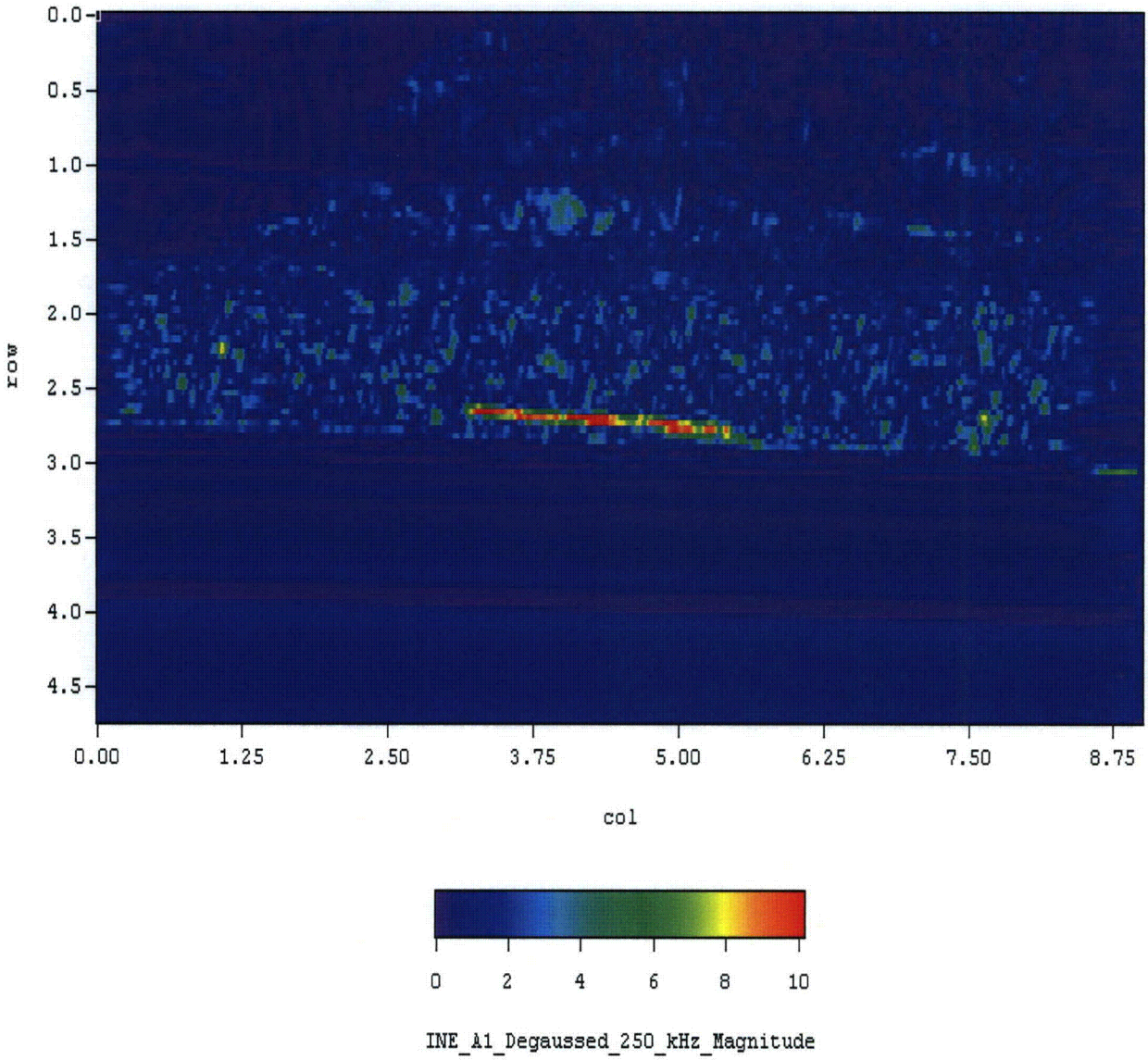

Figure B.3 Magnitude Plot of WOG Specimen INE-A-1

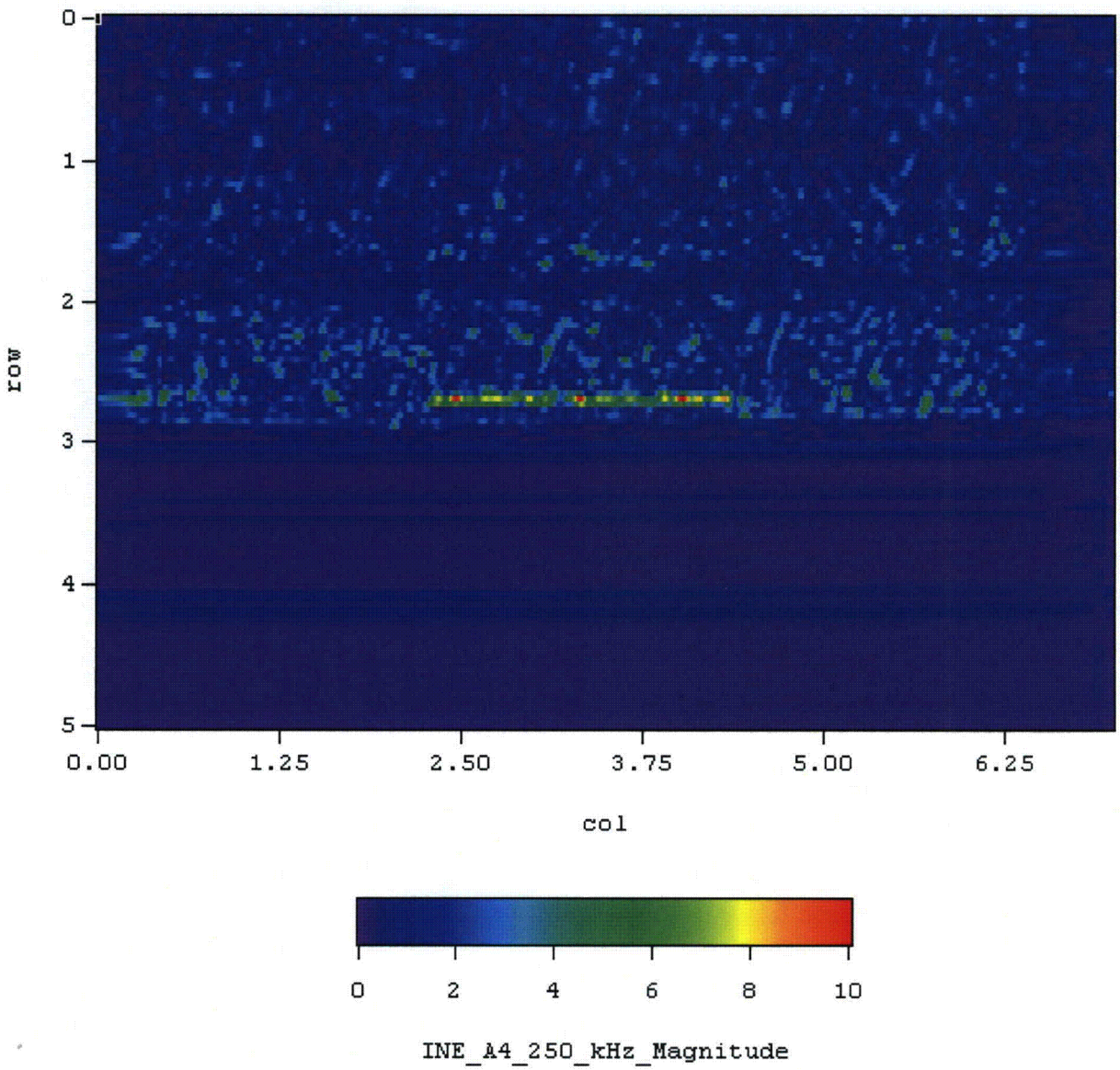

Figure B.4 Magnitude Plot of WOG Specimen INE-A-4

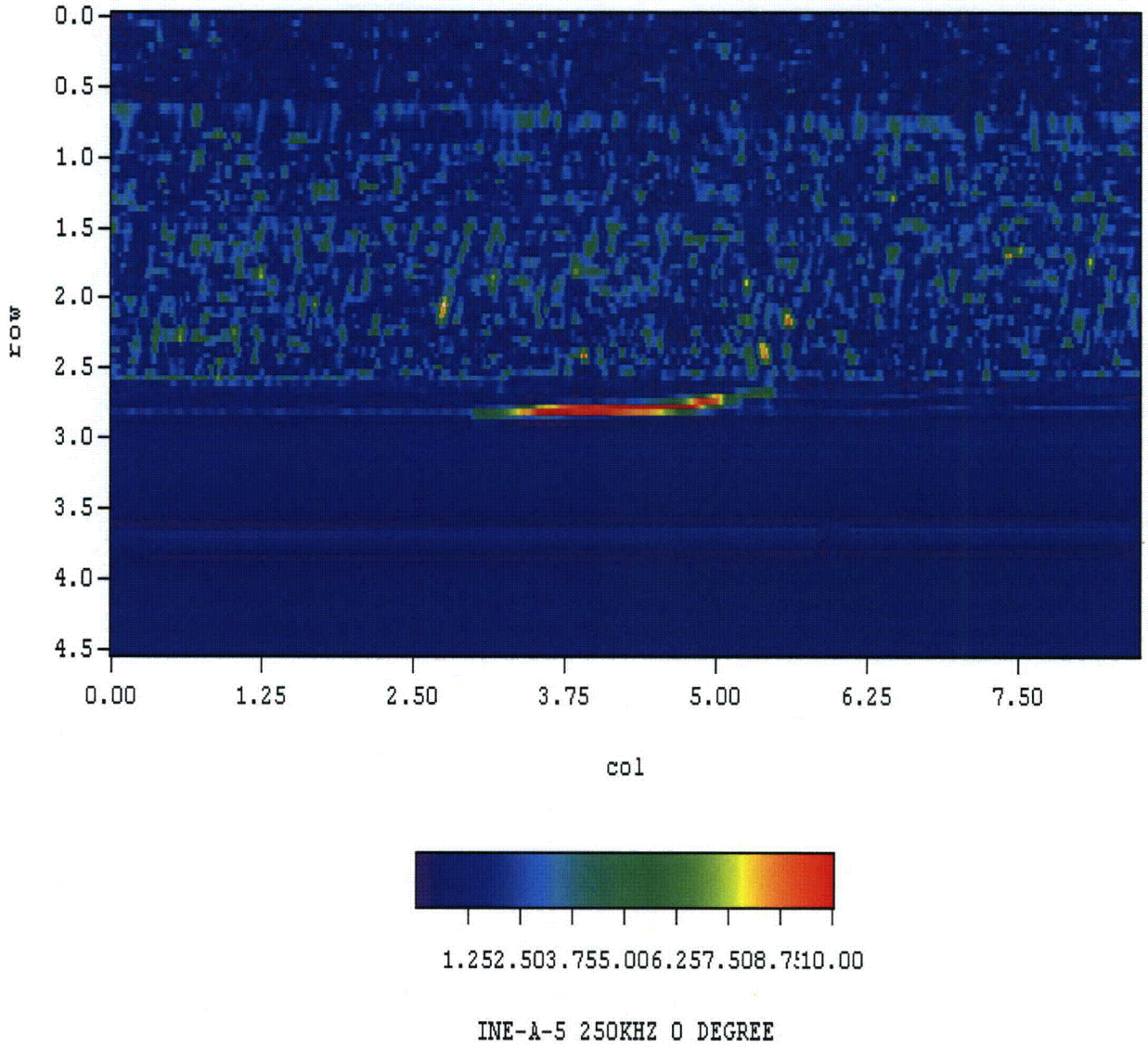

Figure B.5 Magnitude Plot of WOG Specimen INE-A-5

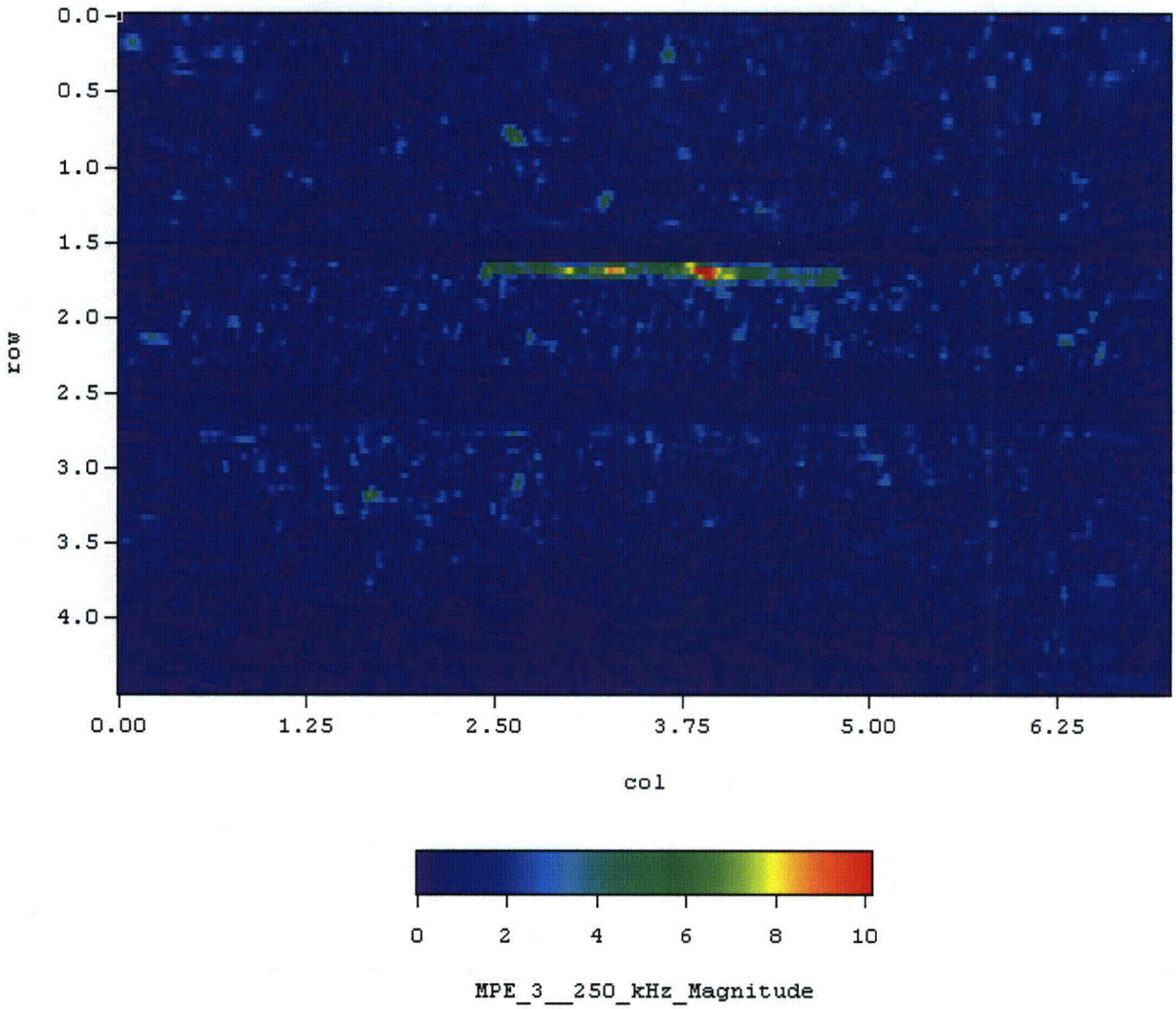

Figure B.6 Magnitude Plot of WOG Specimen MPE-3

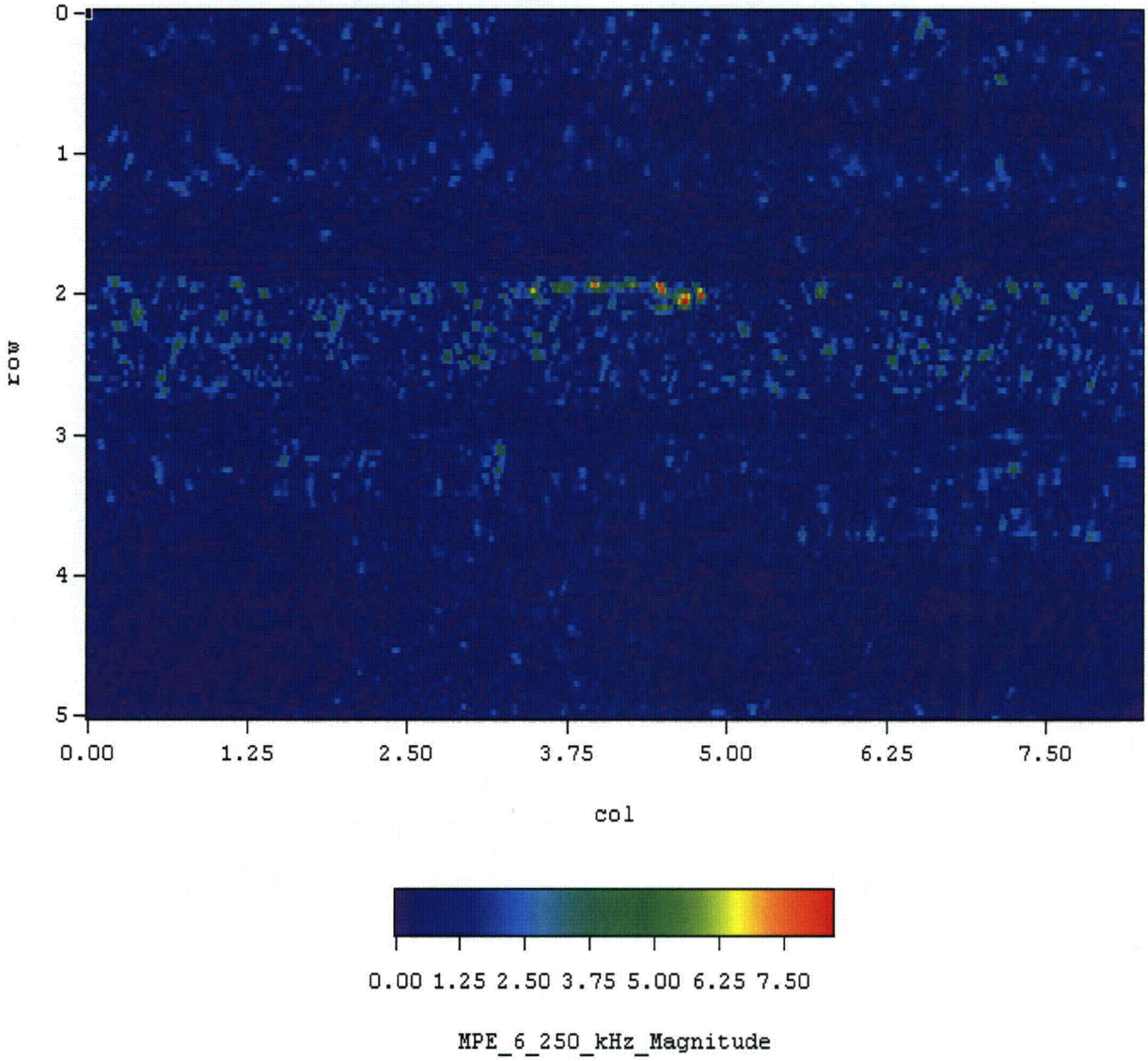

Figure B.7 Magnitude Plot of WOG Specimen MPE-6

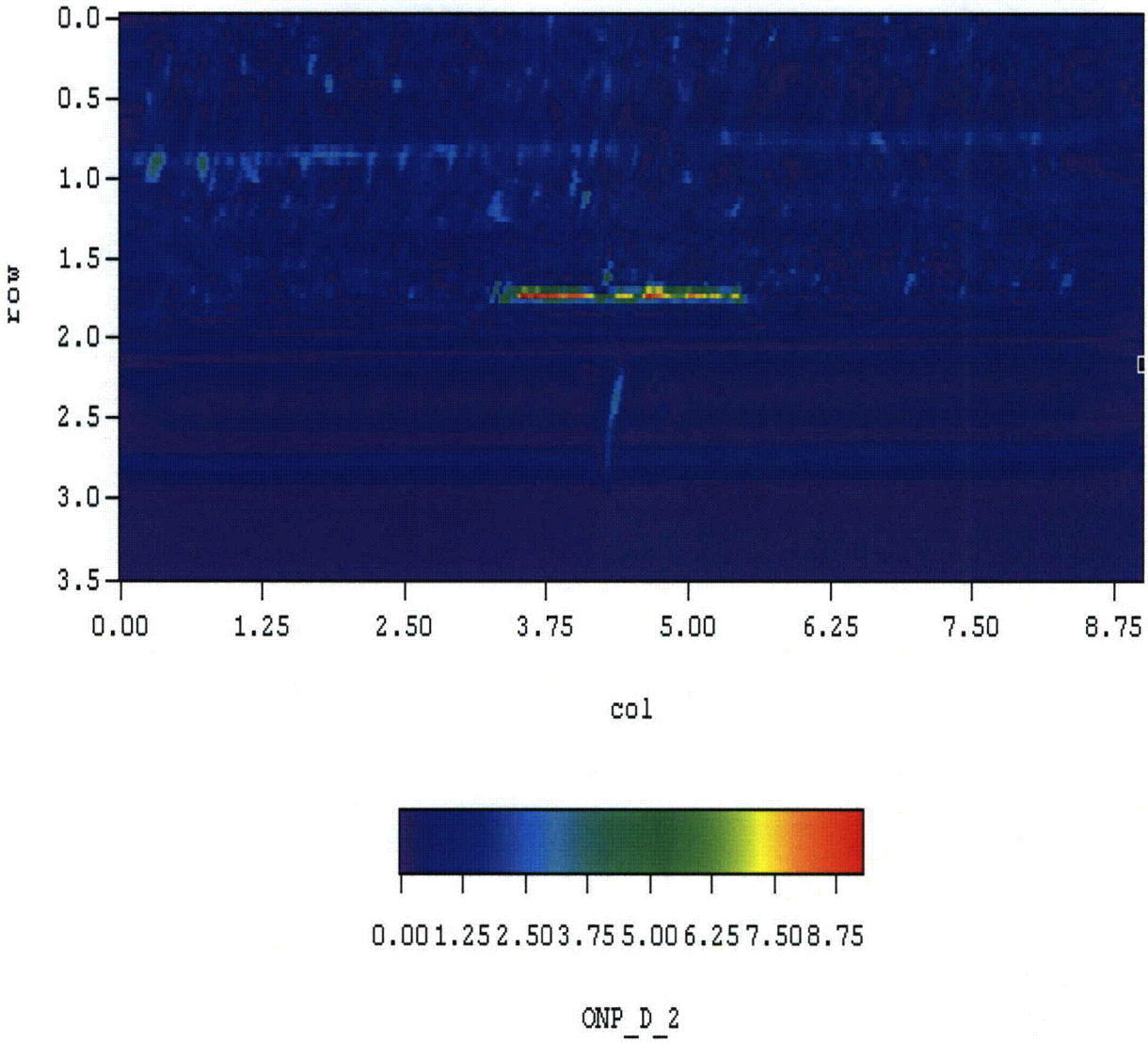

Figure B.8 Magnitude Plot of WOG Specimen ONP-D-2

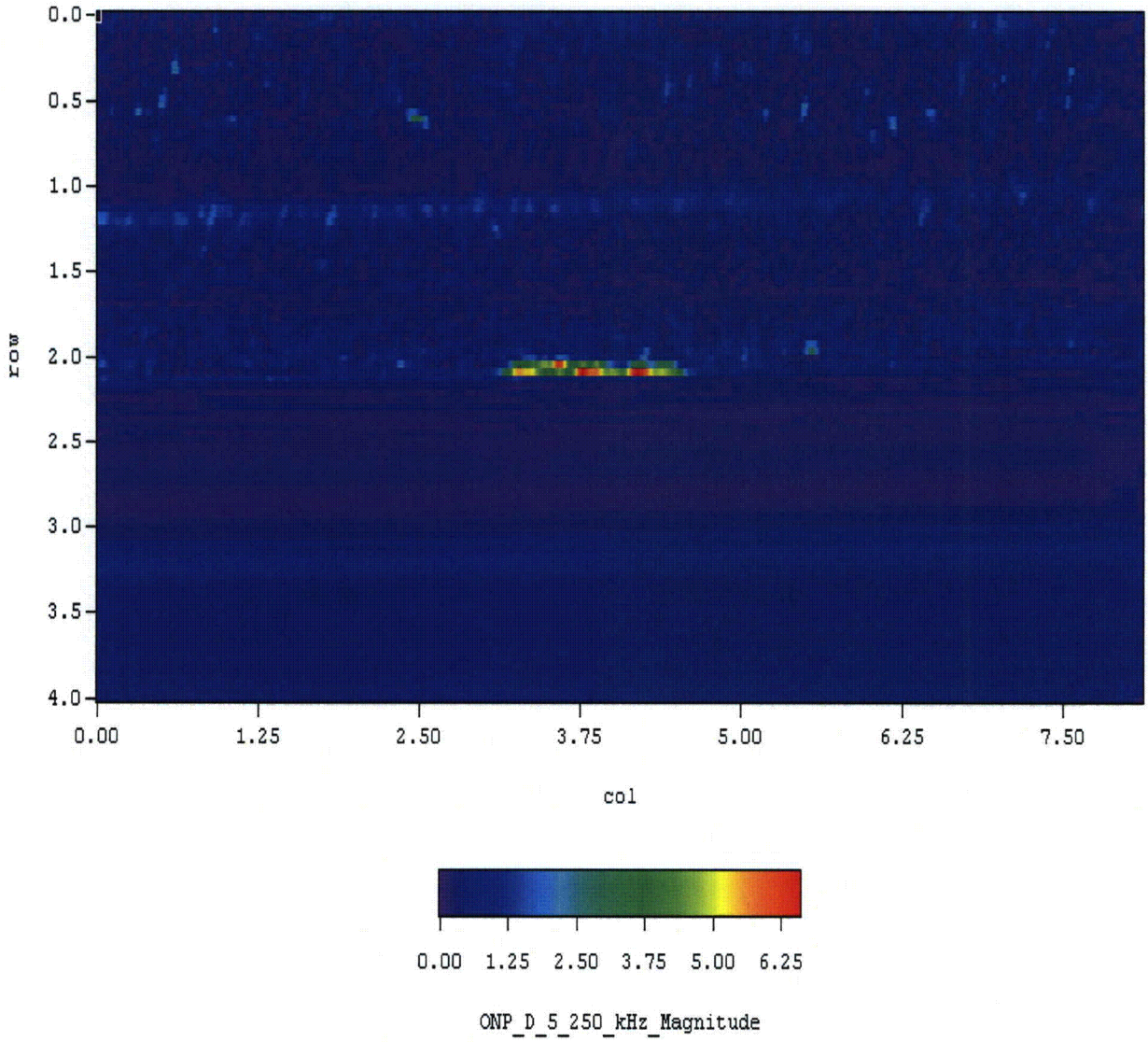

Figure B.9 Magnitude Plot of WOG Specimen ONP-D-5

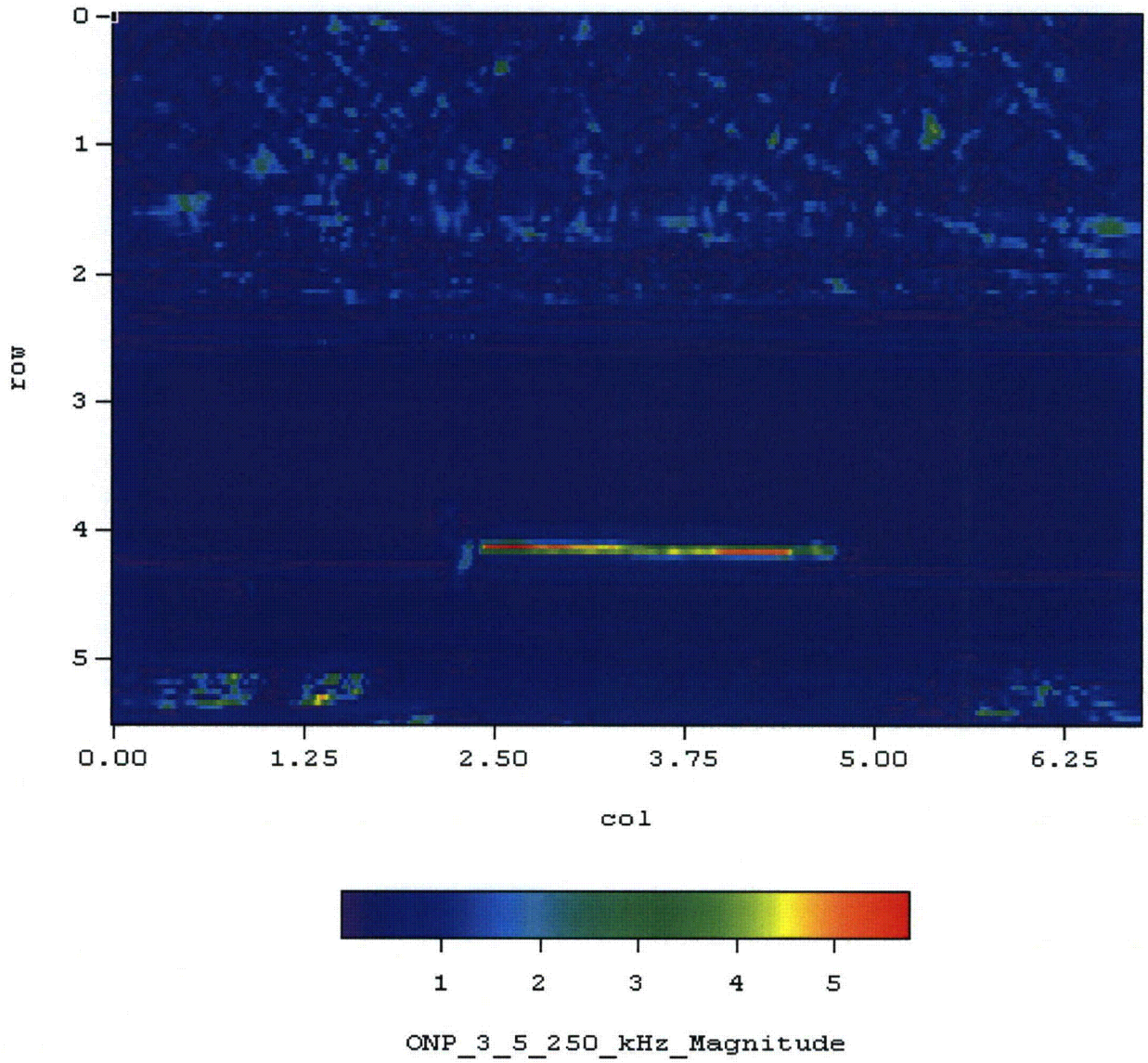

Figure B.10 Magnitude Plot of WOG Specimen ONP-3-5

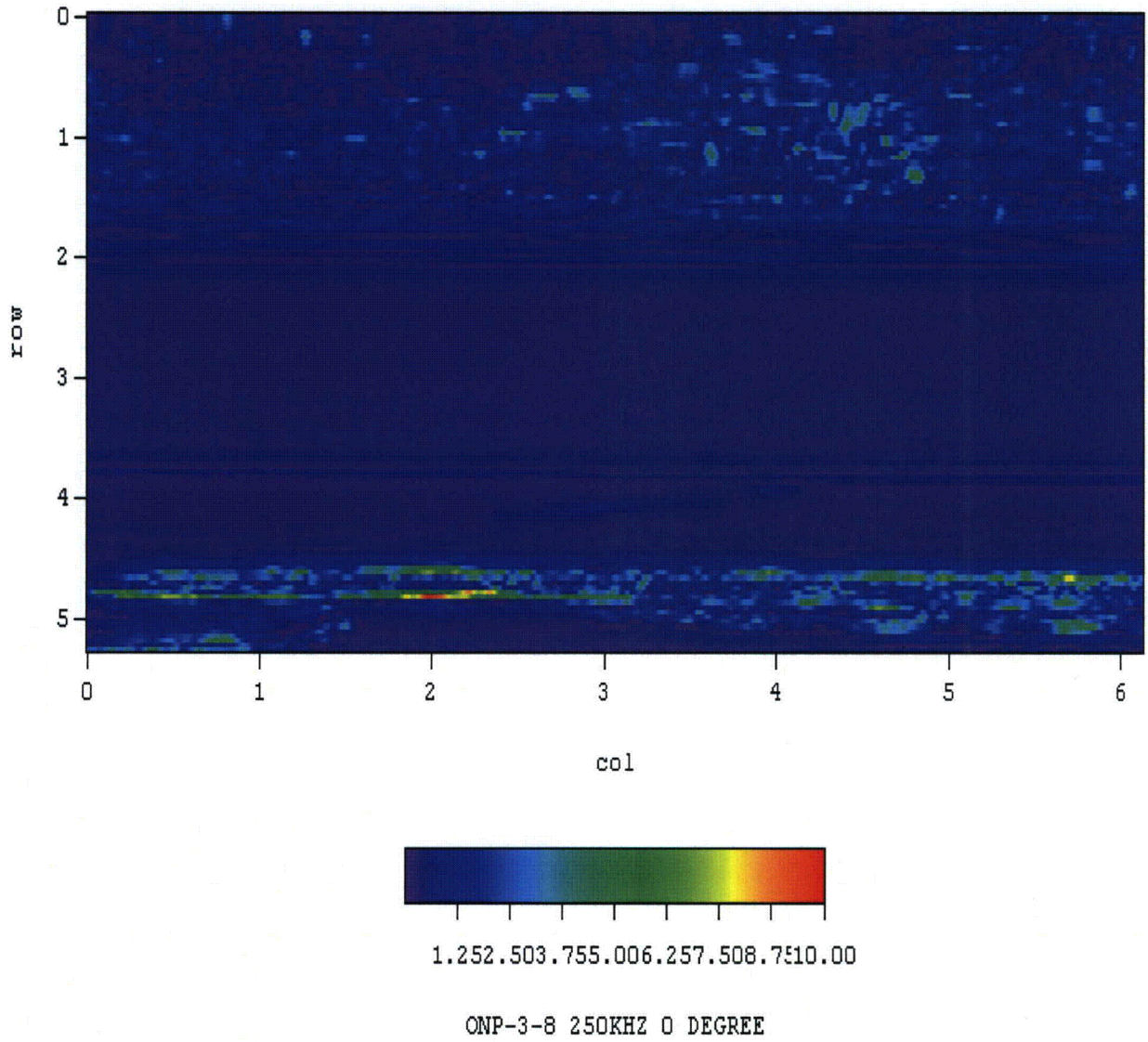

Figure B.11 Magnitude Plot of WOG Specimen ONP-3-8

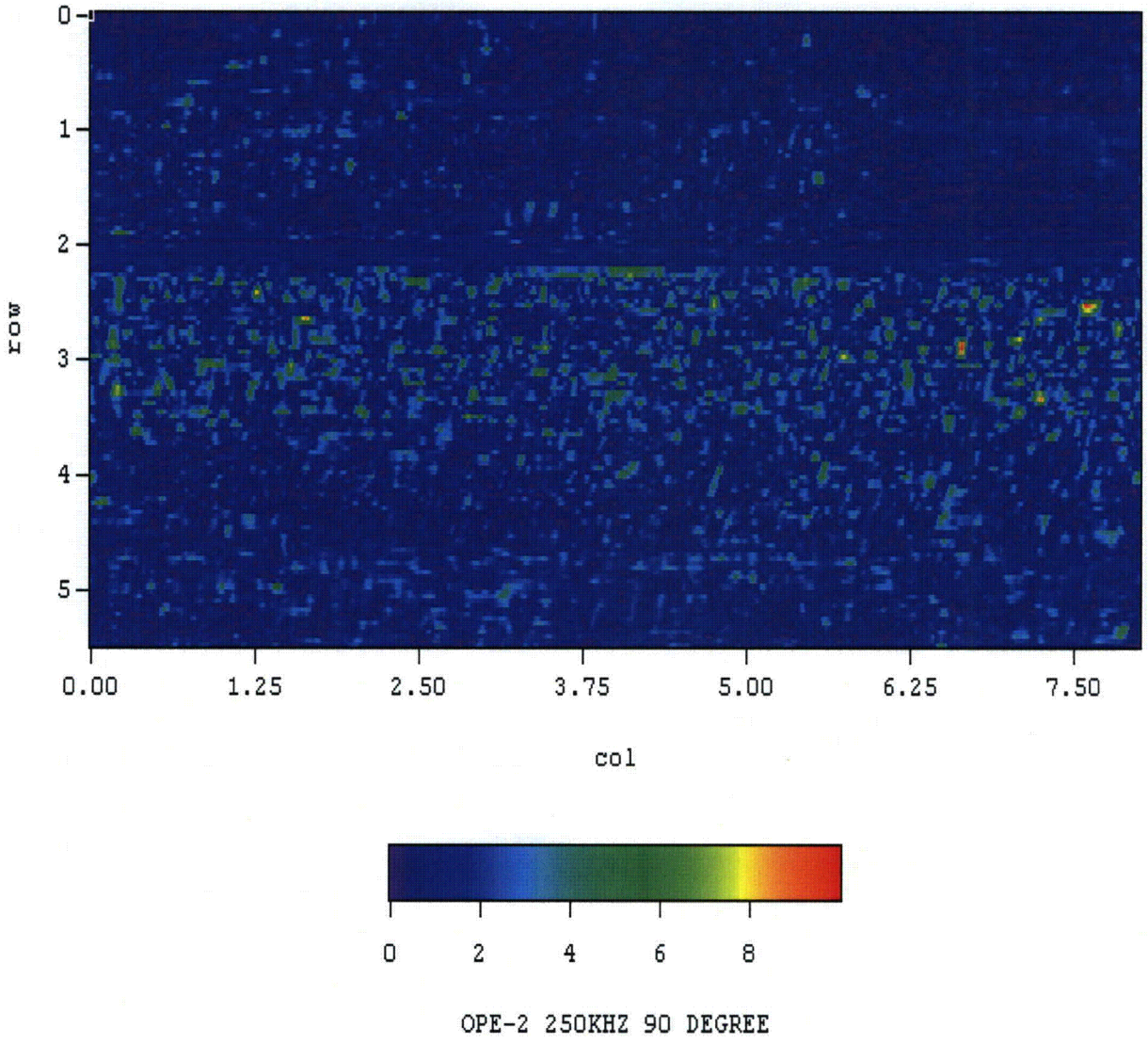

Figure B.12 Magnitude Plot of WOG Specimen OPE-2

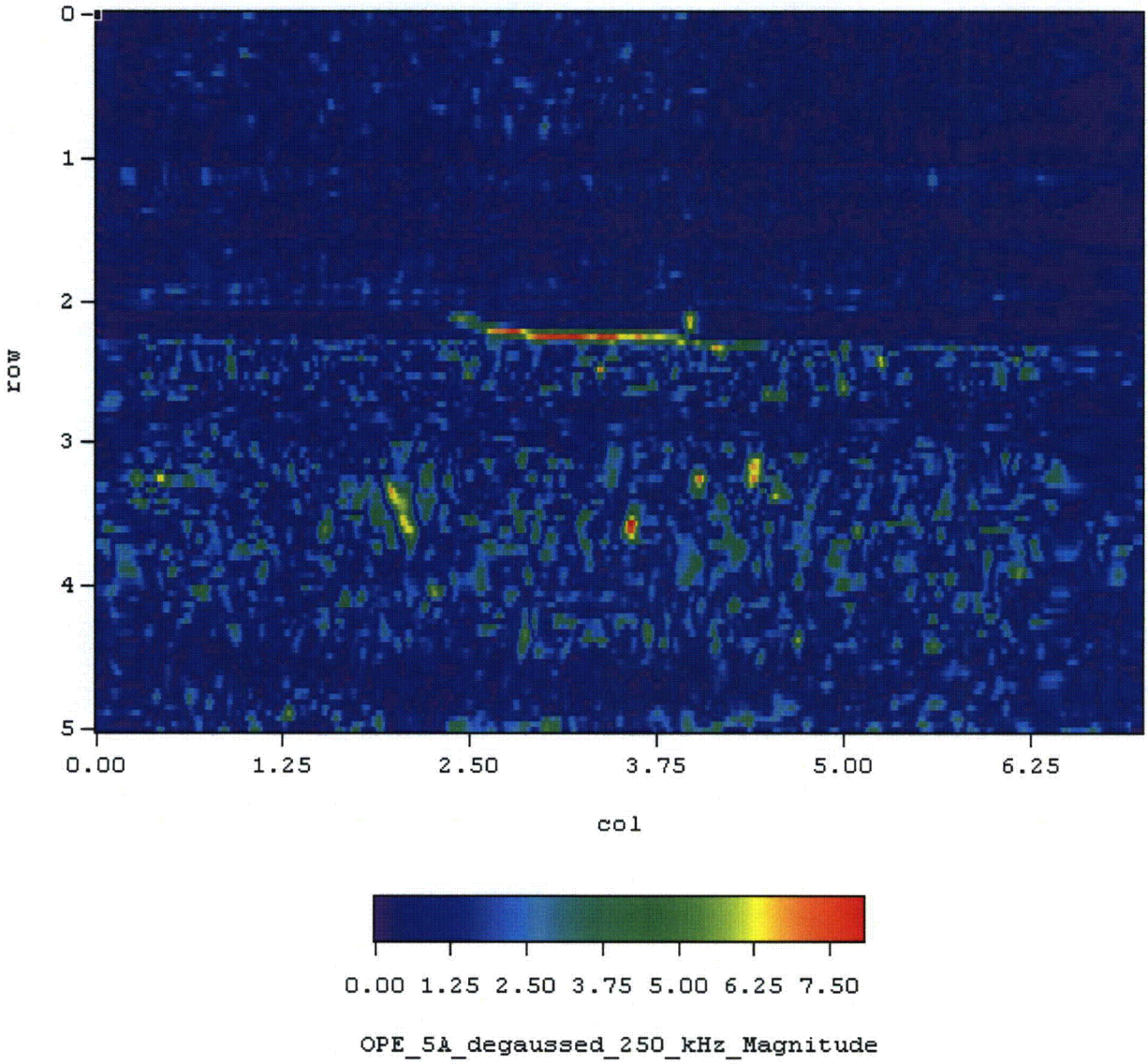

Figure B.13 Magnitude Plot of WOG Specimen OPE-5

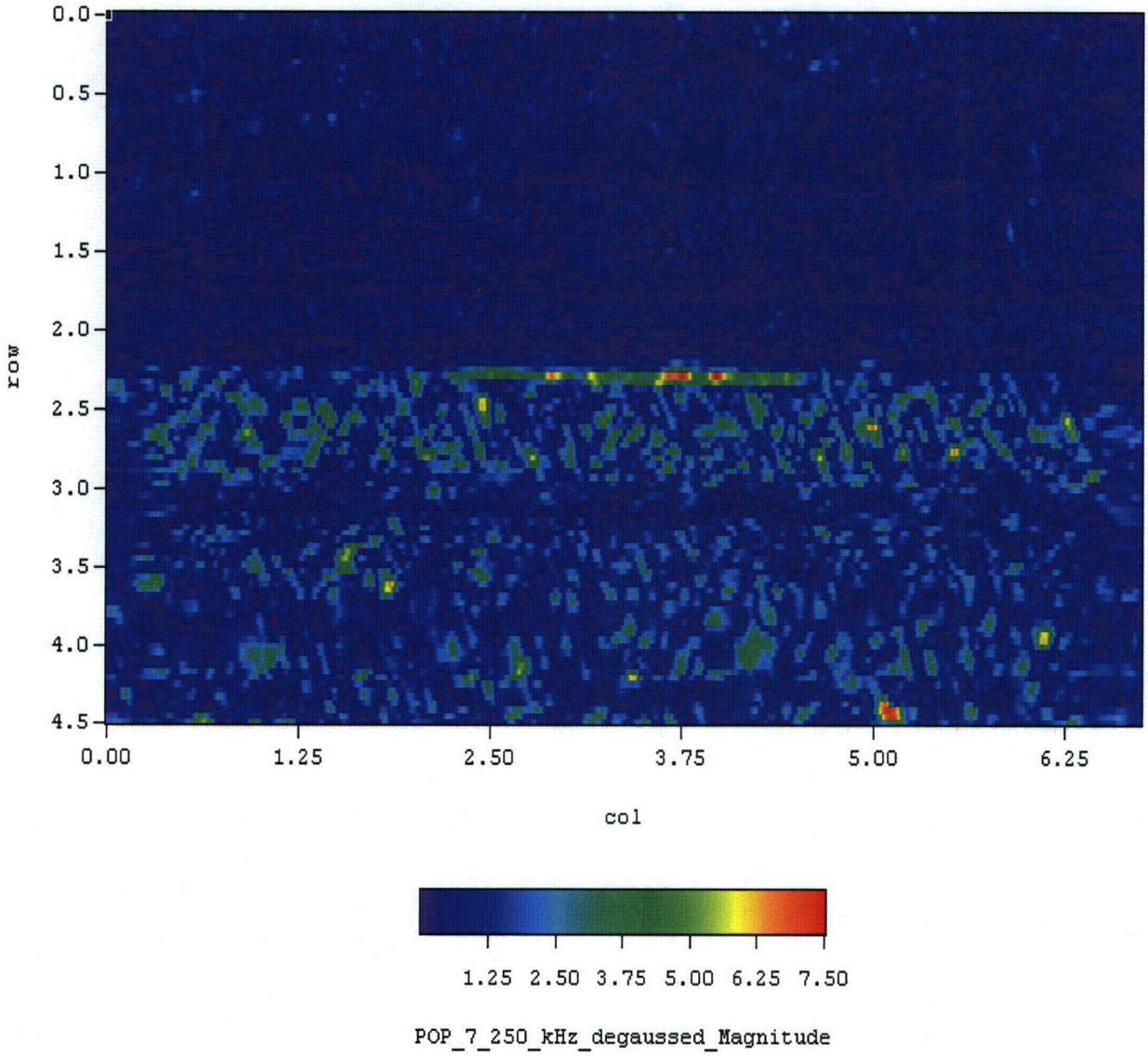

Figure B.14 Magnitude Plot of WOG Specimen POP-7

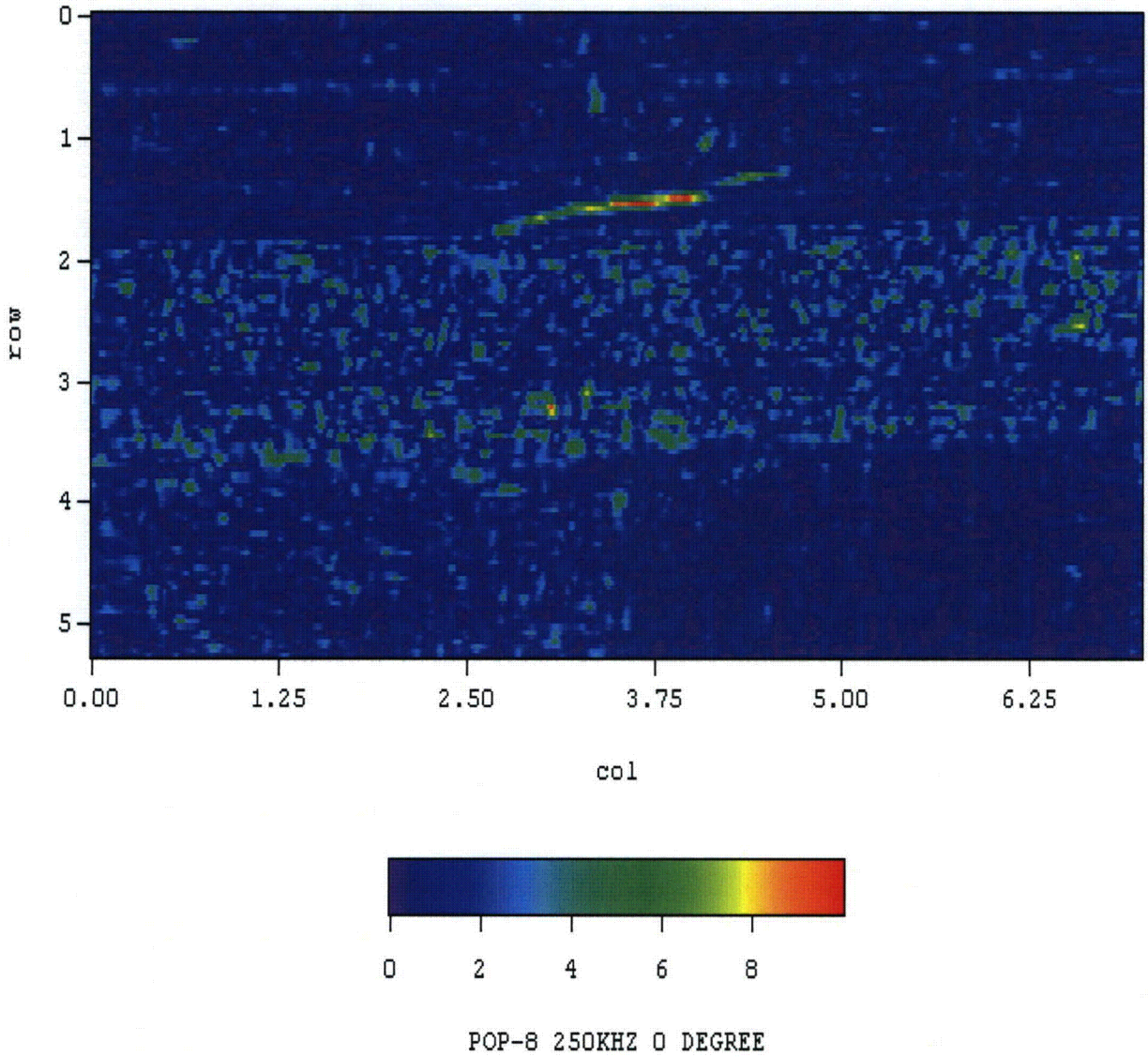

Figure B.15 Magnitude Plot of WOG Specimen POP-8

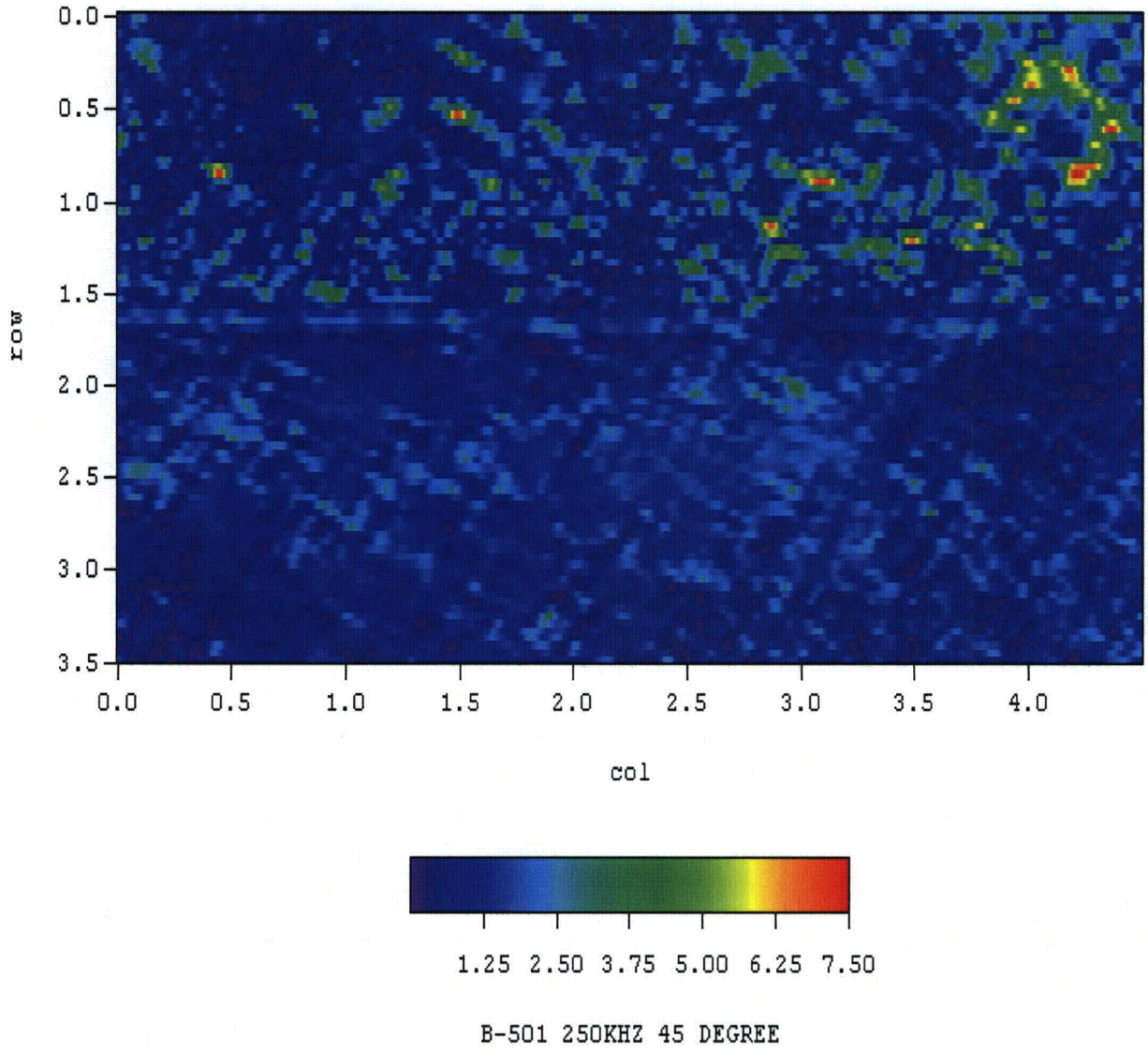

Figure B.16 Magnitude Plot of PNNL Specimen B-501

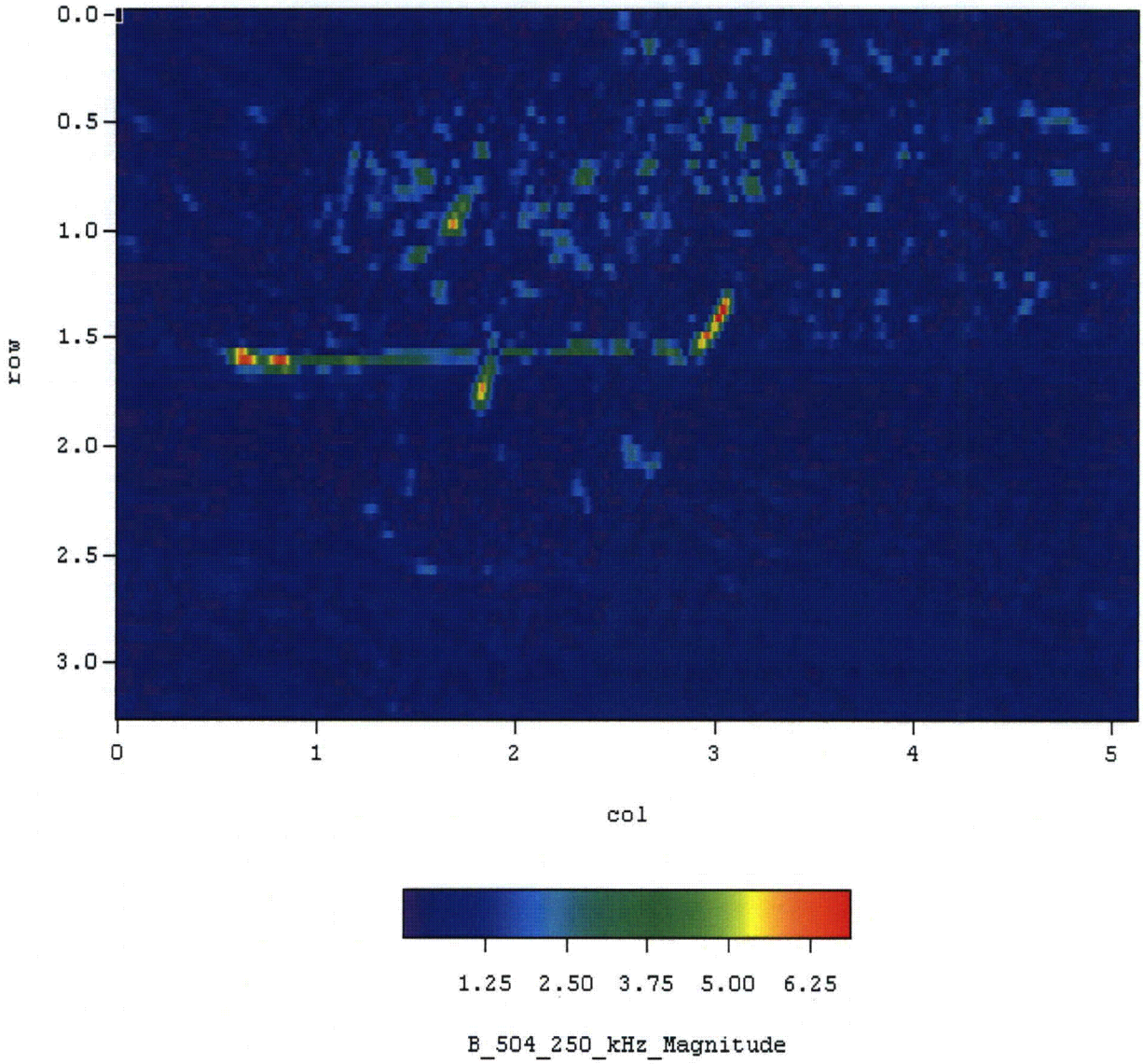

Figure B.17 Magnitude Plot of PNNL Specimen B-504

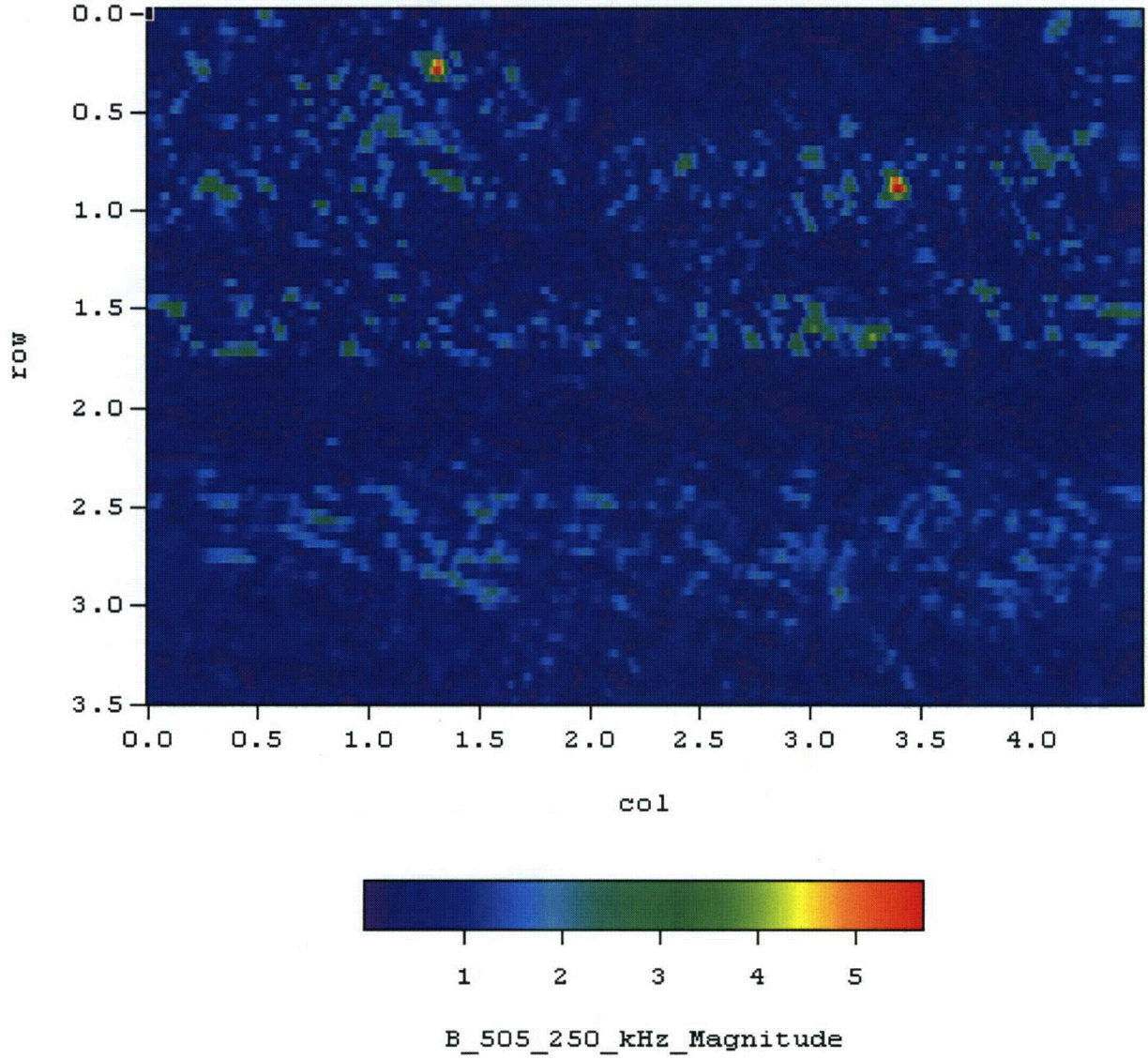

Figure B.18 Magnitude Plot of PNNL Specimen B-505

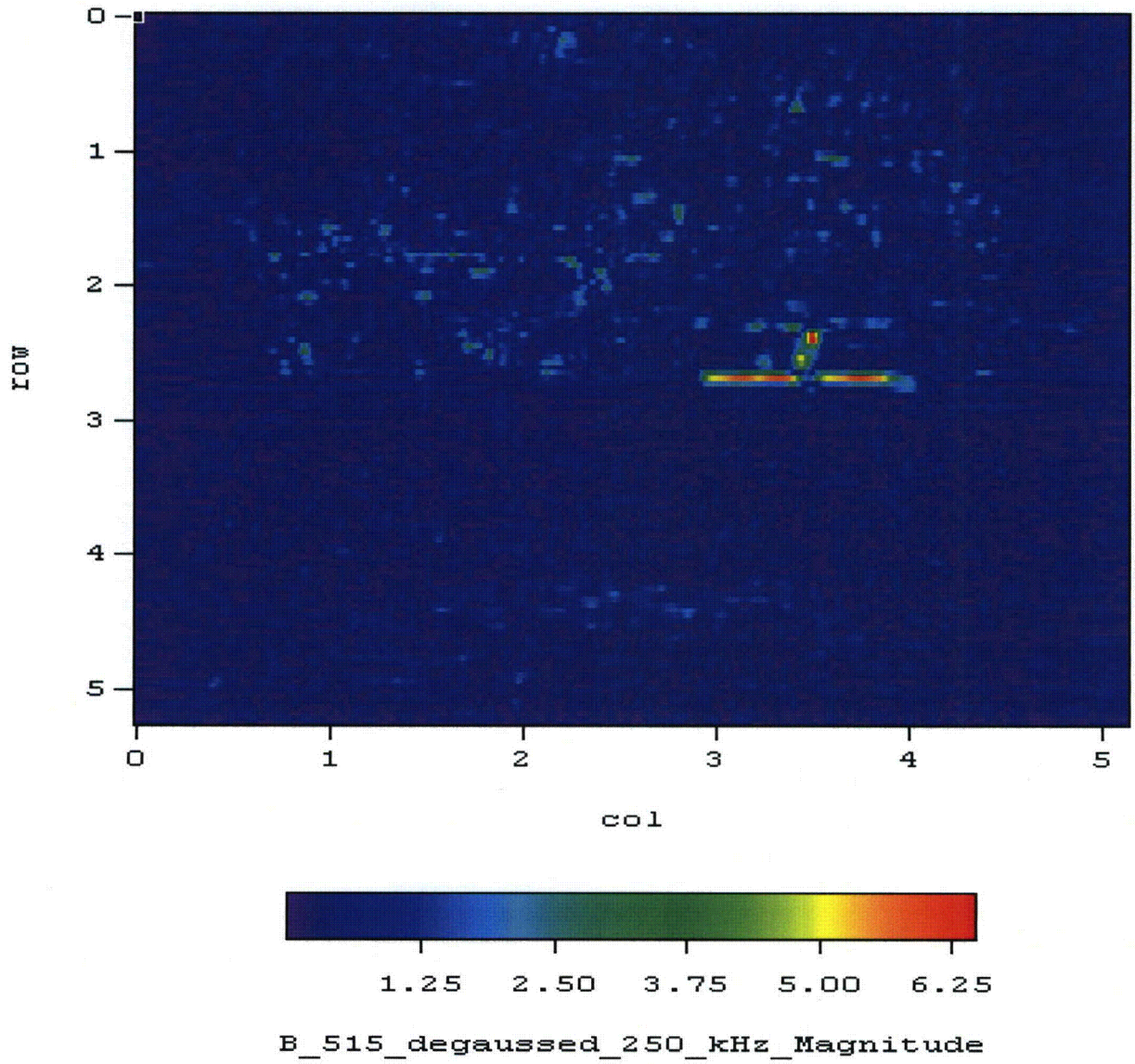

Figure B.19 Magnitude Plot of PNNL Specimen B-515

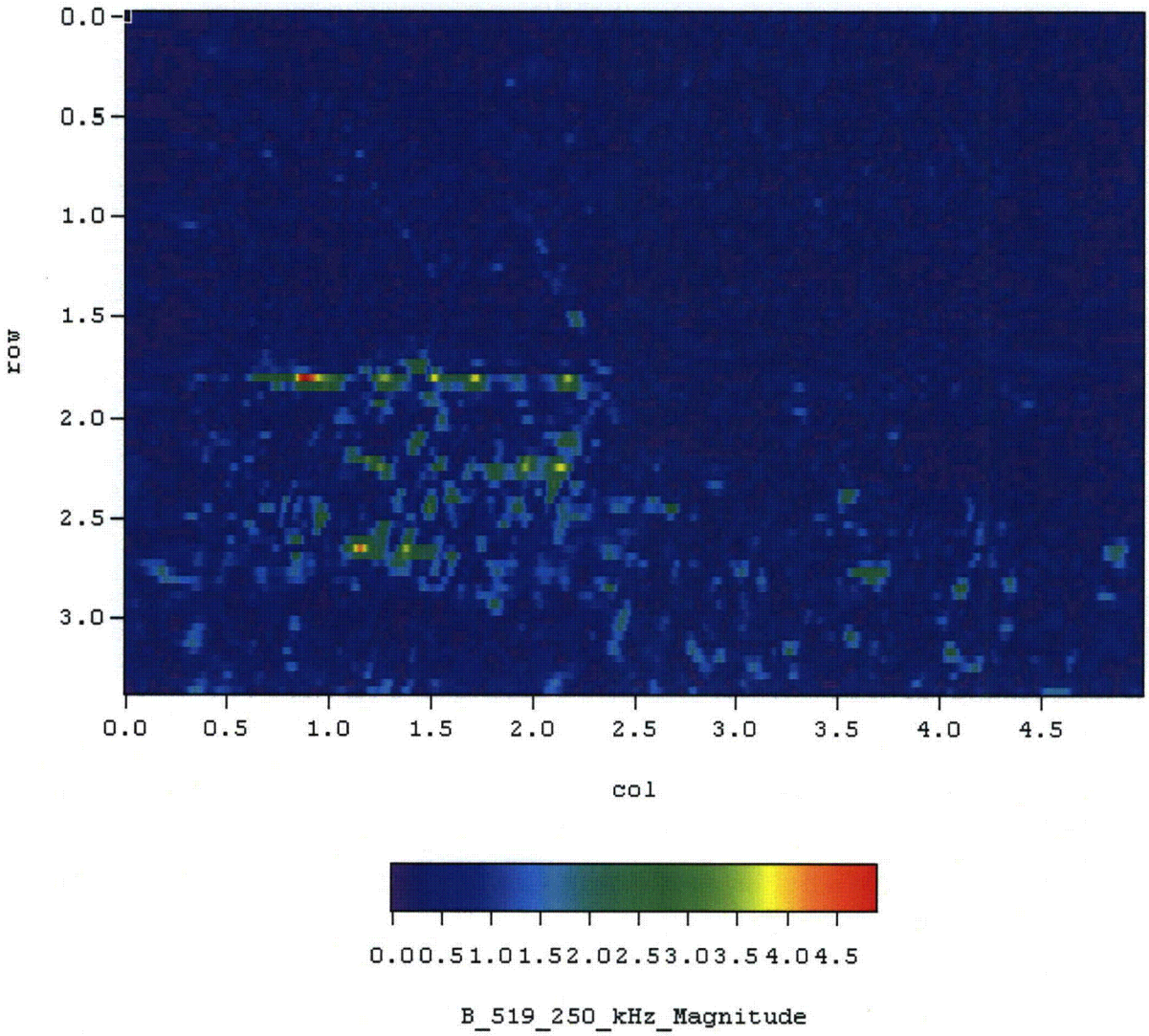

Figure B.20 Magnitude Plot of PNNL Specimen B-519

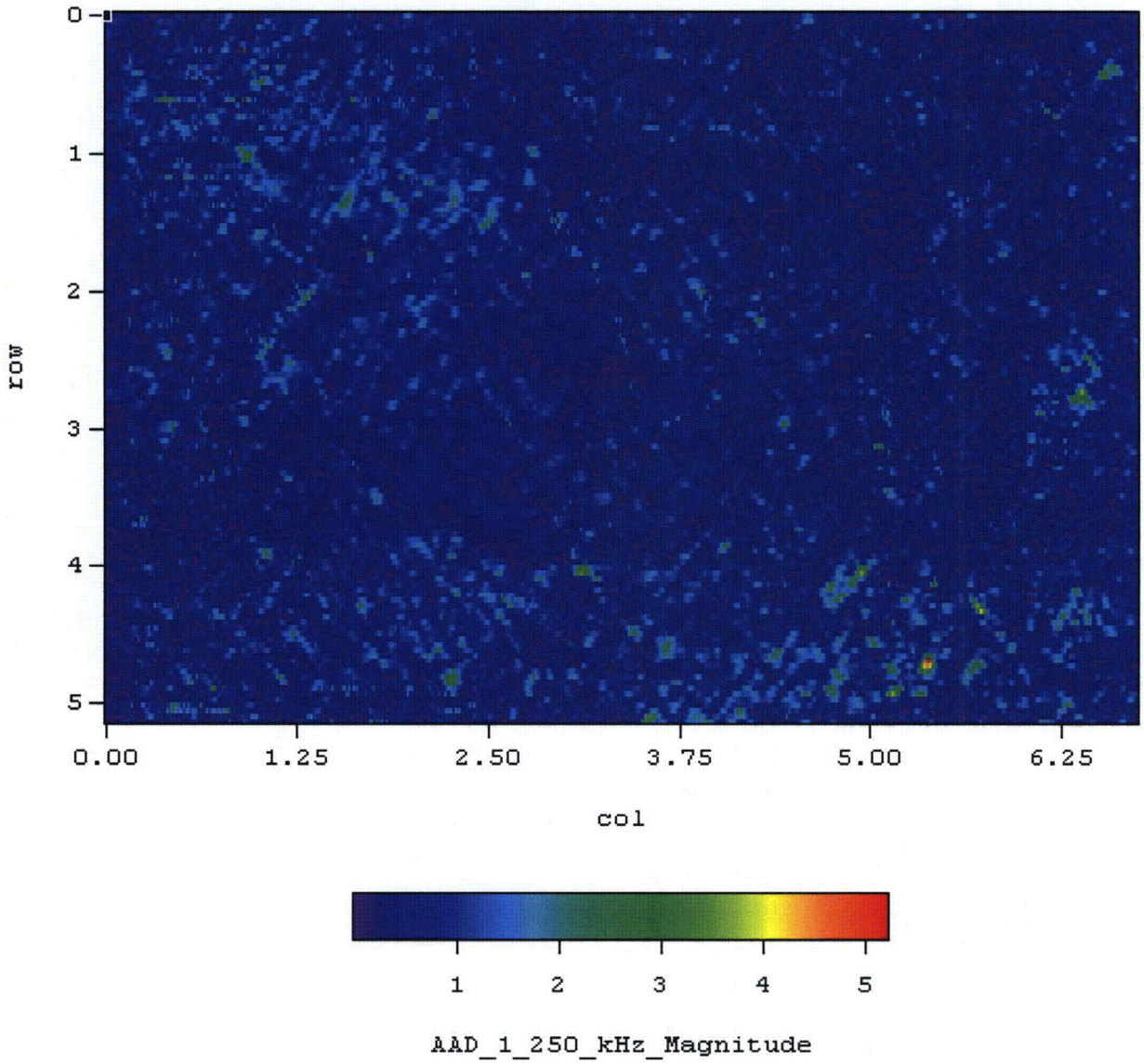

Figure B.21 Magnitude Plot of Southwest Research Institute Specimen AAD-1

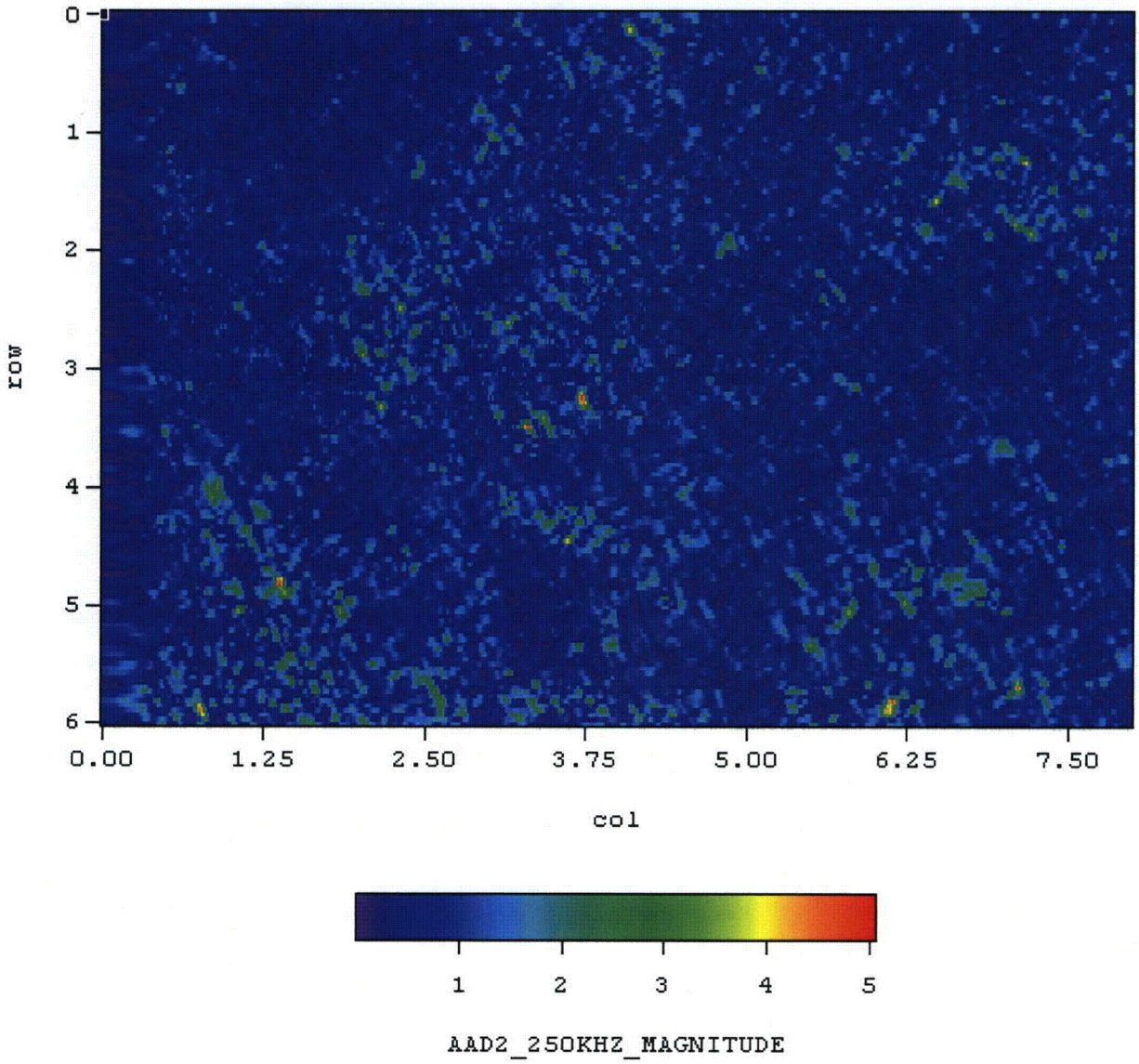

Figure B.22 Magnitude Plot of Southwest Research Institute Specimen AAD-2

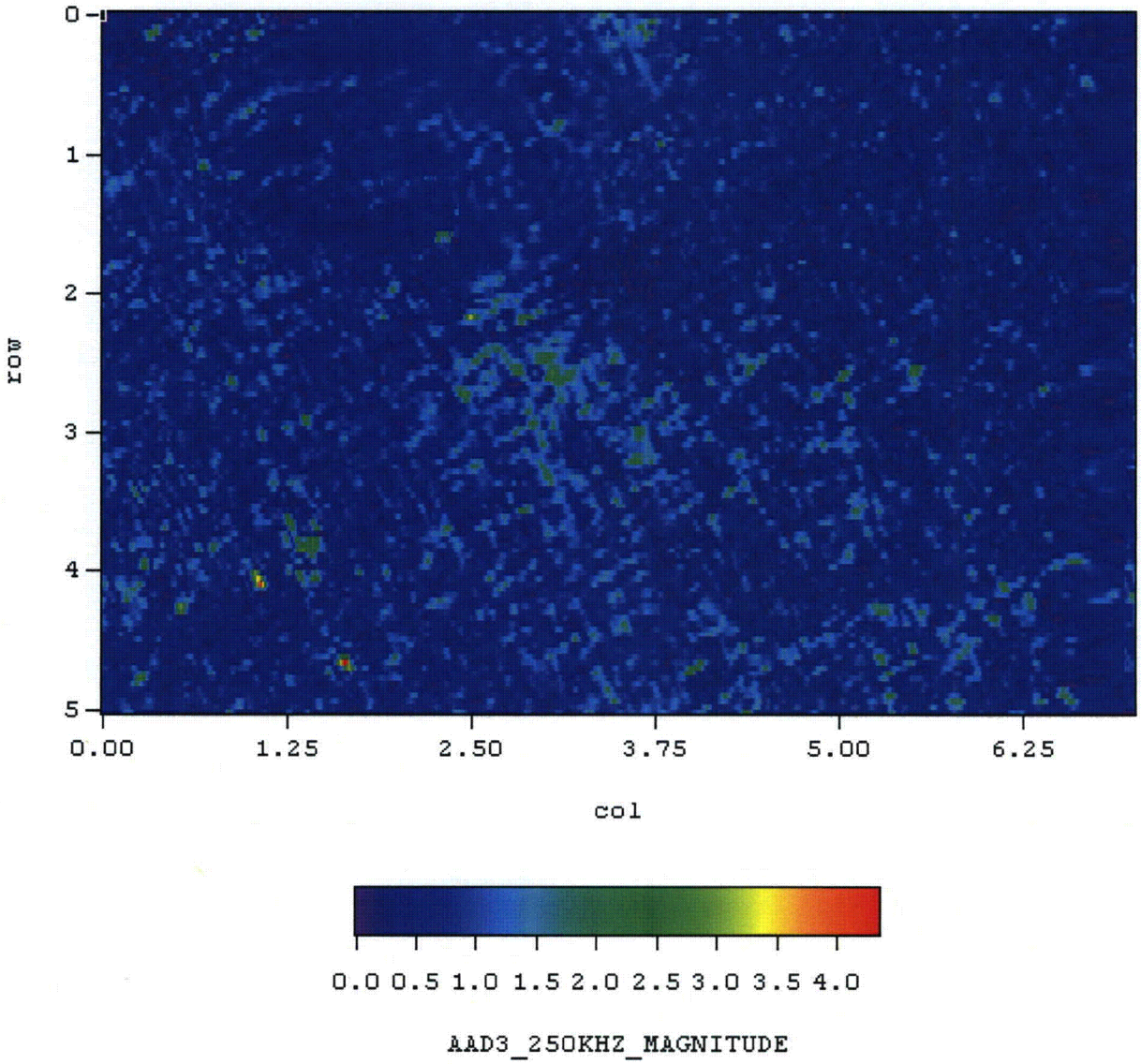

Figure B.23 Magnitude Plot of Southwest Research Institute Specimen AAD-3

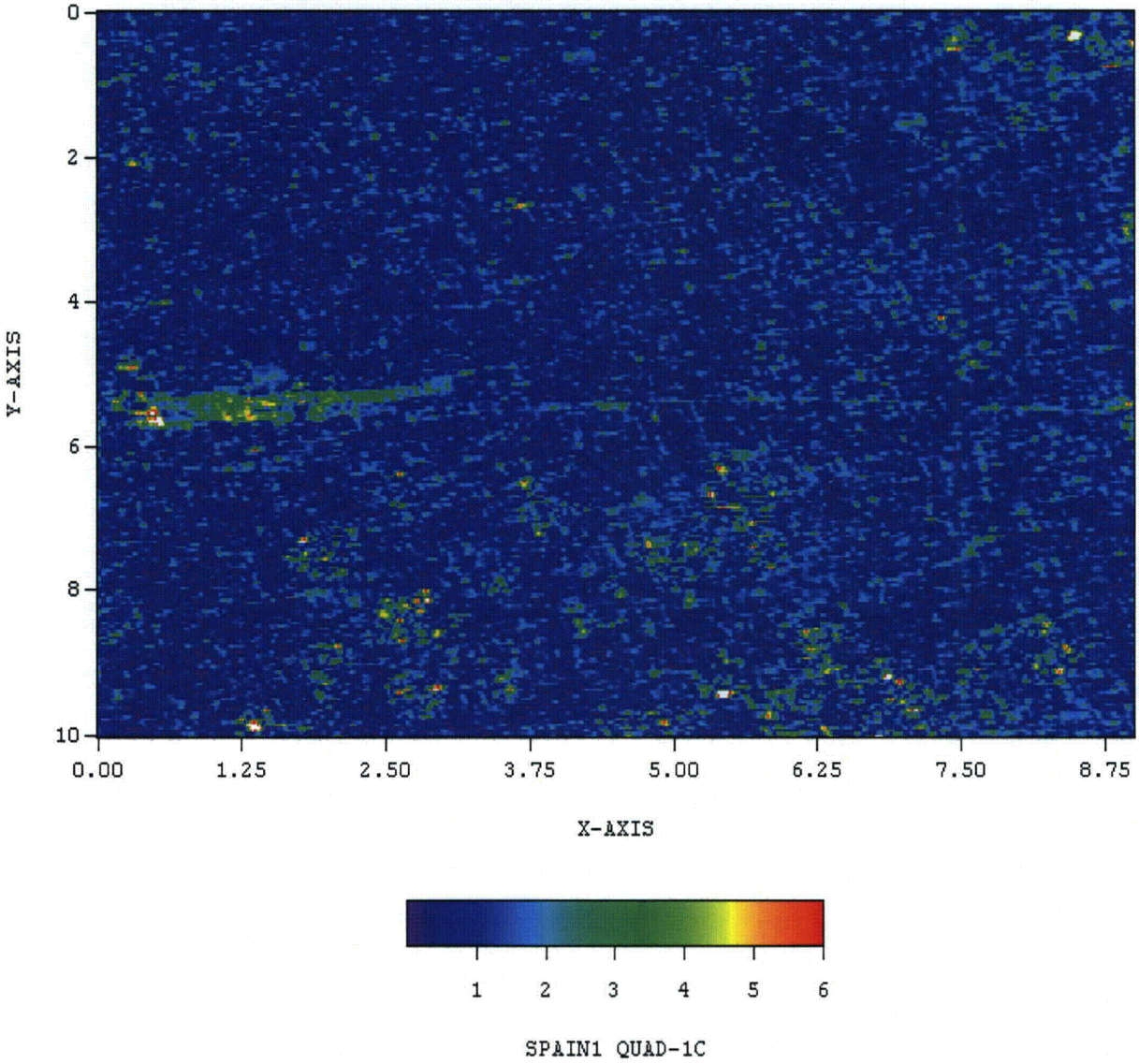

Figure B.24 Magnitude Plot of EPRI NDE Center Spanish Spool Piece Specimen (right side, Quadrant 1)

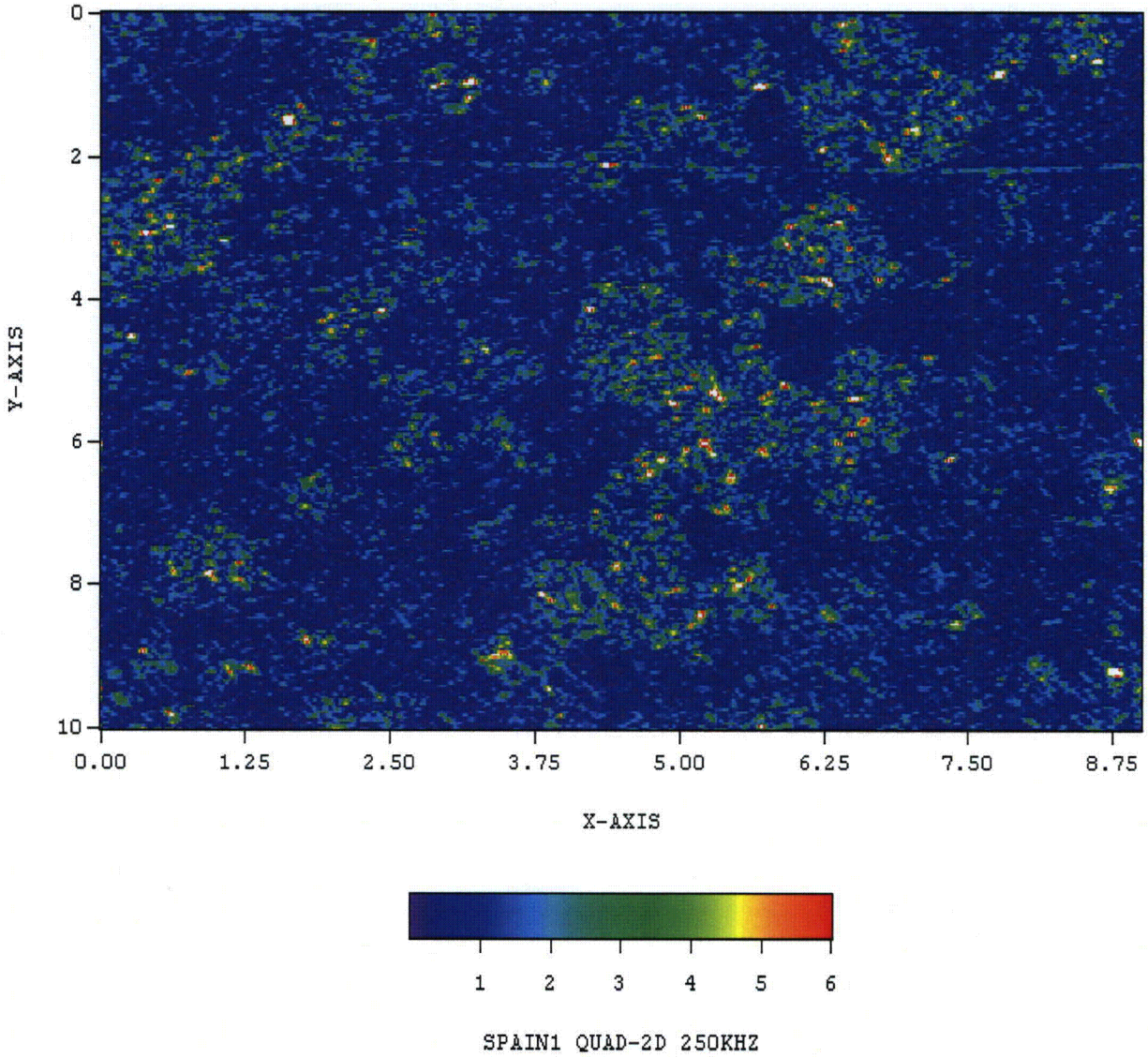

Figure B.25 Magnitude Plot of EPRI NDE Center Spanish Spool Piece Specimen (right side, Quadrant 2)

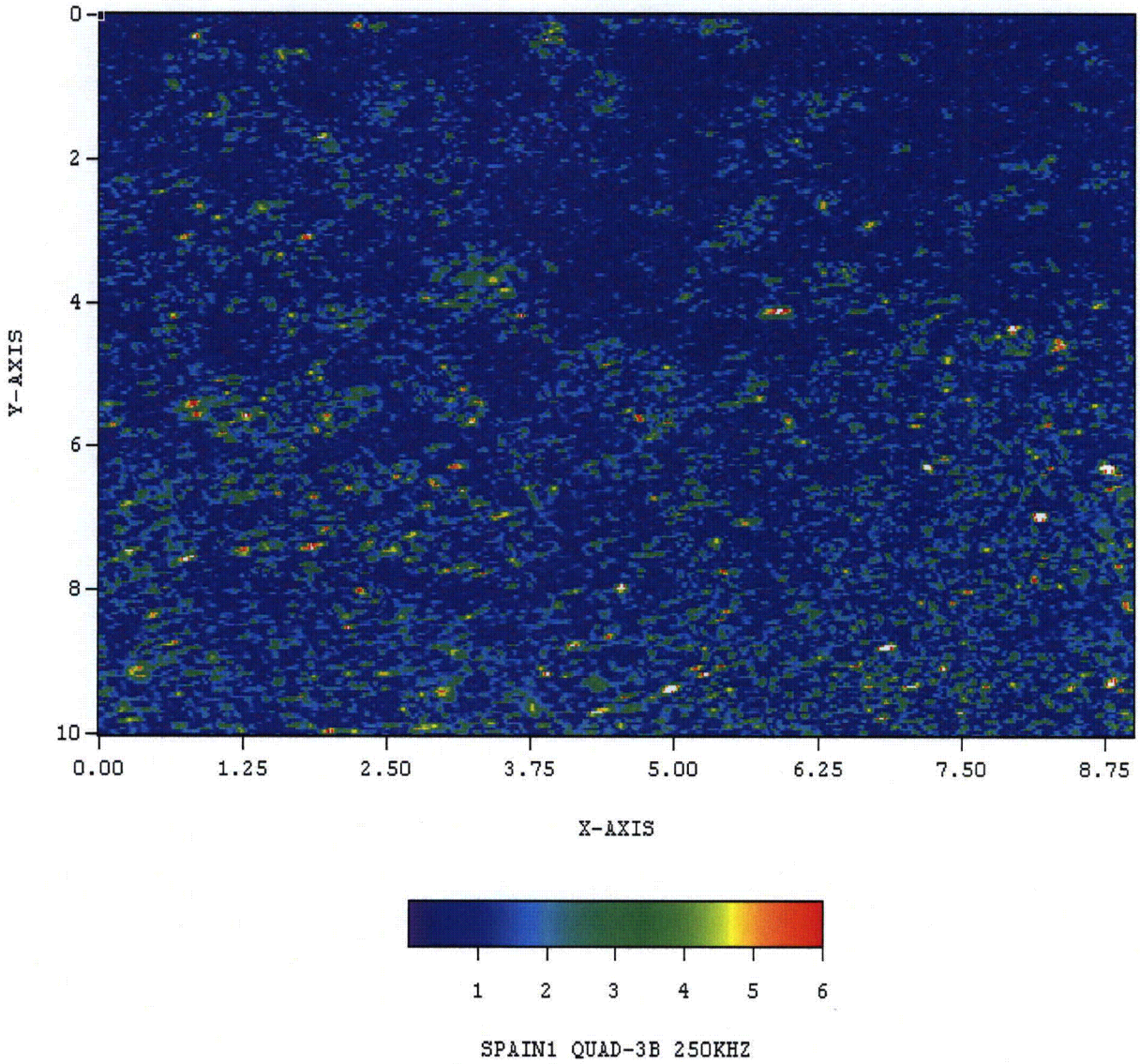

Figure B.26 Magnitude Plot of EPRI NDE Center Spanish Spool Piece Specimen (right side, Quadrant 3)

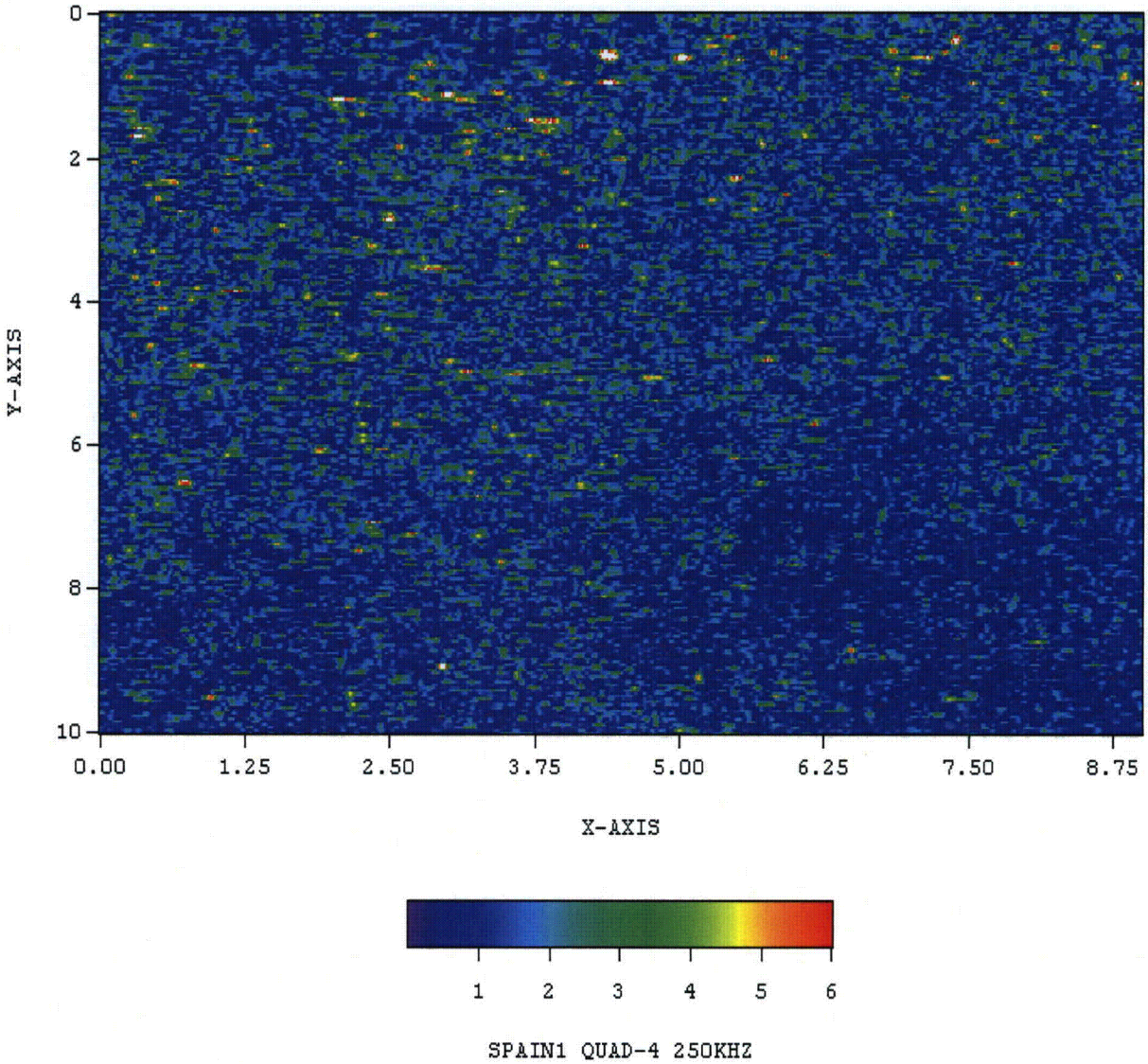

Figure B.27 Magnitude Plot of EPRI NDE Center Spanish Spool Piece Specimen (right side, Quadrant 4)

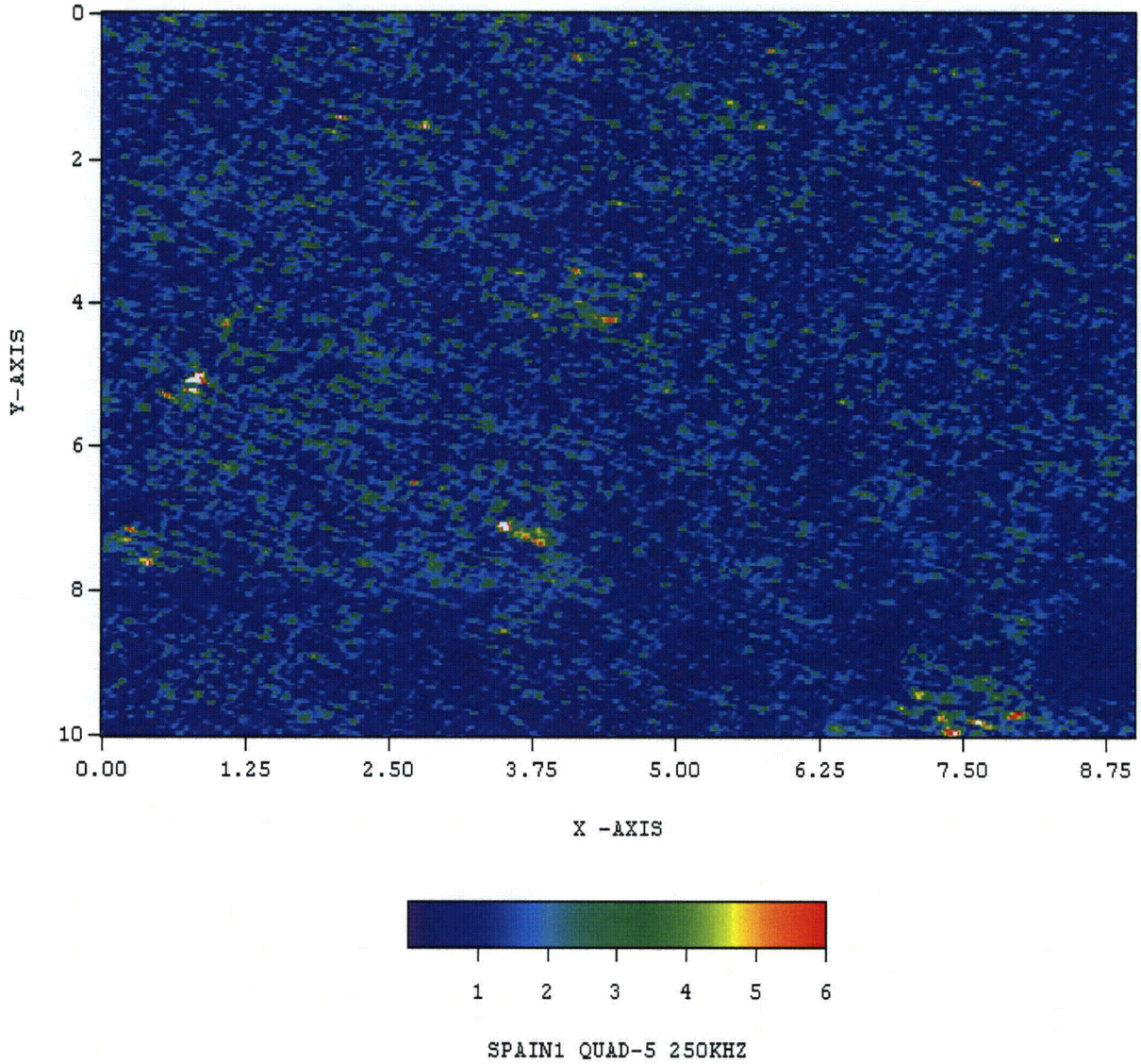

Figure B.28 Magnitude Plot of EPRI NDE Center Spanish Spool Piece Specimen (right side, Quadrant 5)

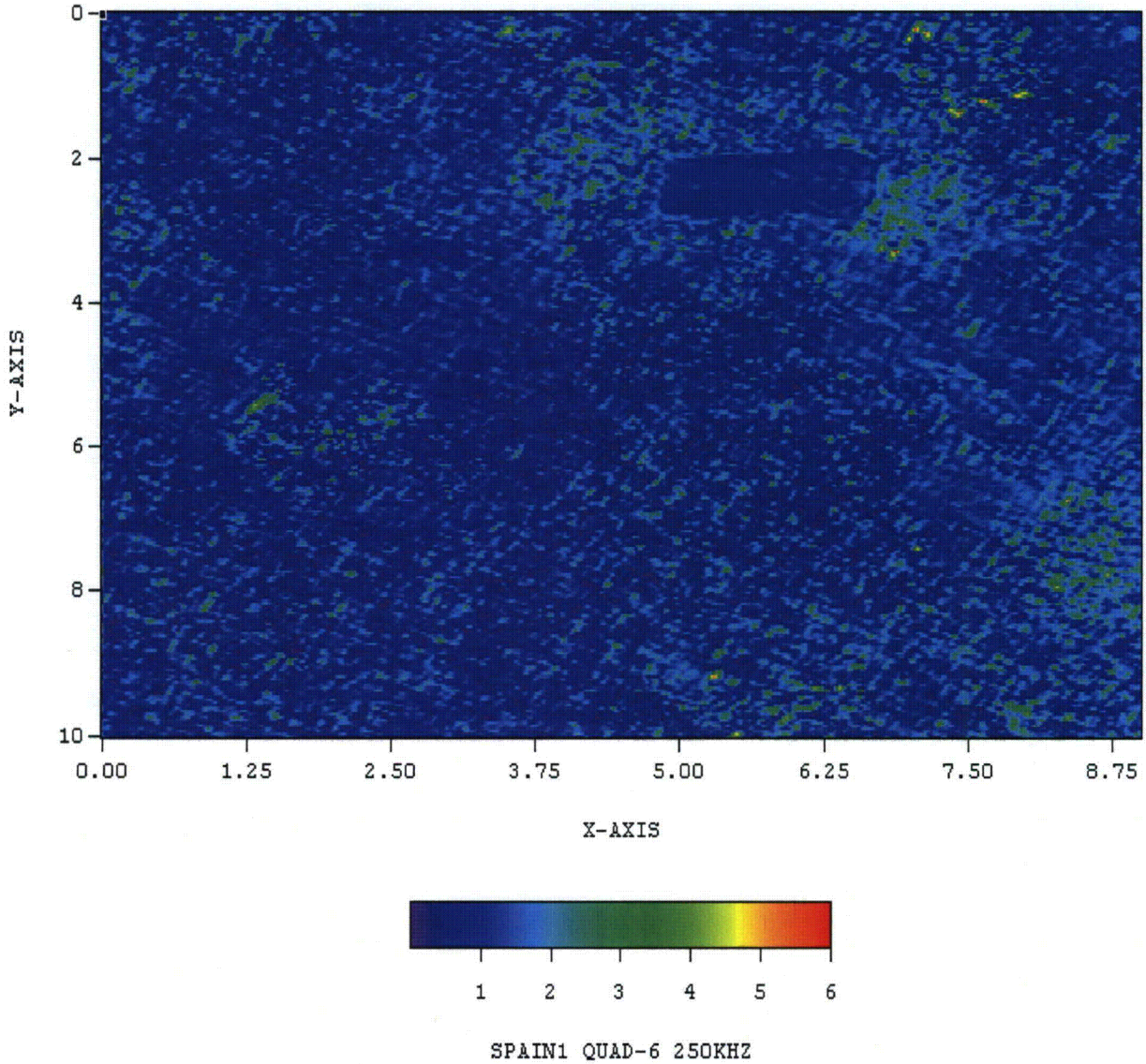

Figure B.29 Magnitude Plot of EPRI NDE Center Spanish Spool Piece Specimen (right side, Quadrant 6)

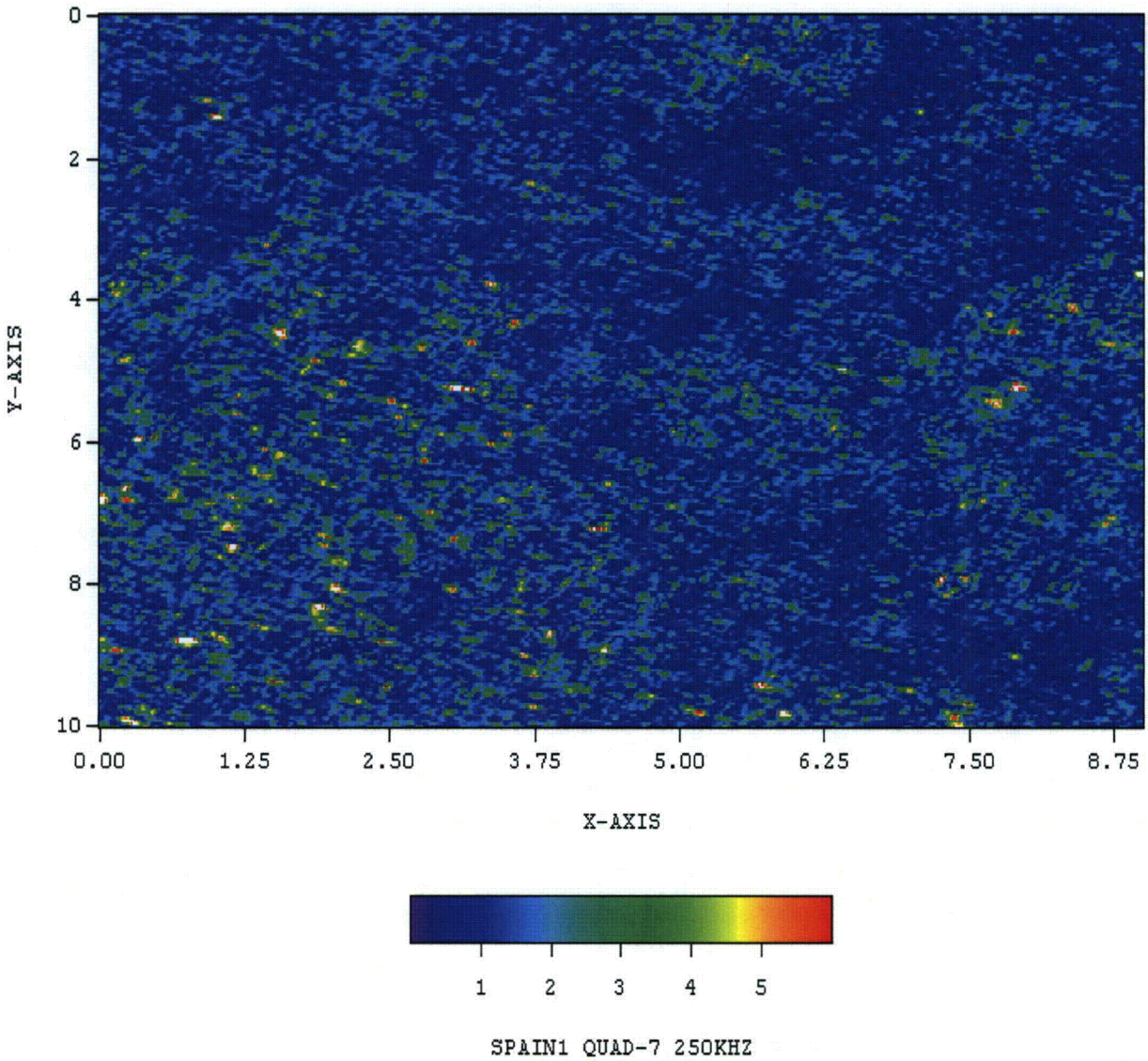

Figure B.30 Magnitude Plot of EPRI NDE Center Spanish Spool Piece Specimen (right side, Quadrant 7)

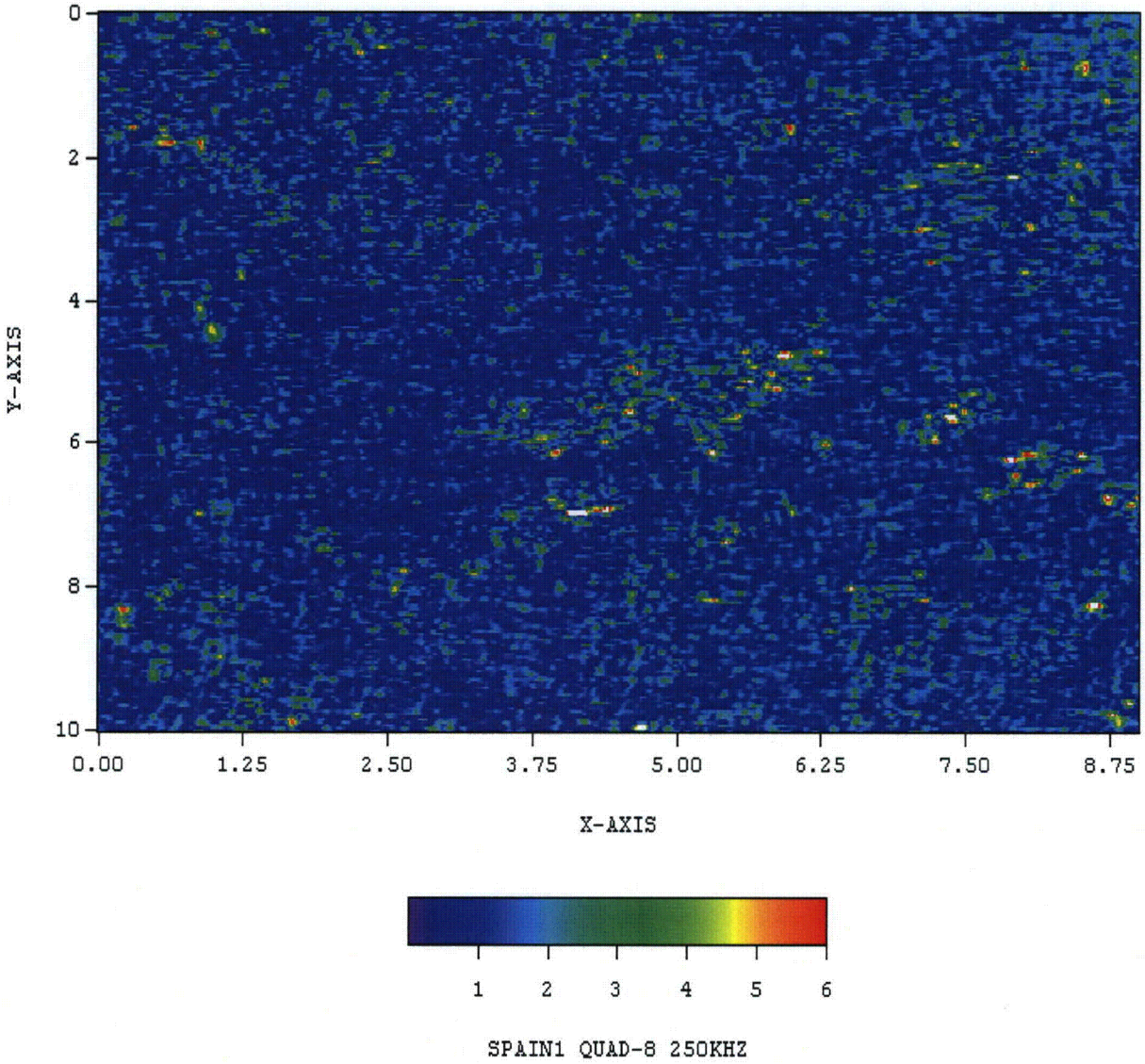

Figure B.31 Magnitude Plot of EPRI NDE Center Spanish Spool Piece Specimen (right side, Quadrant 8)

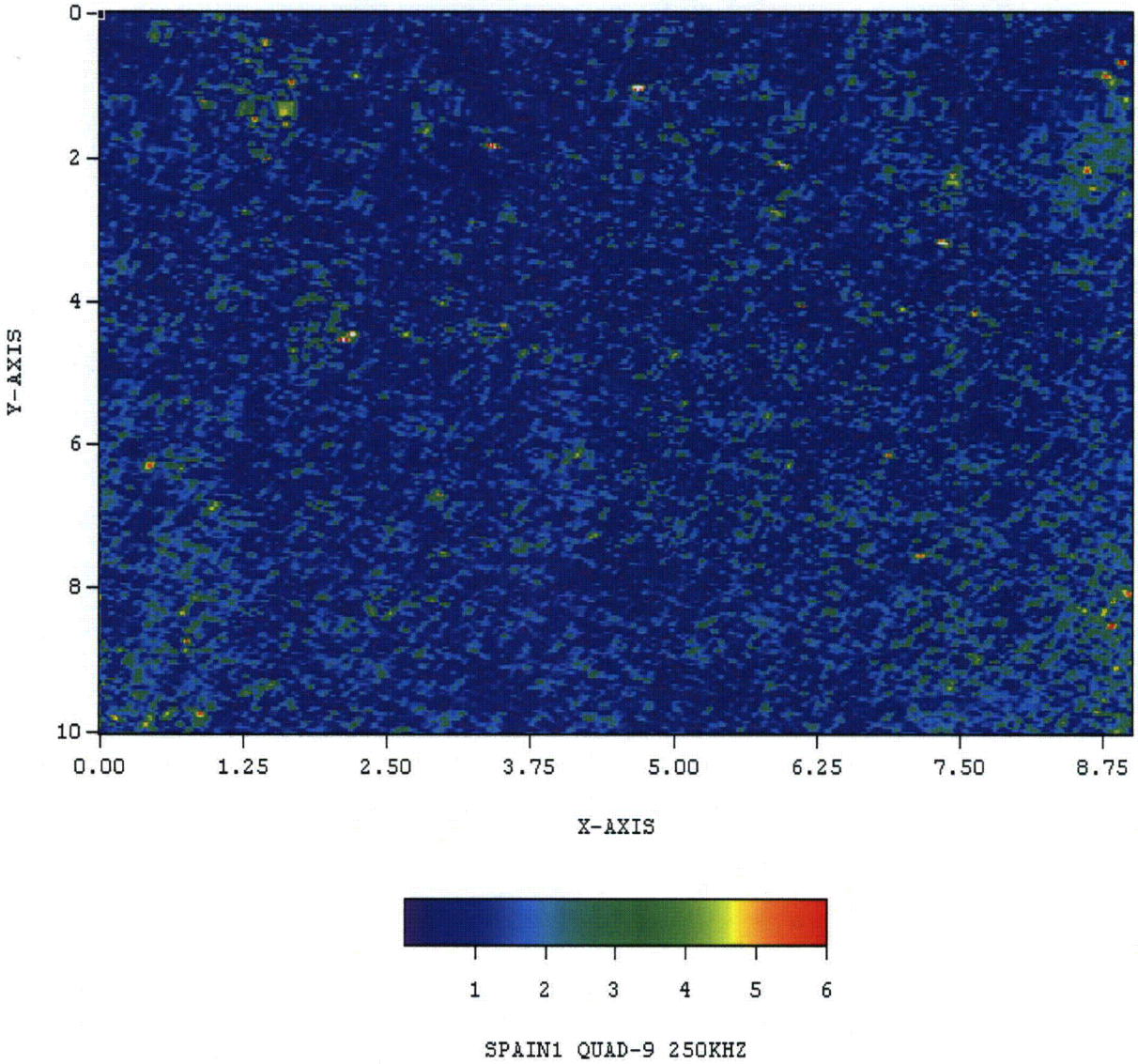

Figure B.32 Magnitude Plot of EPRI NDE Center Spanish Spool Piece Specimen (right side, Quadrant 9)

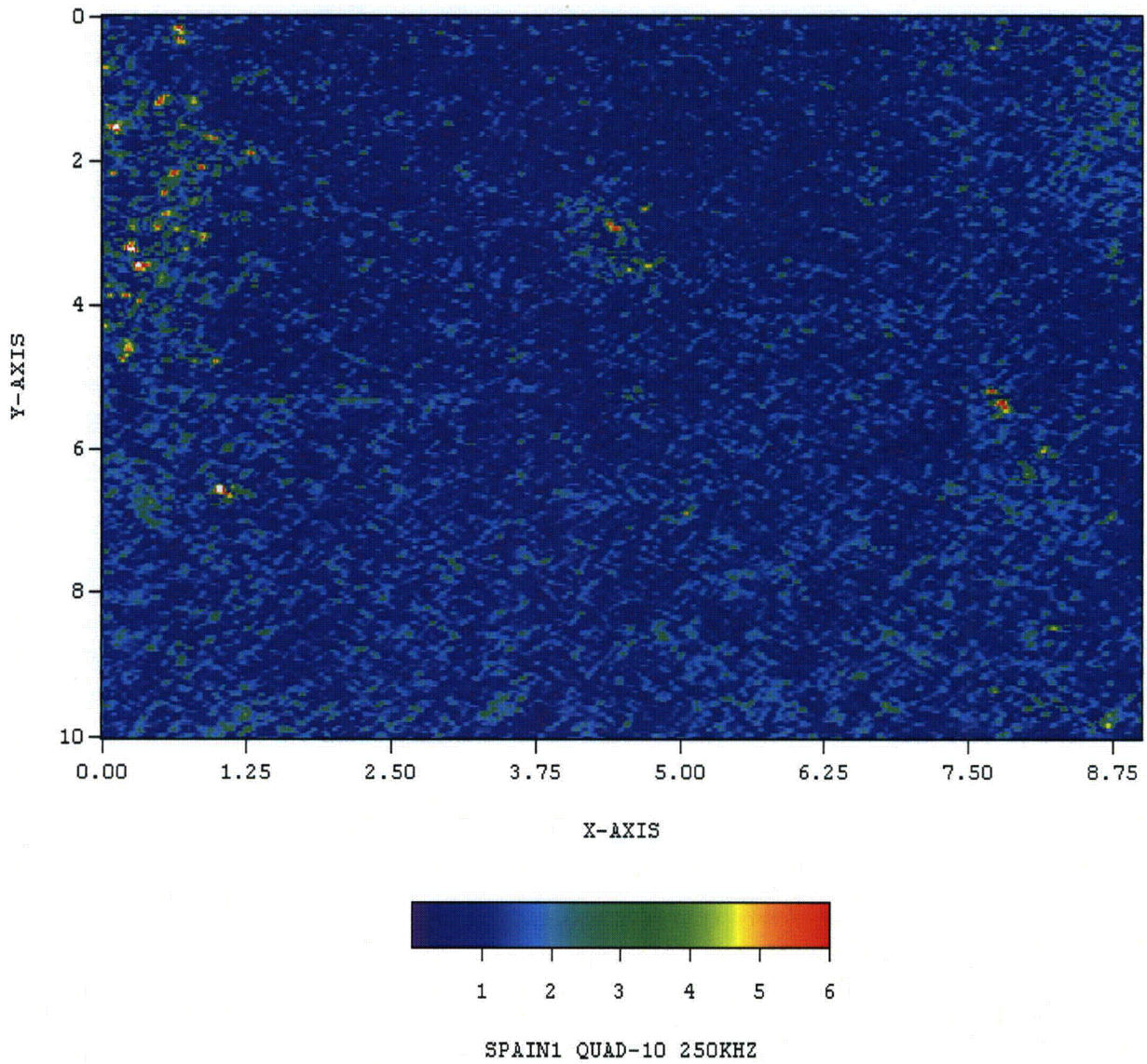

Figure B.33 Magnitude Plot of EPRI NDE Center Spanish Spool Piece Specimen (right side, Quadrant 10)

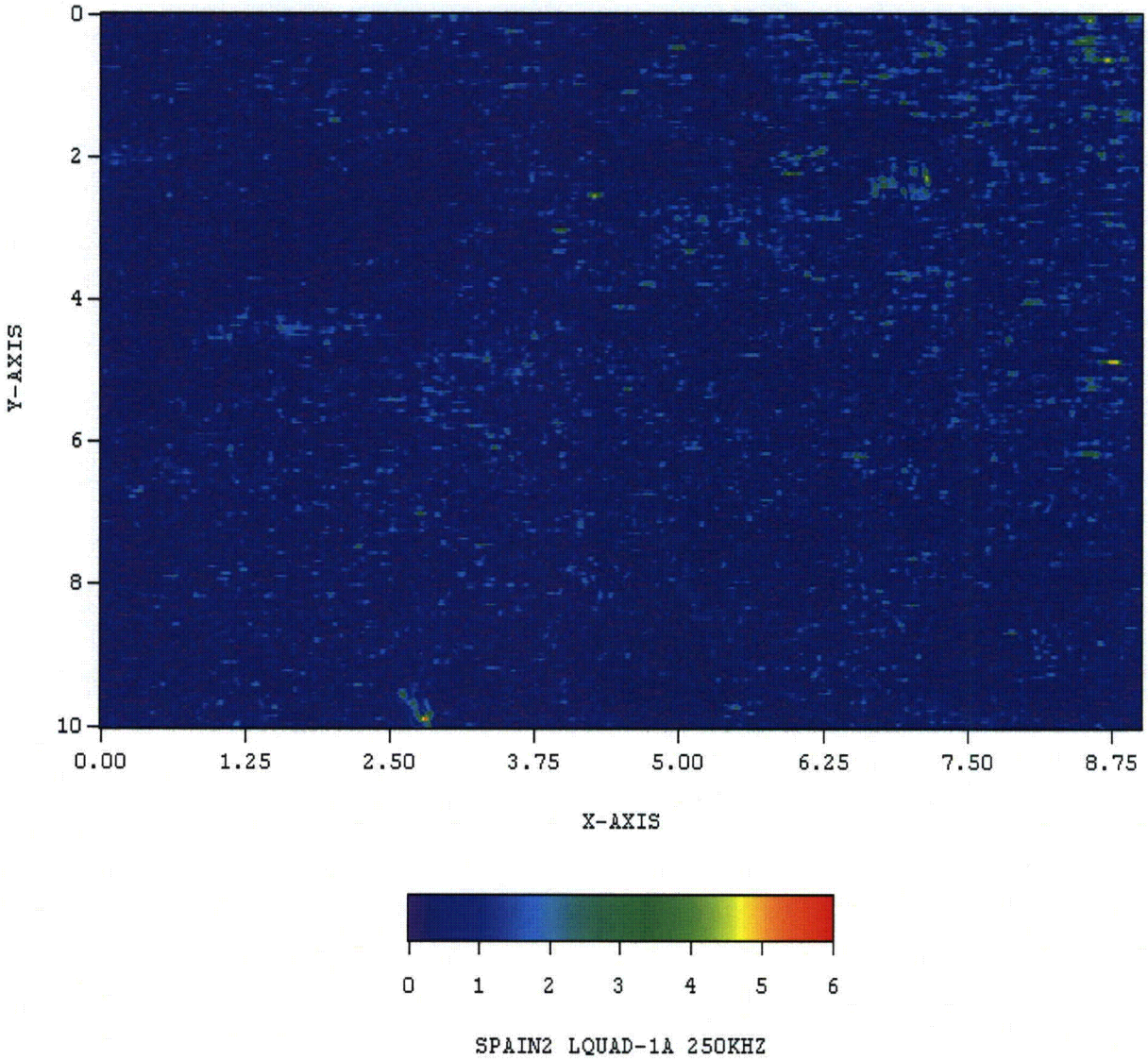

Figure B.34 Magnitude Plot of EPRI NDE Center Spanish Spool Piece Specimen (left side, Quadrant 1)

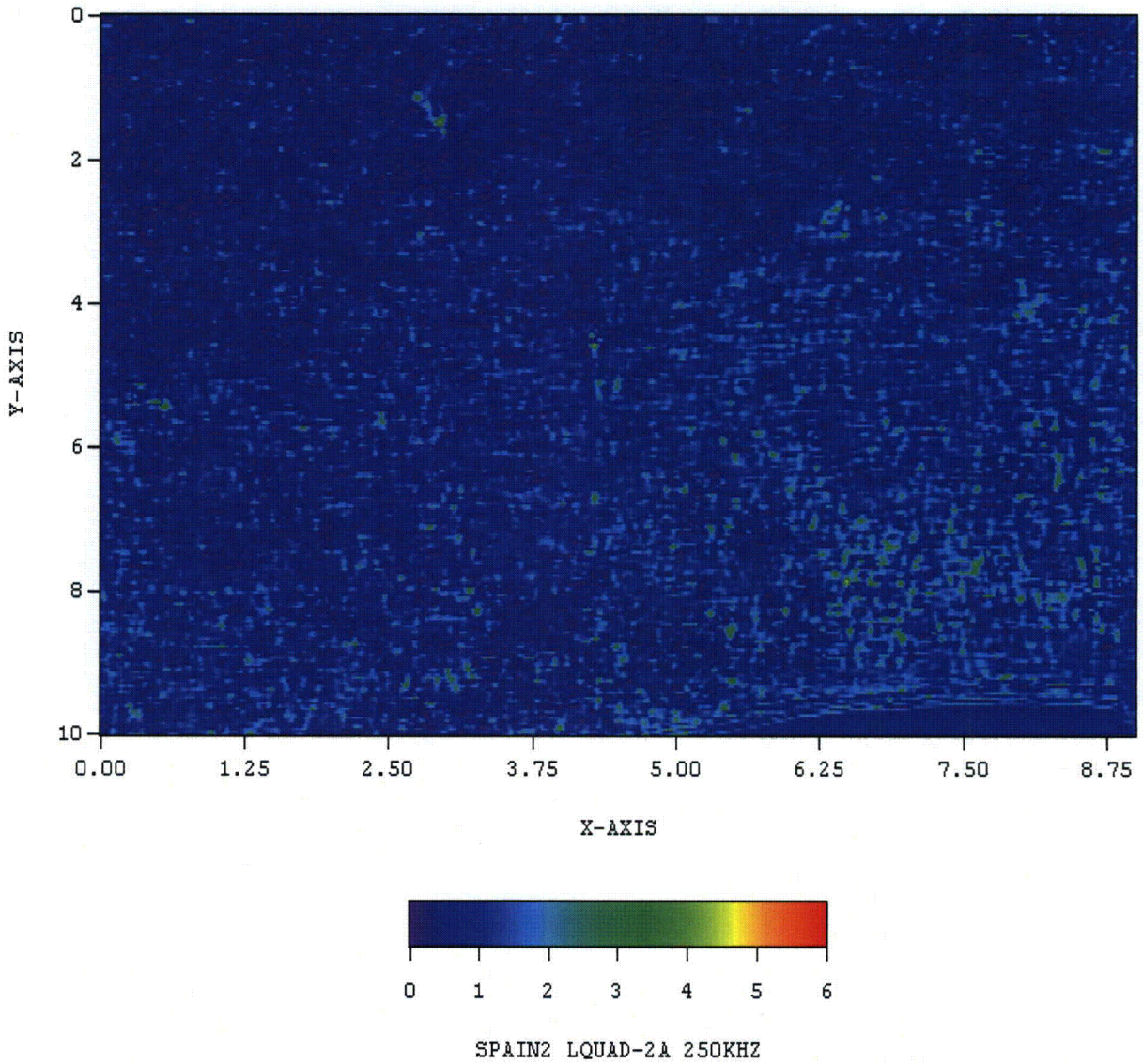

Figure B.35 Magnitude Plot of EPRI NDE Center Spanish Spool Piece Specimen (left side, Quadrant 2)

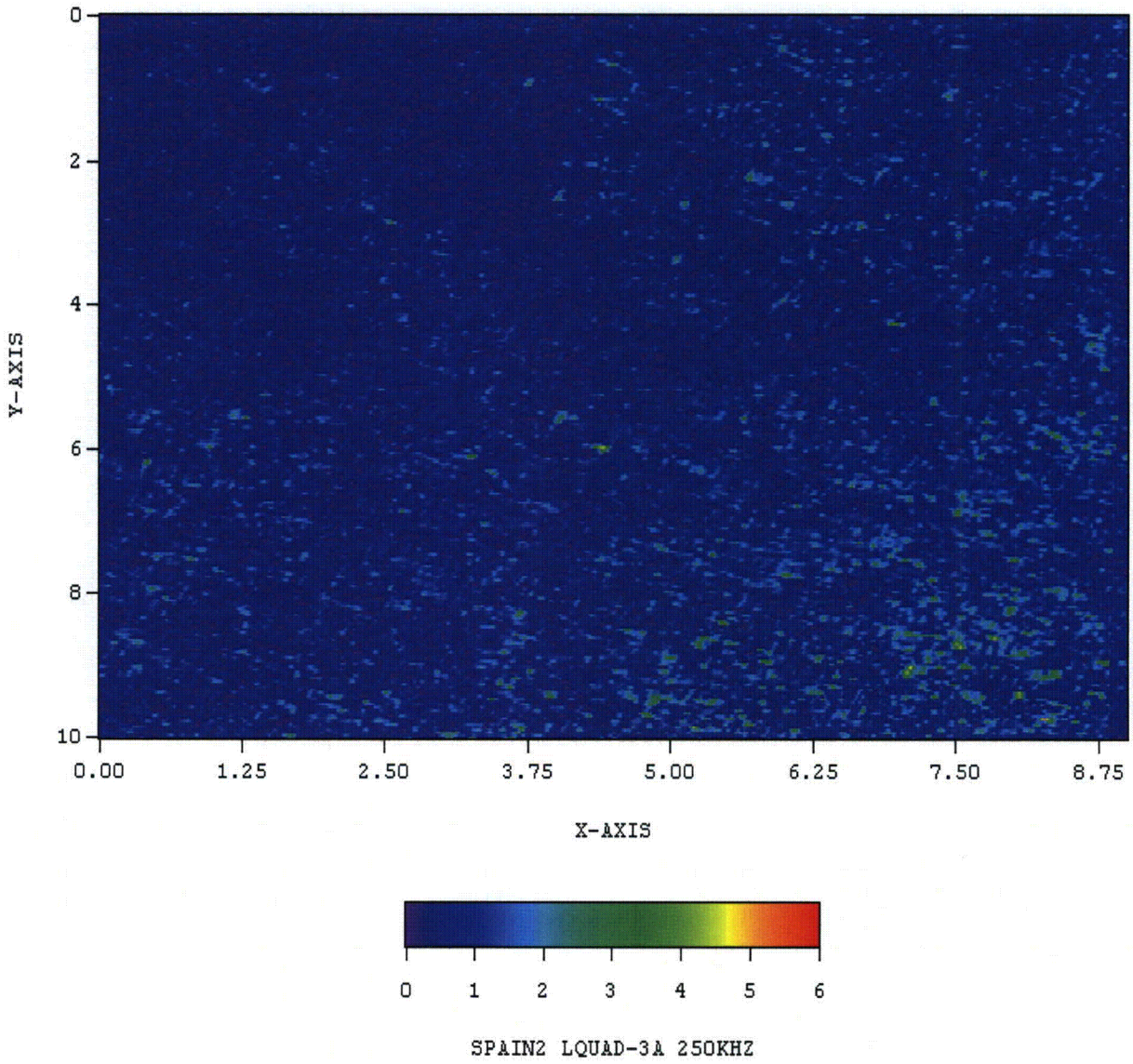

Figure B.36 Magnitude Plot of EPRI NDE Center Spanish Spool Piece Specimen (left side, Quadrant 3)

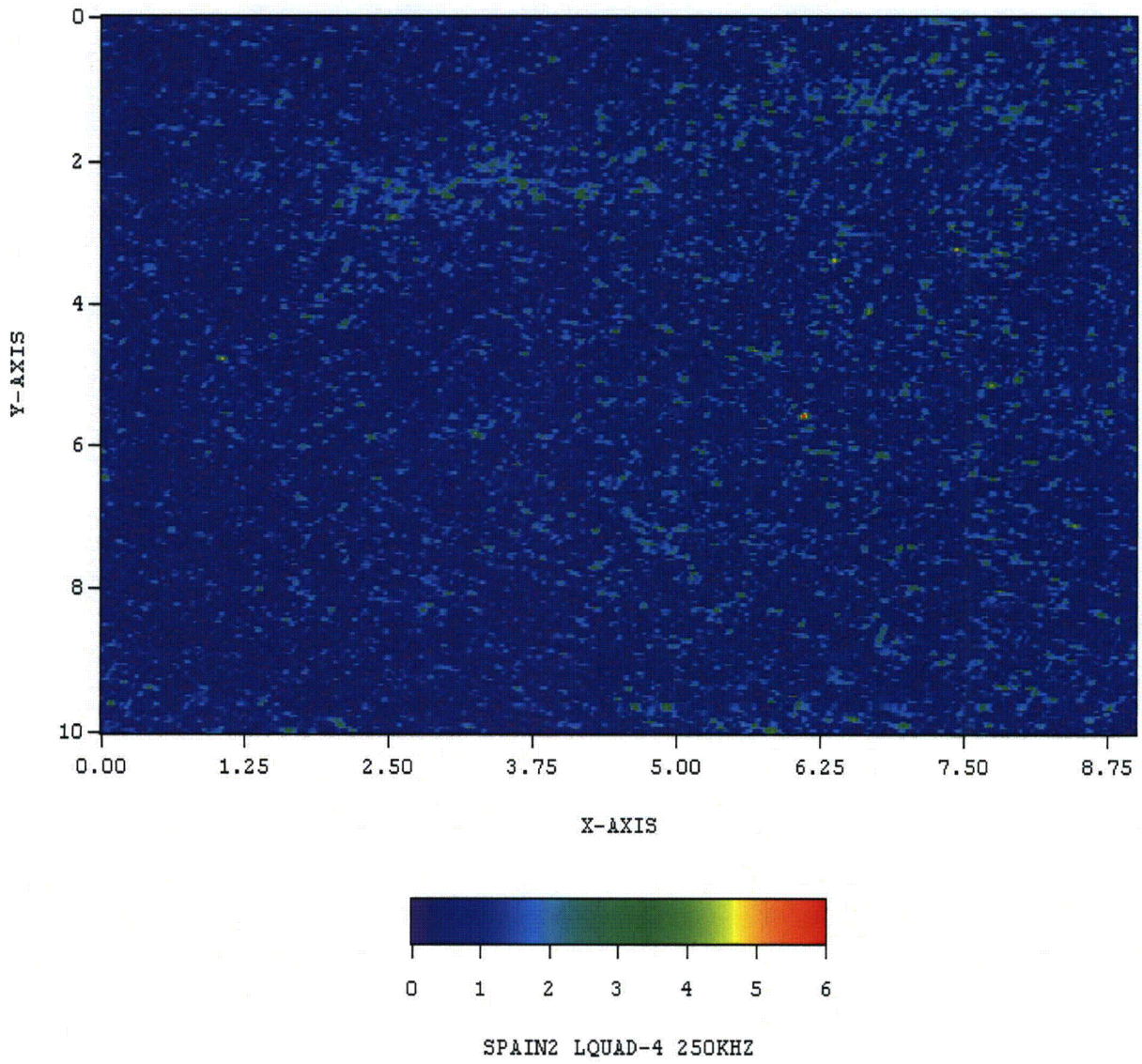

Figure B.37 Magnitude Plot of EPRI NDE Center Spanish Spool Piece Specimen (left side, Quadrant 4)

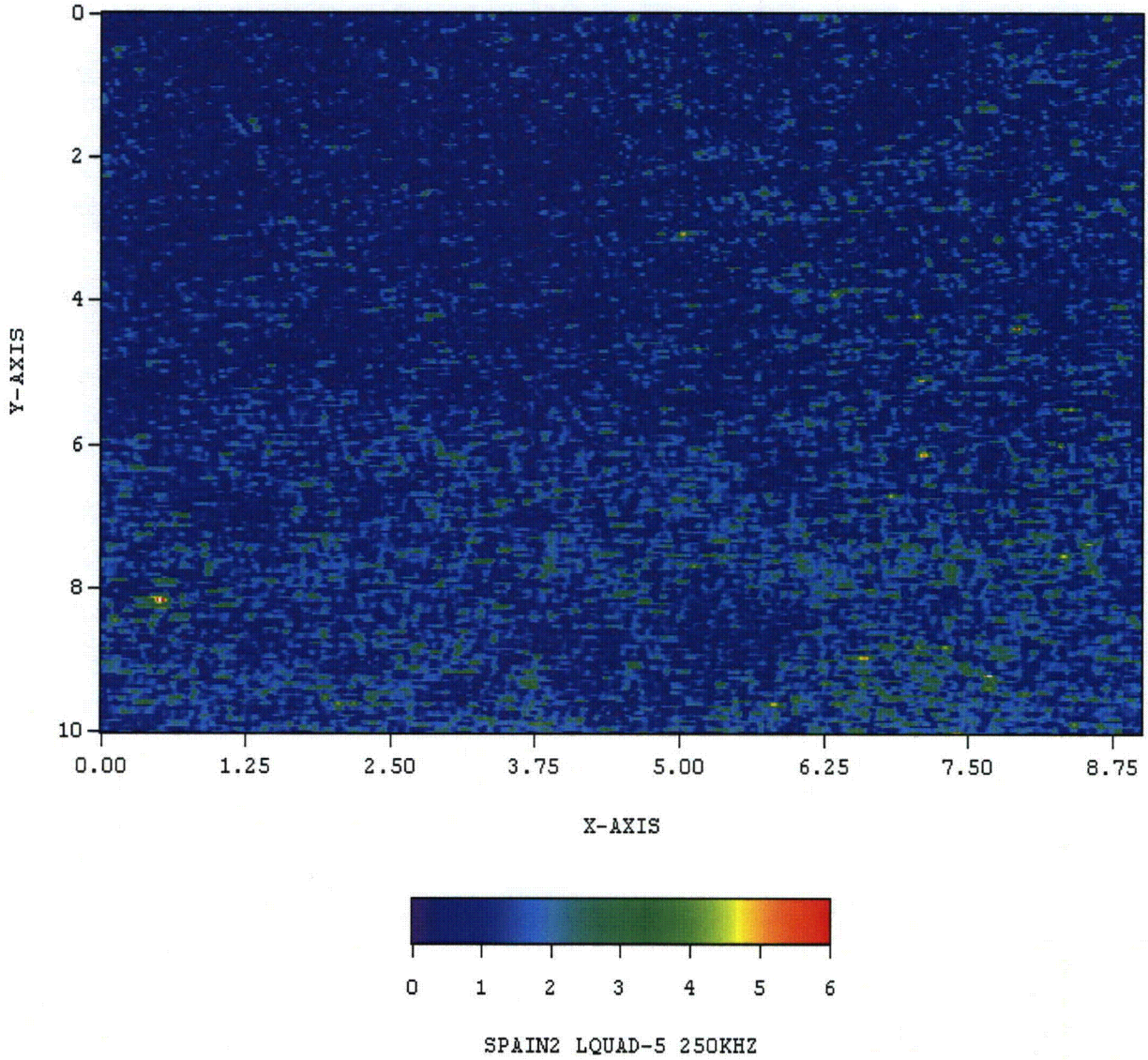

Figure B.38 Magnitude Plot of EPRI NDE Center Spanish Spool Piece Specimen (left side, Quadrant 5)

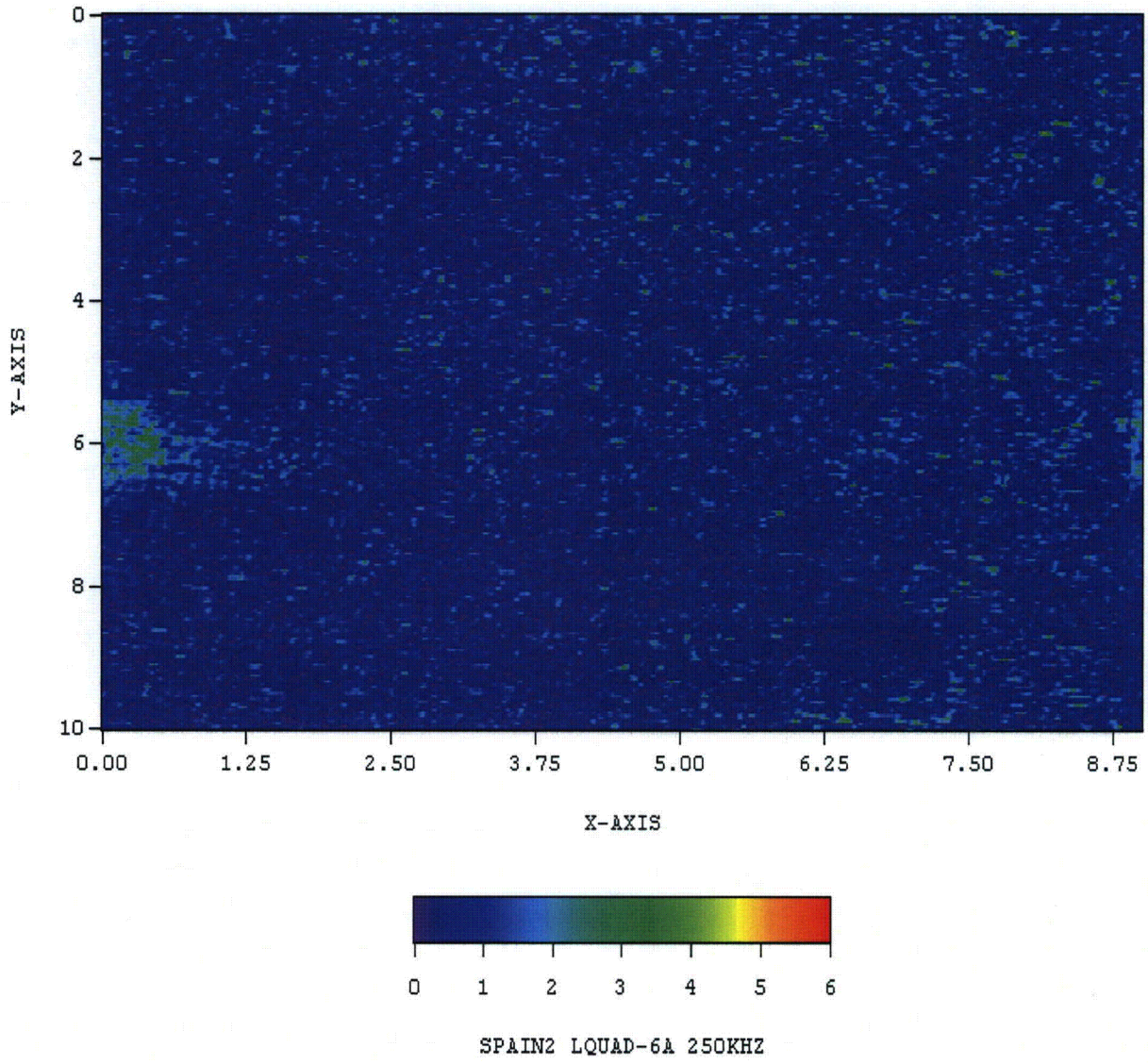

Figure B.39 Magnitude Plot of EPRI NDE Center Spanish Spool Piece Specimen (left side, Quadrant 6)

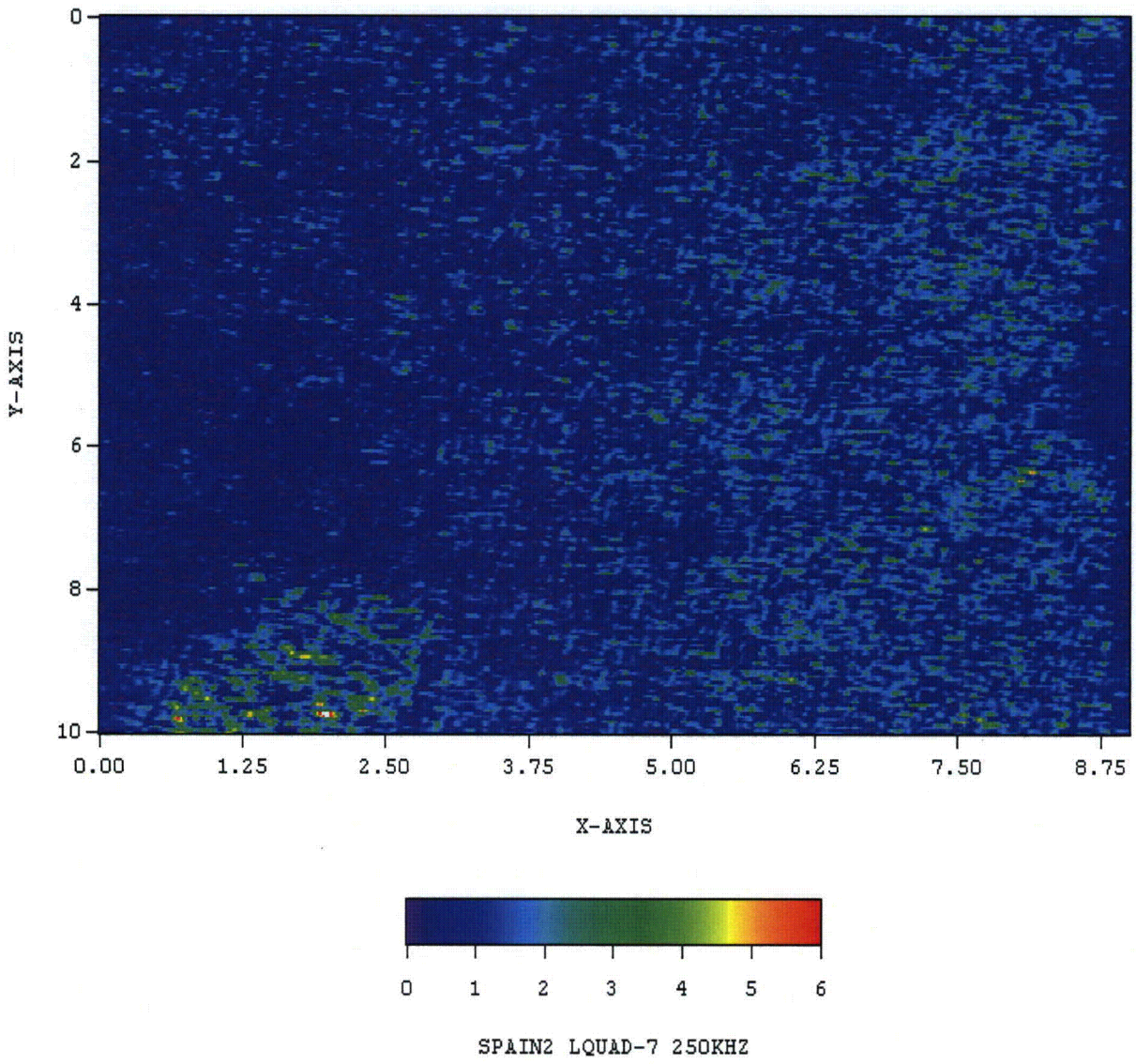

Figure B.40 Magnitude Plot of EPRI NDE Center Spanish Spool Piece Specimen (left side, Quadrant 7)

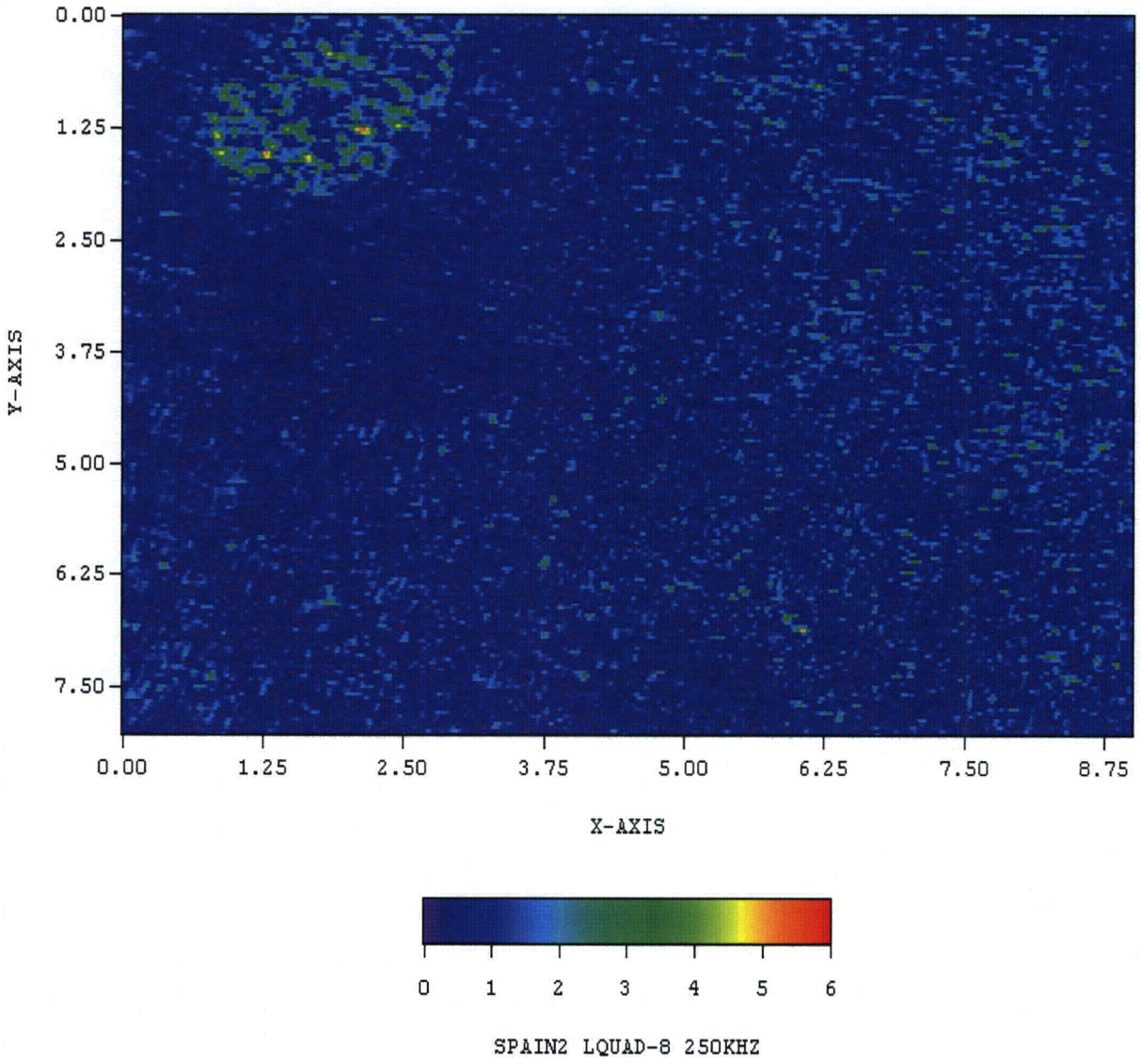

Figure B.41 Magnitude Plot of EPRI NDE Center Spanish Spool Piece Specimen (left side, Quadrant 8)

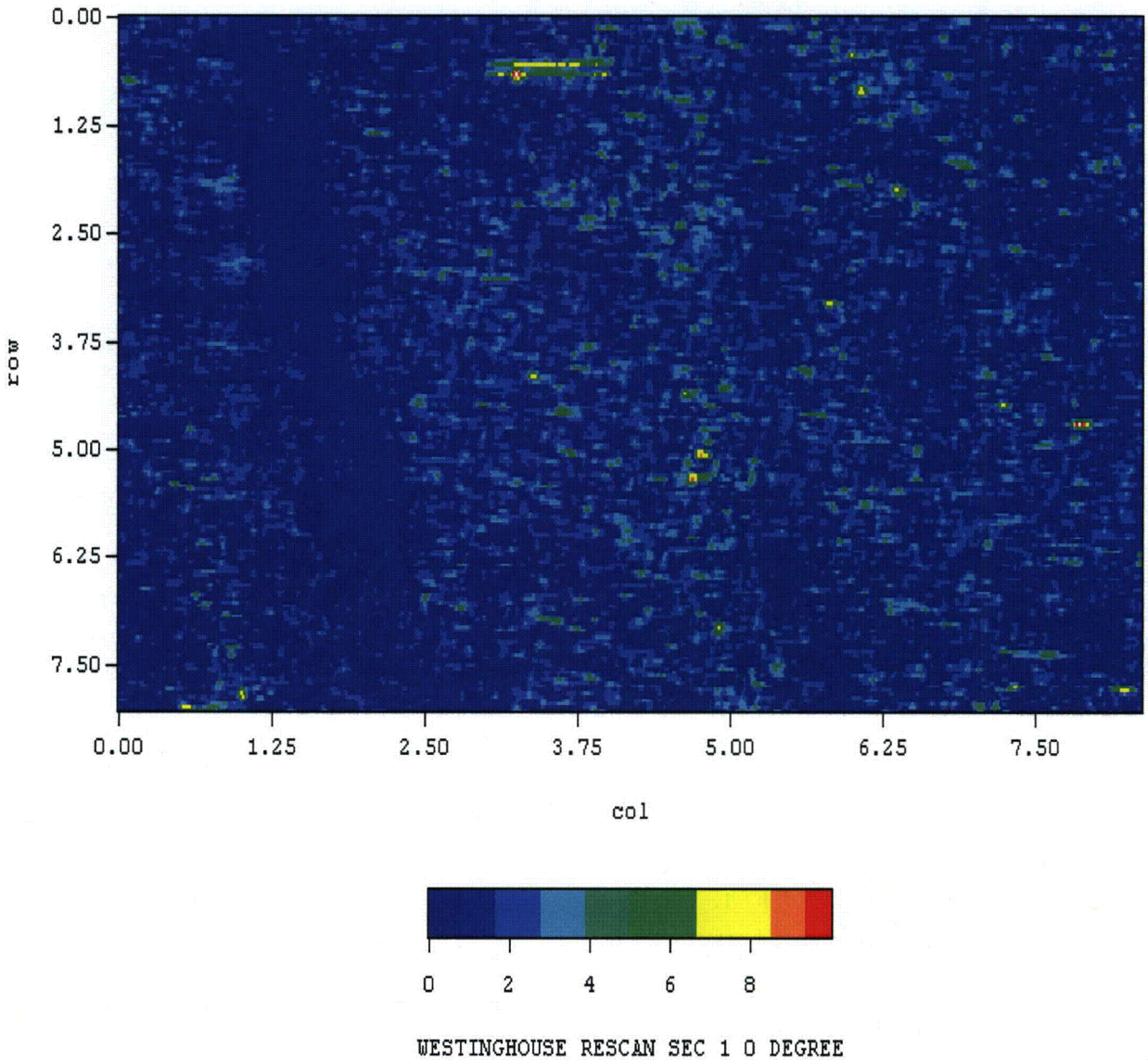

Figure B.42 Magnitude Plot of Westinghouse Spool Piece Specimen Quadrant 1

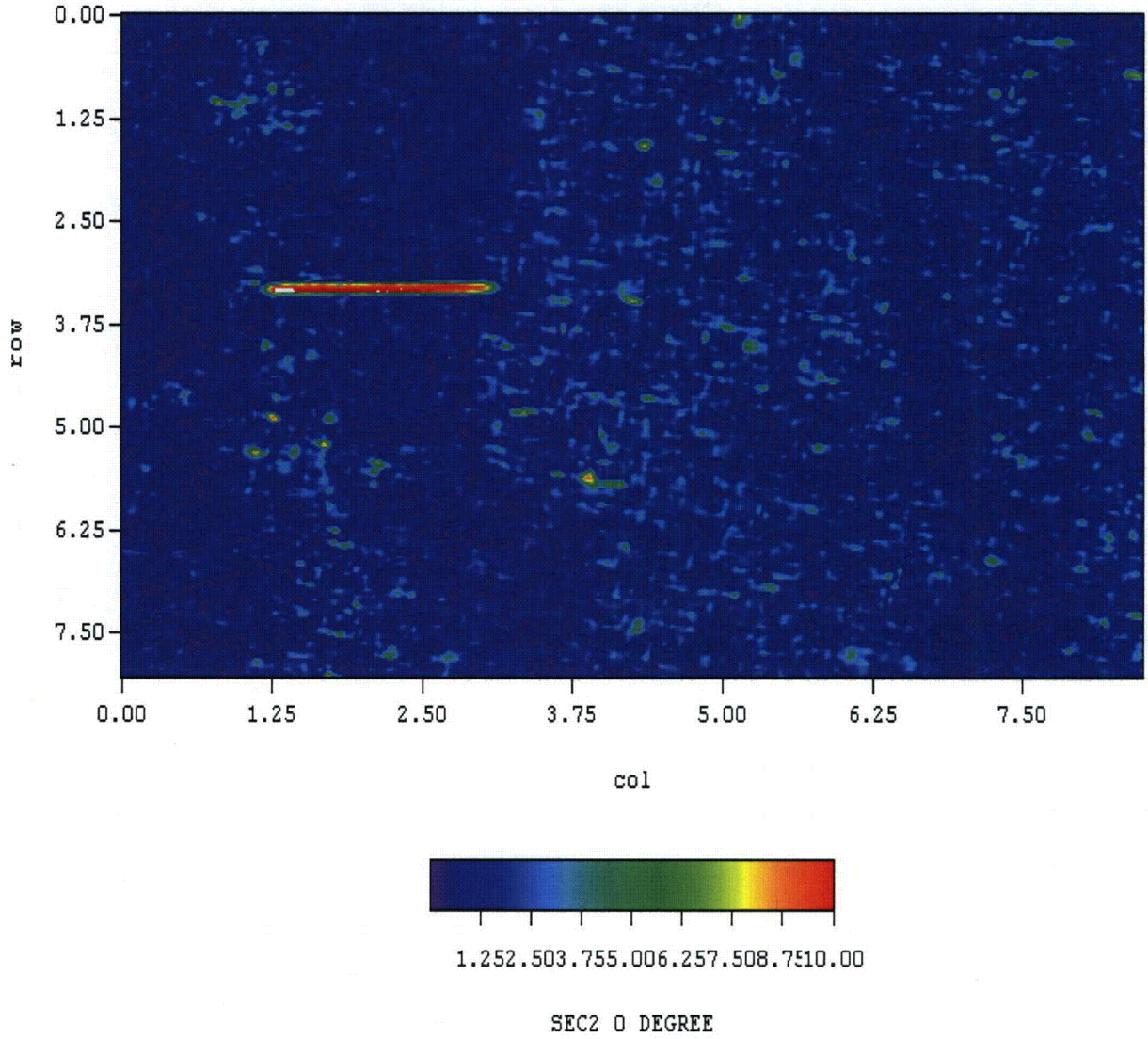

Figure B.43 Magnitude Plot of Westinghouse Spool Piece Specimen Quadrant 2

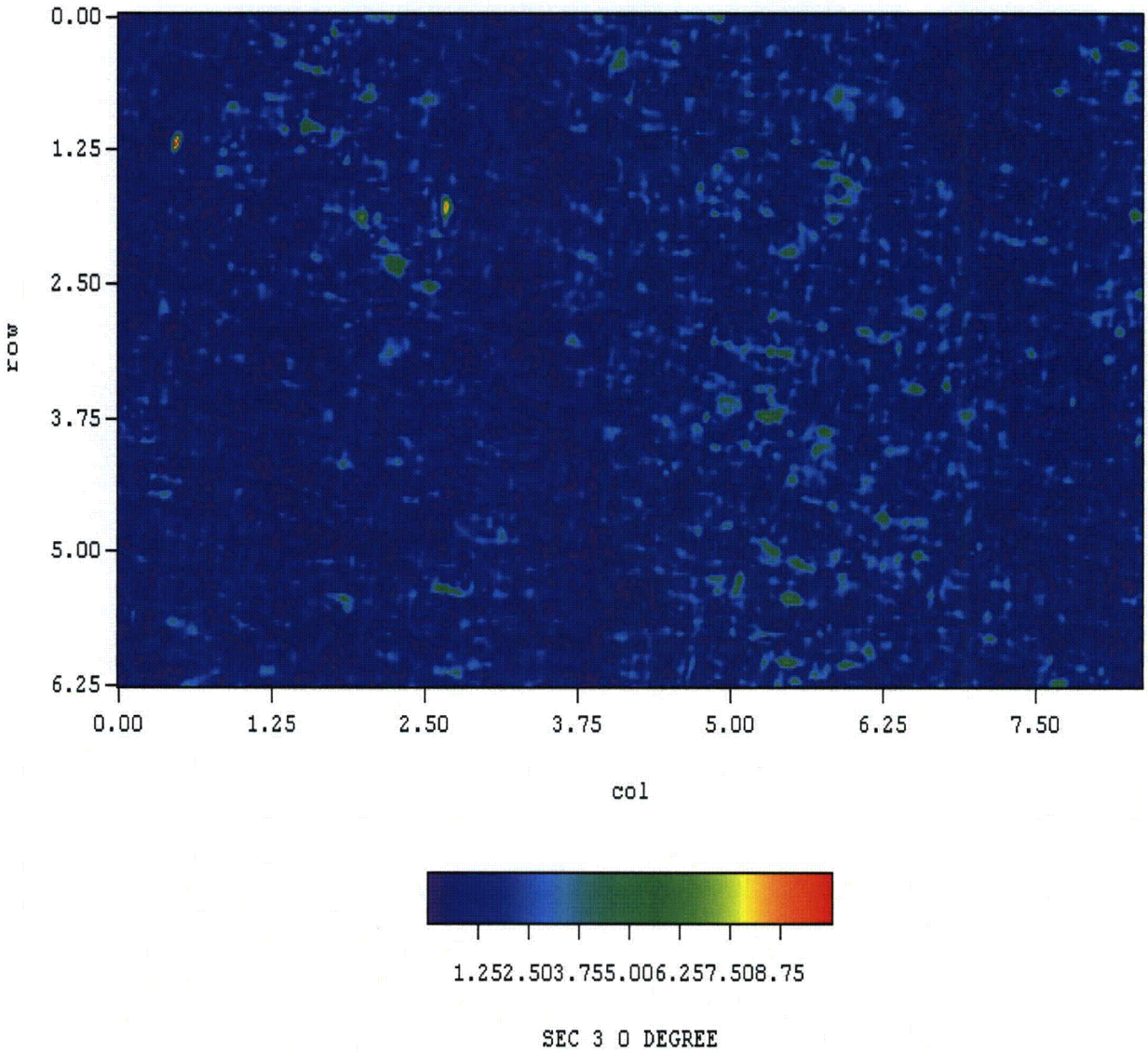

Figure B.44 Magnitude Plot of Westinghouse Spool Piece Specimen Quadrant 3

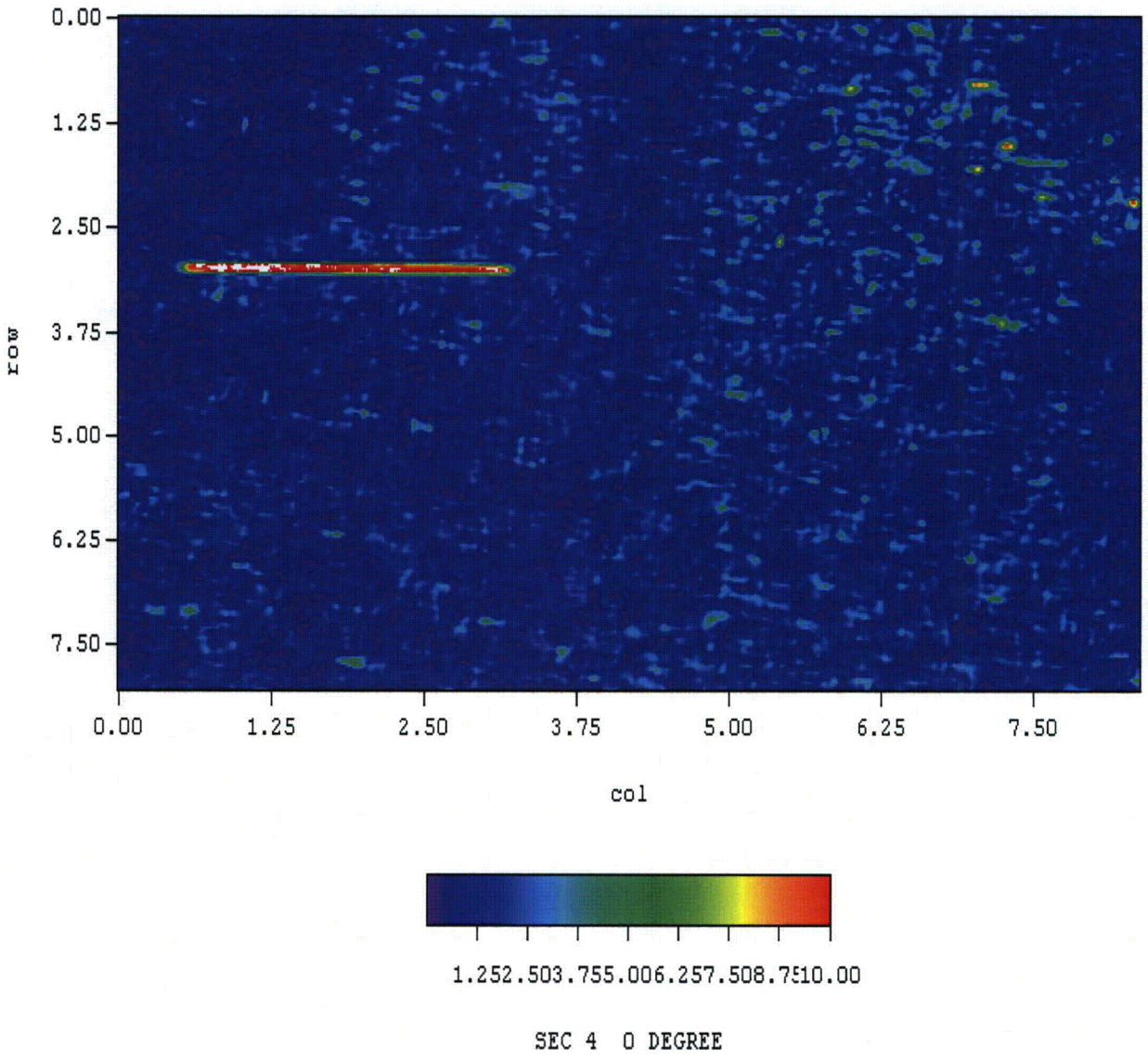

Figure B.45 Magnitude Plot of Westinghouse Spool Piece Specimen Quadrant 4

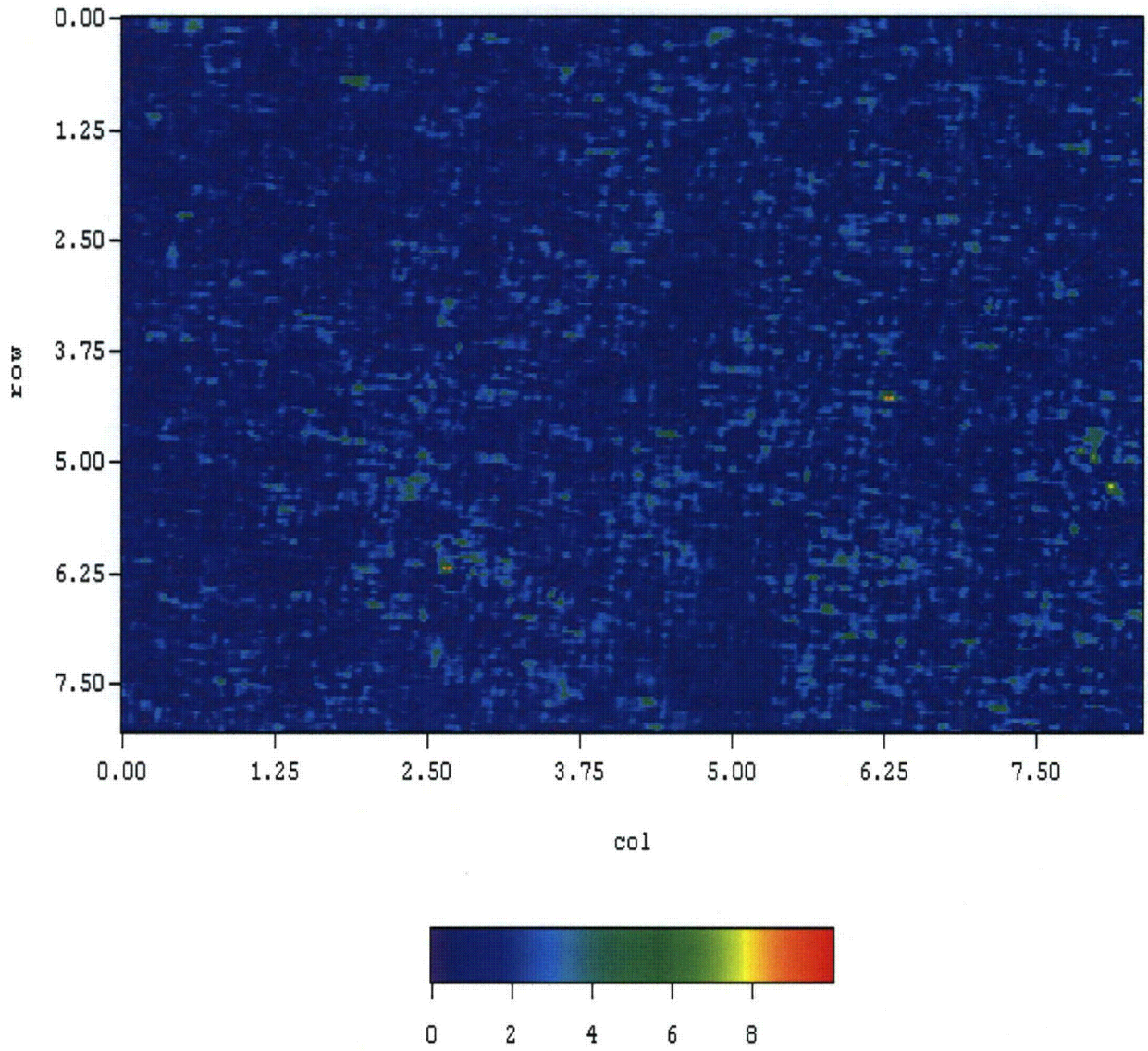

Figure B.46 Magnitude Plot of Westinghouse Spool Piece Specimen Quadrant 5

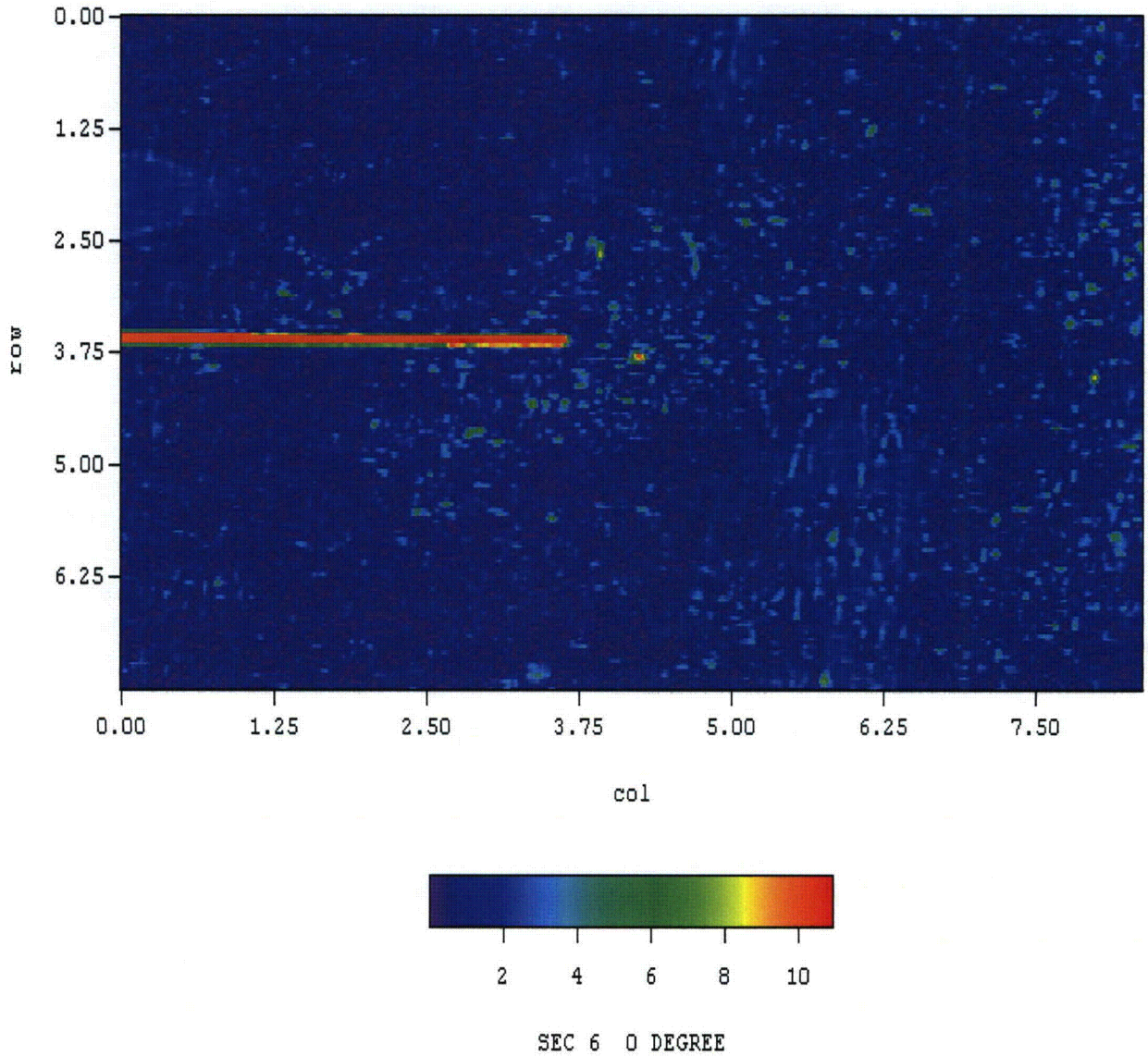

Figure B.47 Magnitude Plot of Westinghouse Spool Piece Specimen Quadrant 6

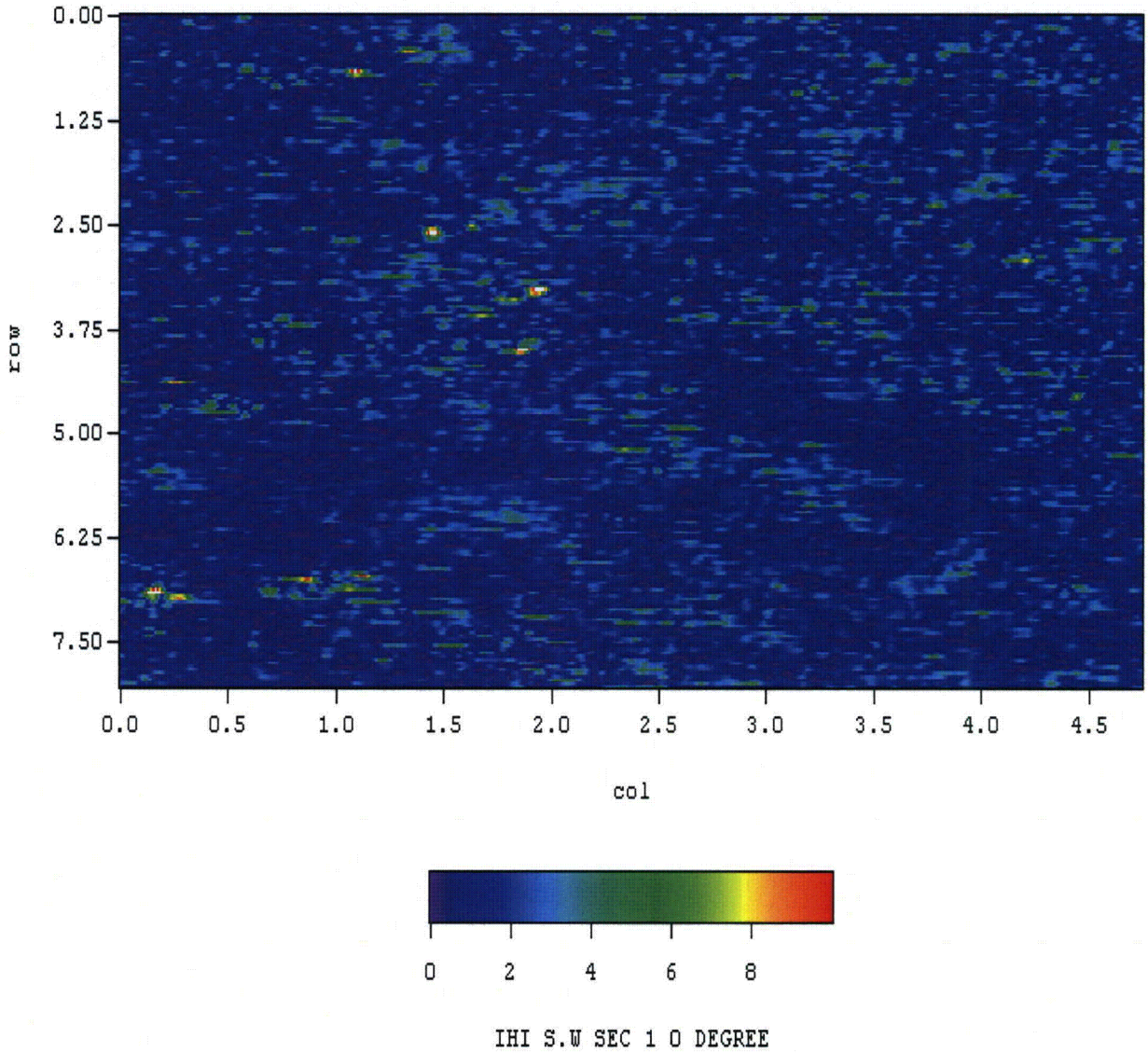

Figure B.48 Magnitude Plot of IHI Southwest Technologies Inc. Spool Piece Specimen Quadrant 1

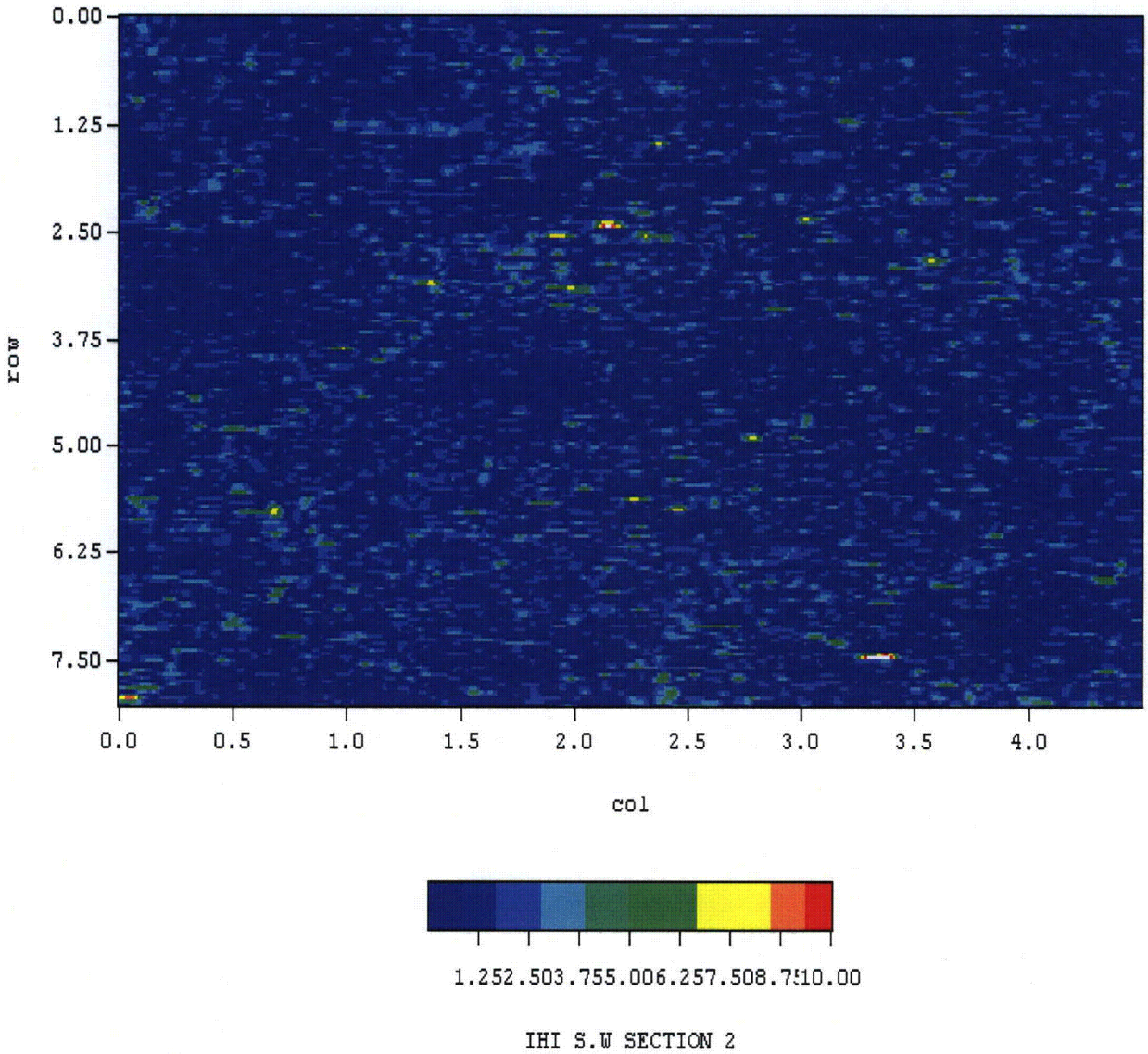

Figure B.49 Magnitude Plot of IHI Southwest Technologies Inc. Spool Piece Specimen Quadrant 2

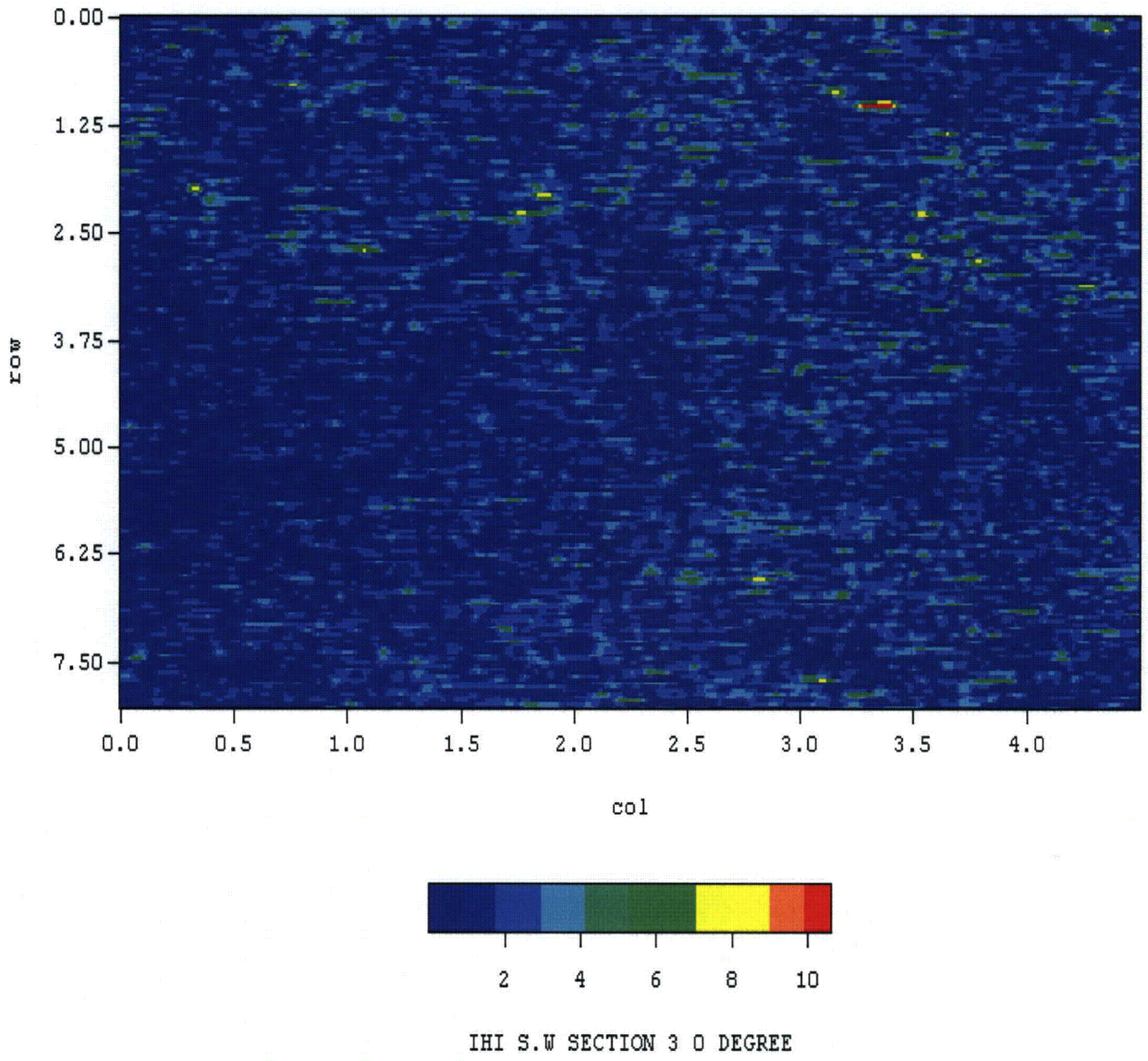

Figure B.50 Magnitude Plot of IHI Southwest Technologies Inc. Spool Piece Specimen Quadrant 3

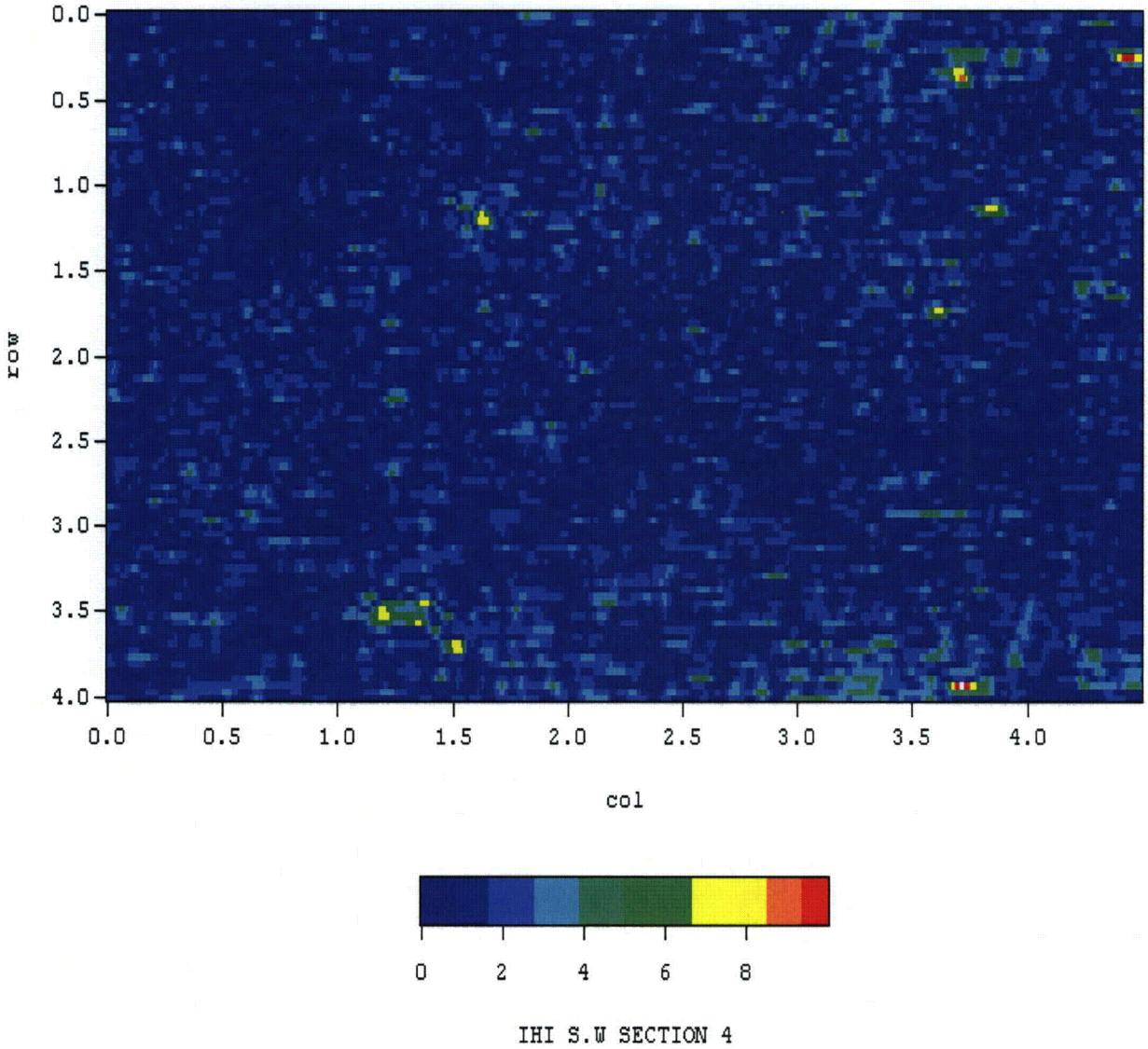

Figure B.51 Magnitude Plot of IHI Southwest Technologies Inc. Spool Piece Specimen Quadrant 4

Appendix C

Phase Plots from Eddy Current Data

Appendix C

Phase Plots from Eddy Current Data

All plots in Appendix C have vertical and horizontal axes that are in units of inches (25.4 mm).

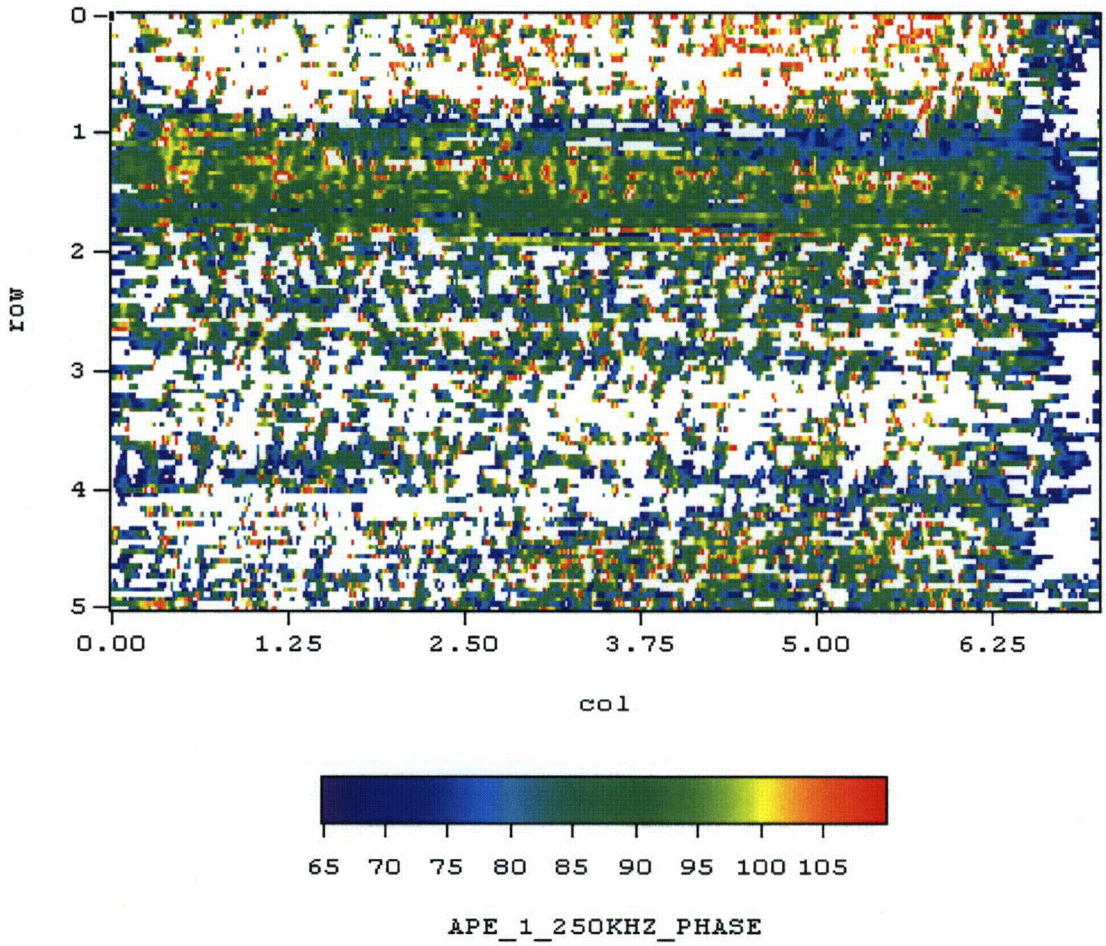

Figure C.1 Phase Response Plot of WOG Specimen APE-1

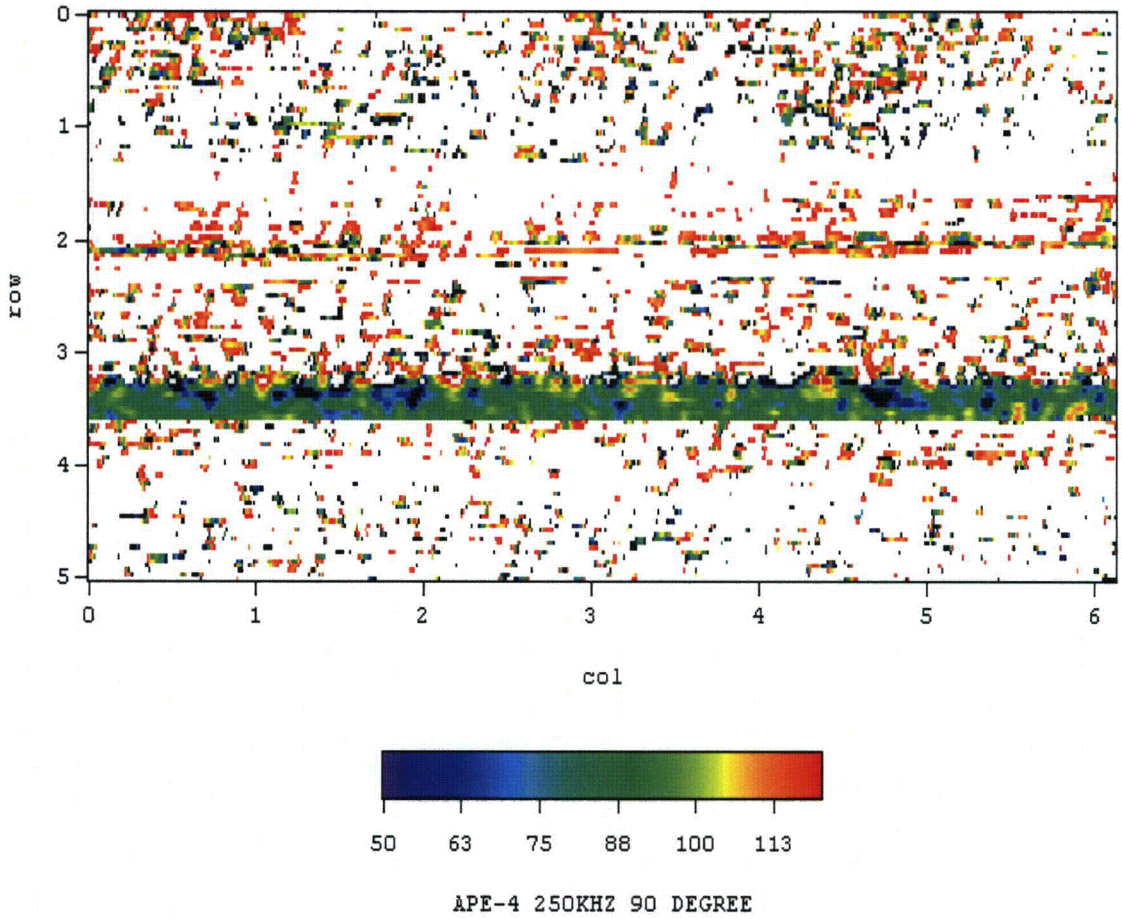

Figure C.2 Phase Response Plot of WOG Specimen APE-4

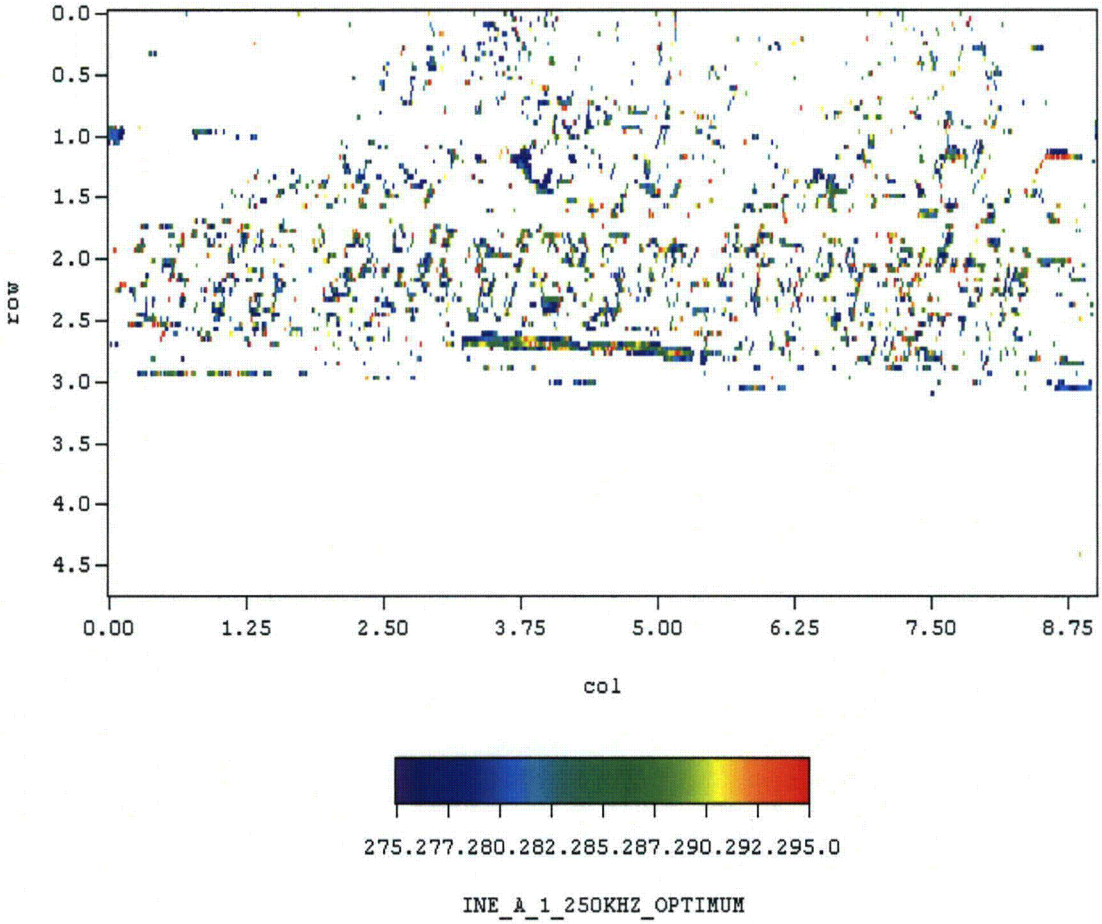

Figure C.3 Phase Response Plot of WOG Specimen INE-A-1

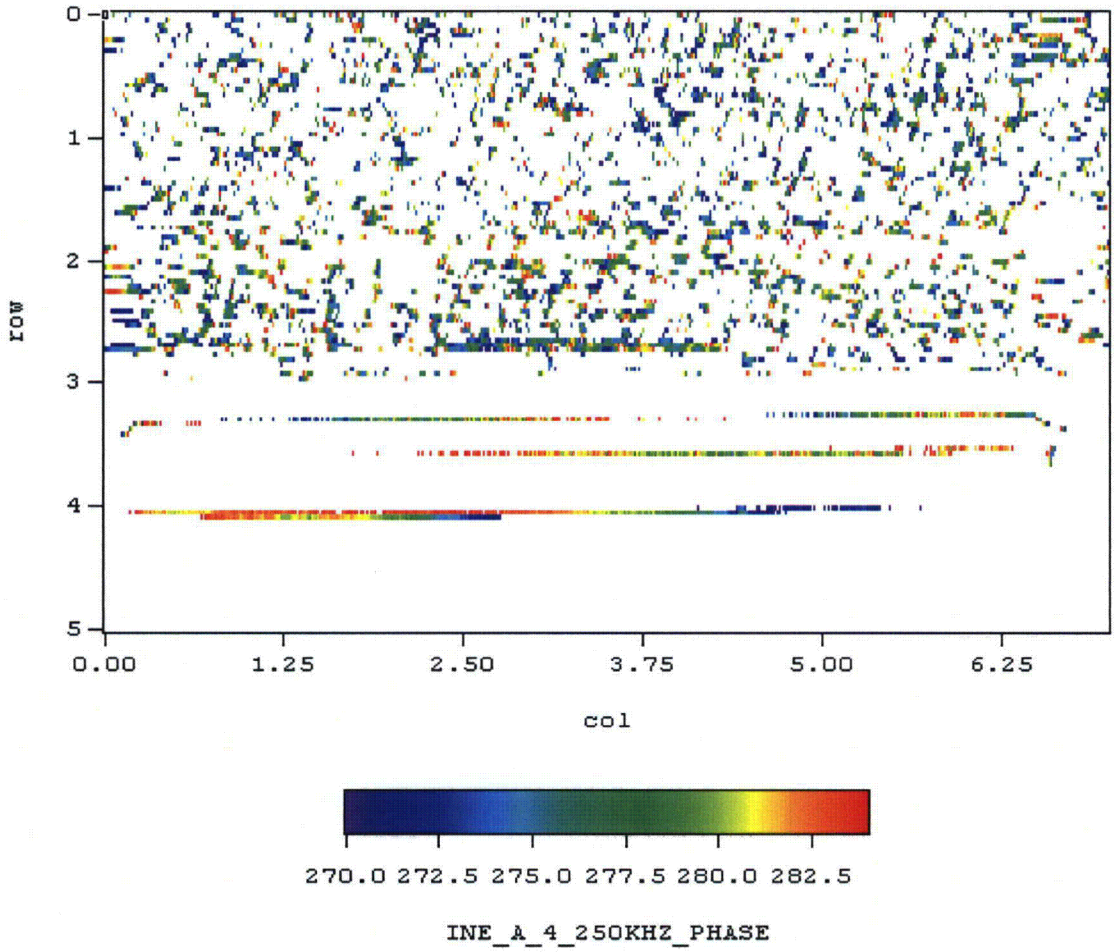

Figure C.4 Phase Response Plot of WOG Specimen INE-A-4

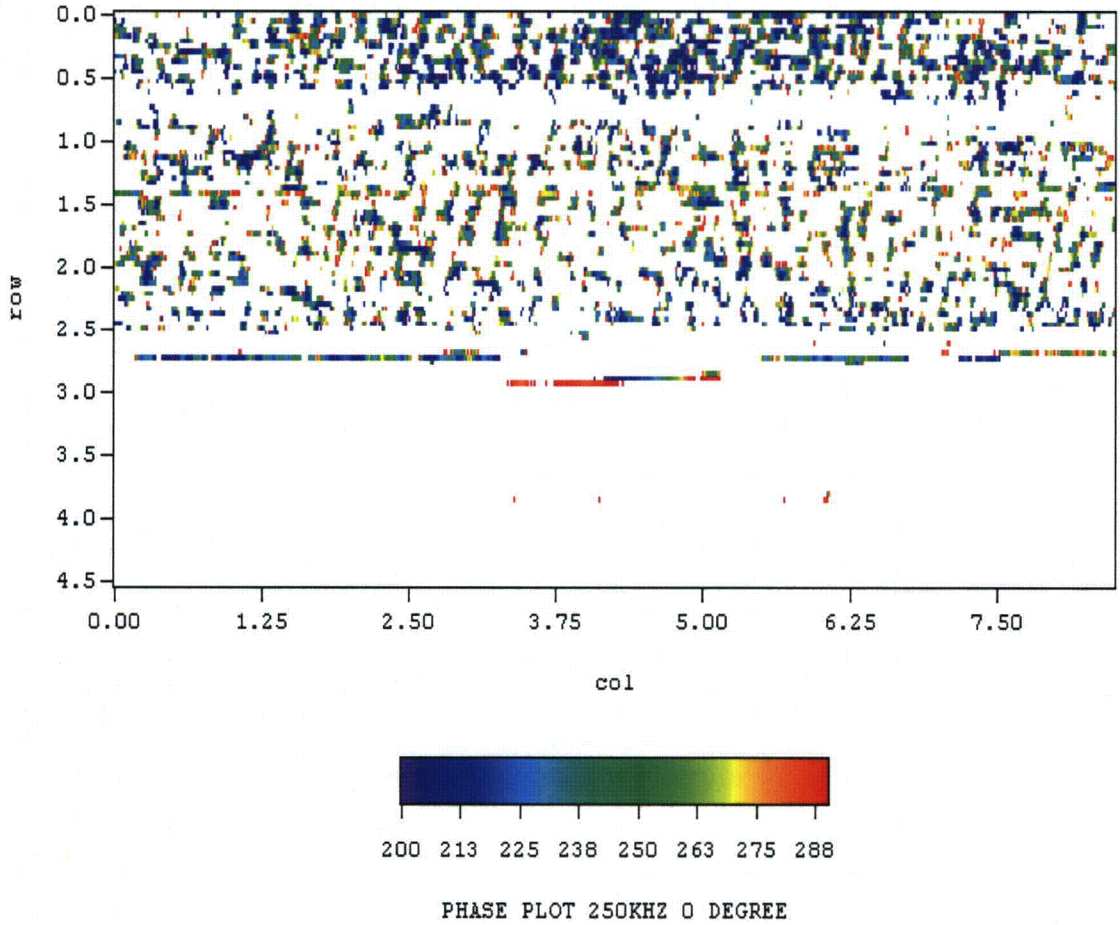

Figure C.5 Phase Response Plot of WOG Specimen INE-A-5

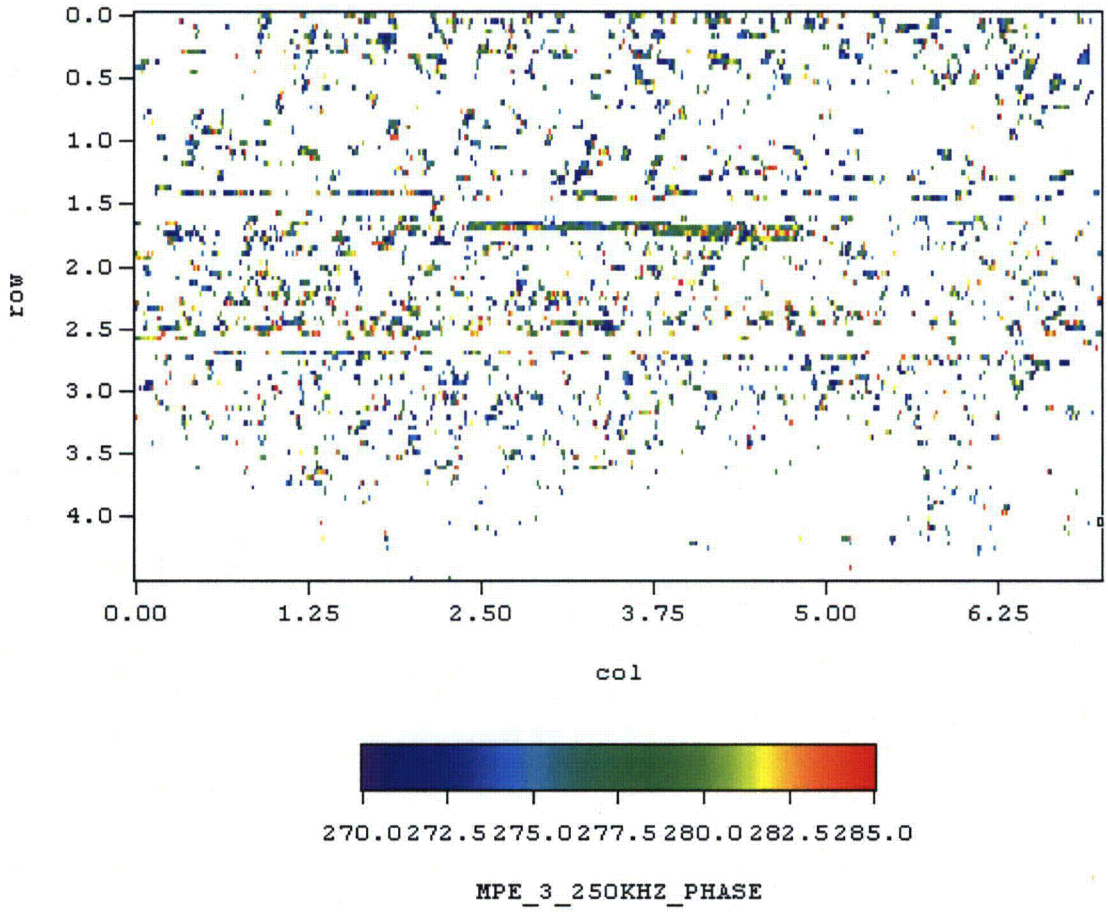

Figure C.6 Phase Response Plot of WOG Specimen MPE-3

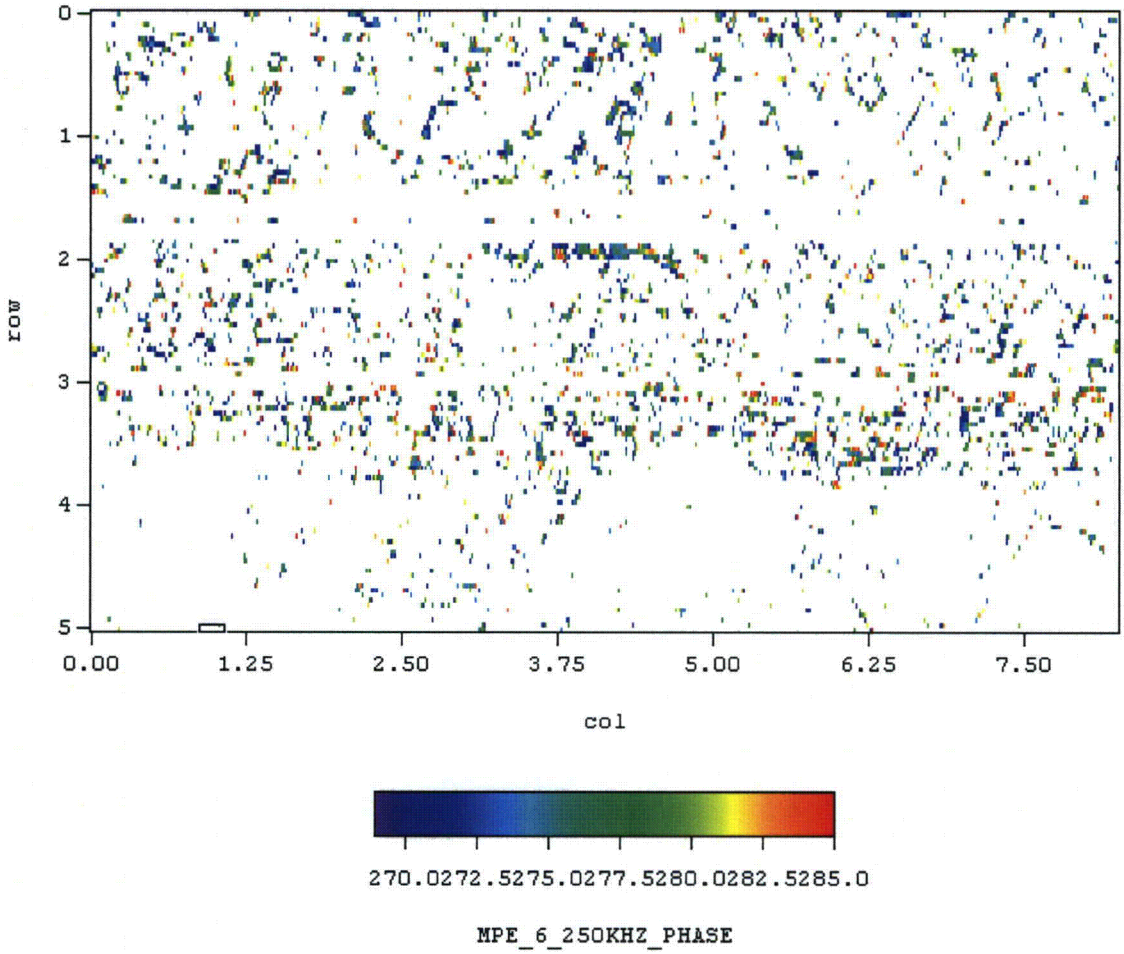

Figure C.7 Phase Response Plot of WOG Specimen MPE-6

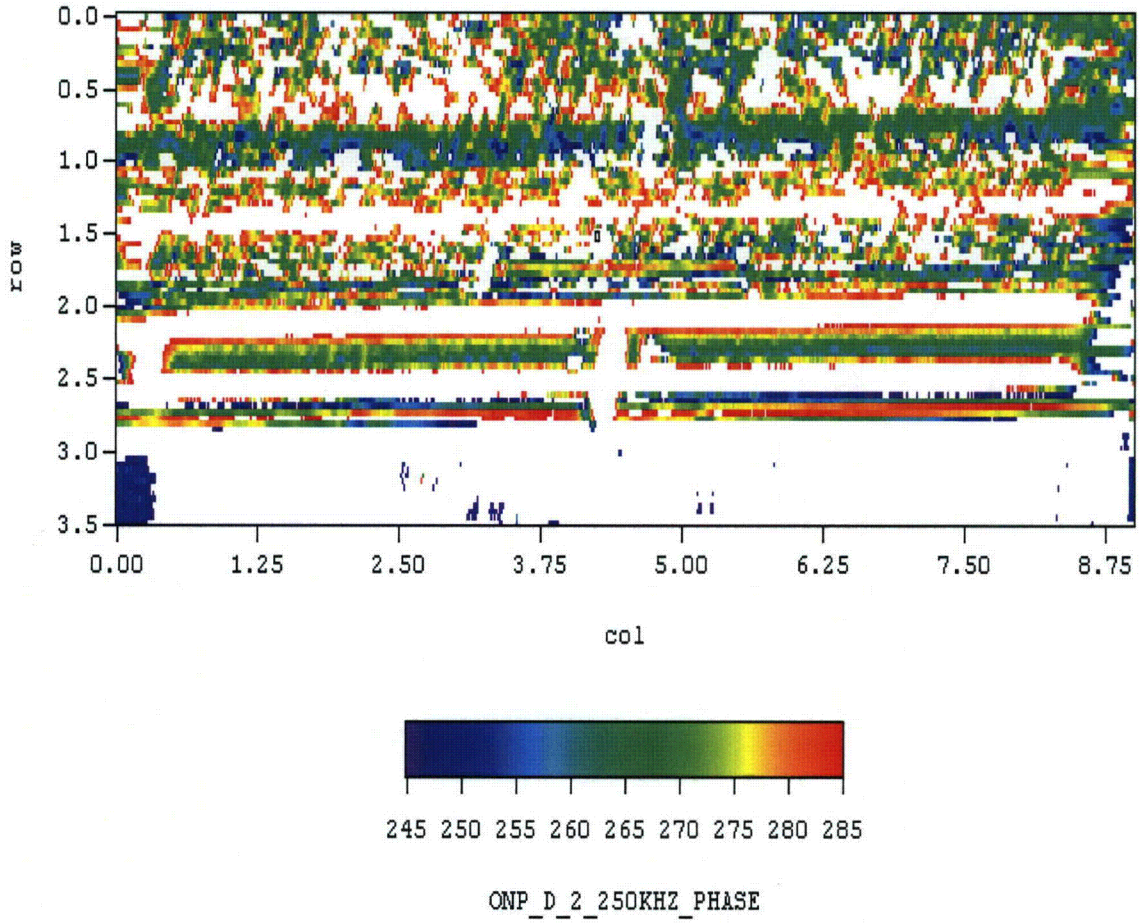

Figure C.8 Phase Response Plot of WOG Specimen ONP-D-2

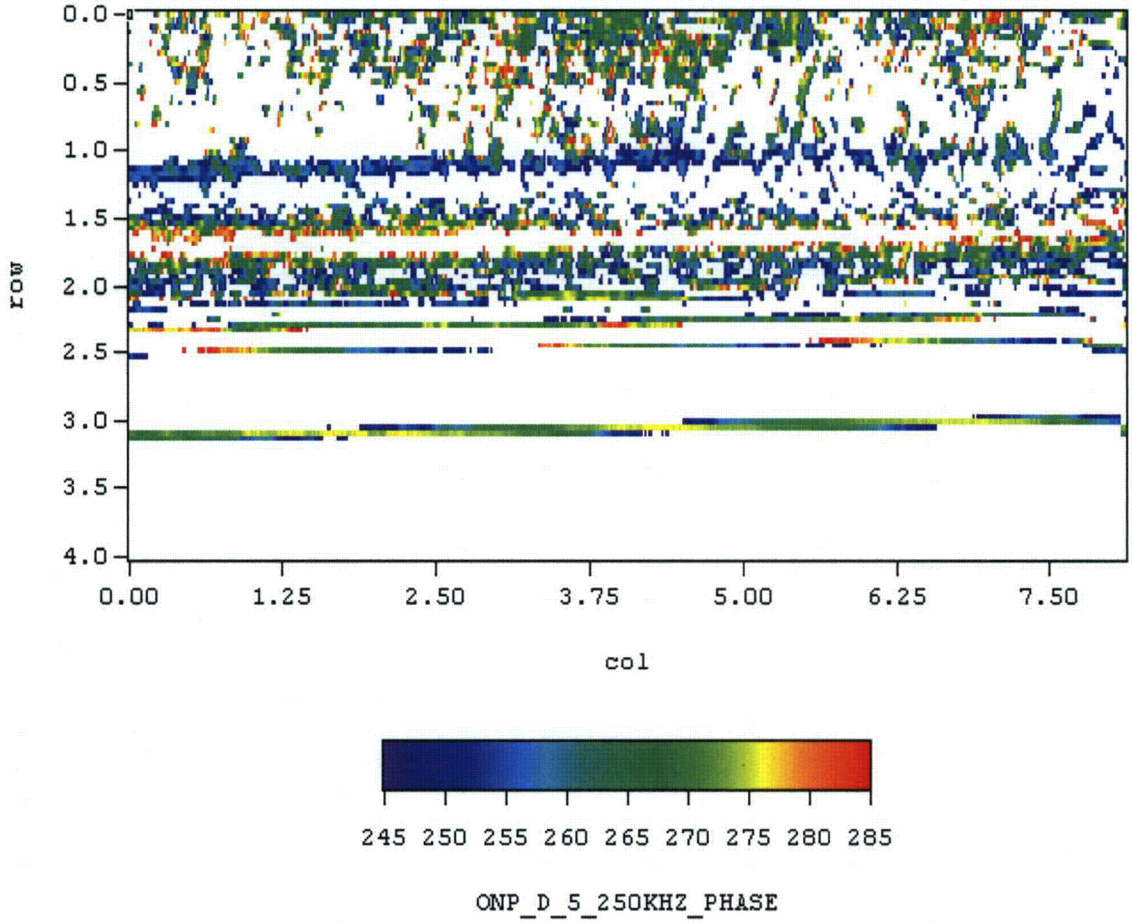

Figure C.9 Phase Response Plot of WOG Specimen ONP-D-5

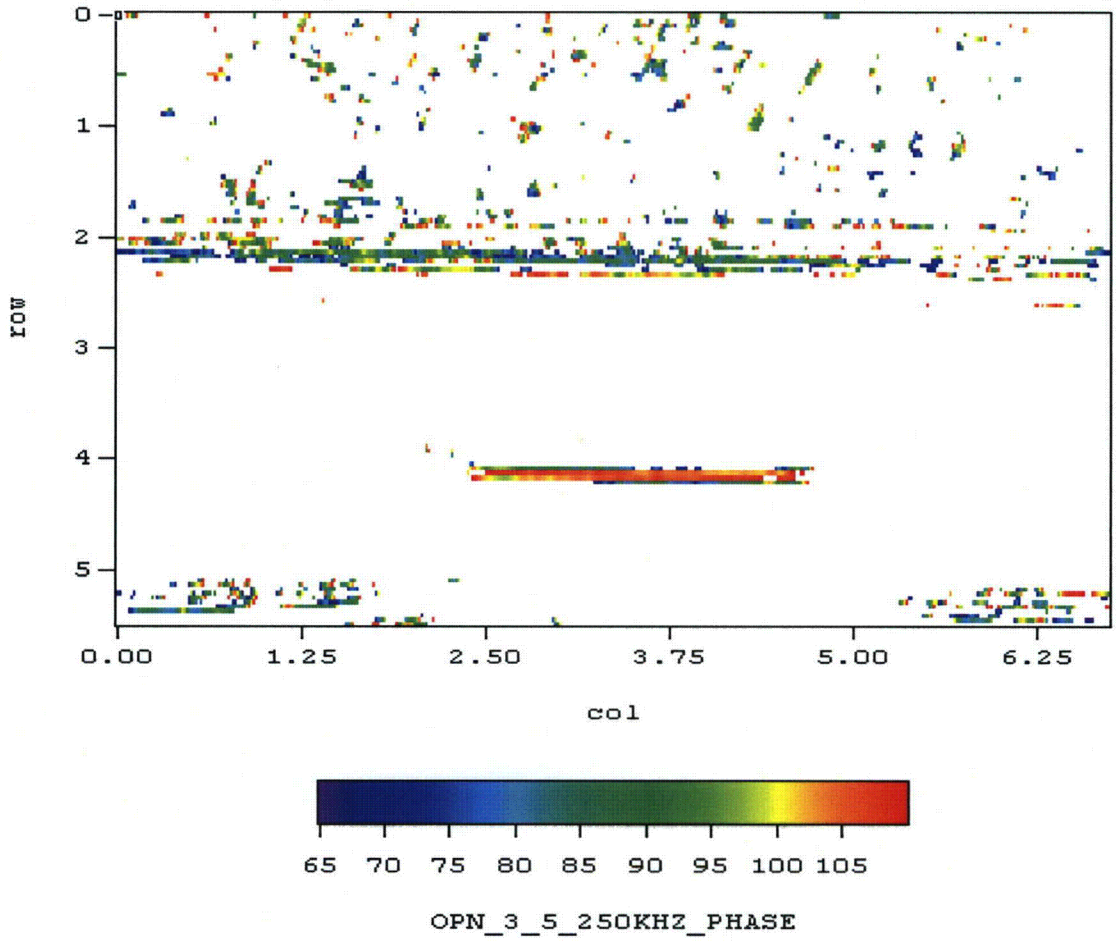

Figure C.10 Phase Response Plot of WOG Specimen ONP-3-5

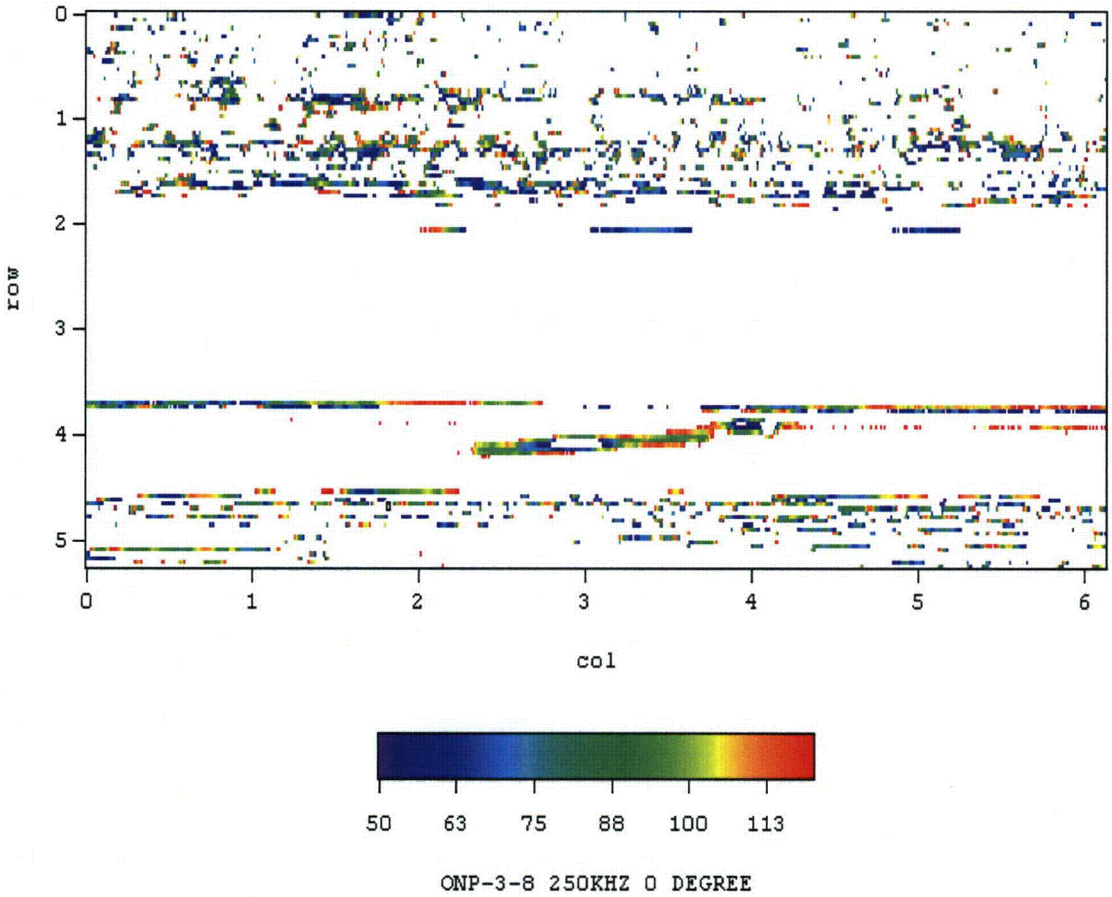

Figure C.11 Phased Response Plot of WOG Specimen ONP-3-8

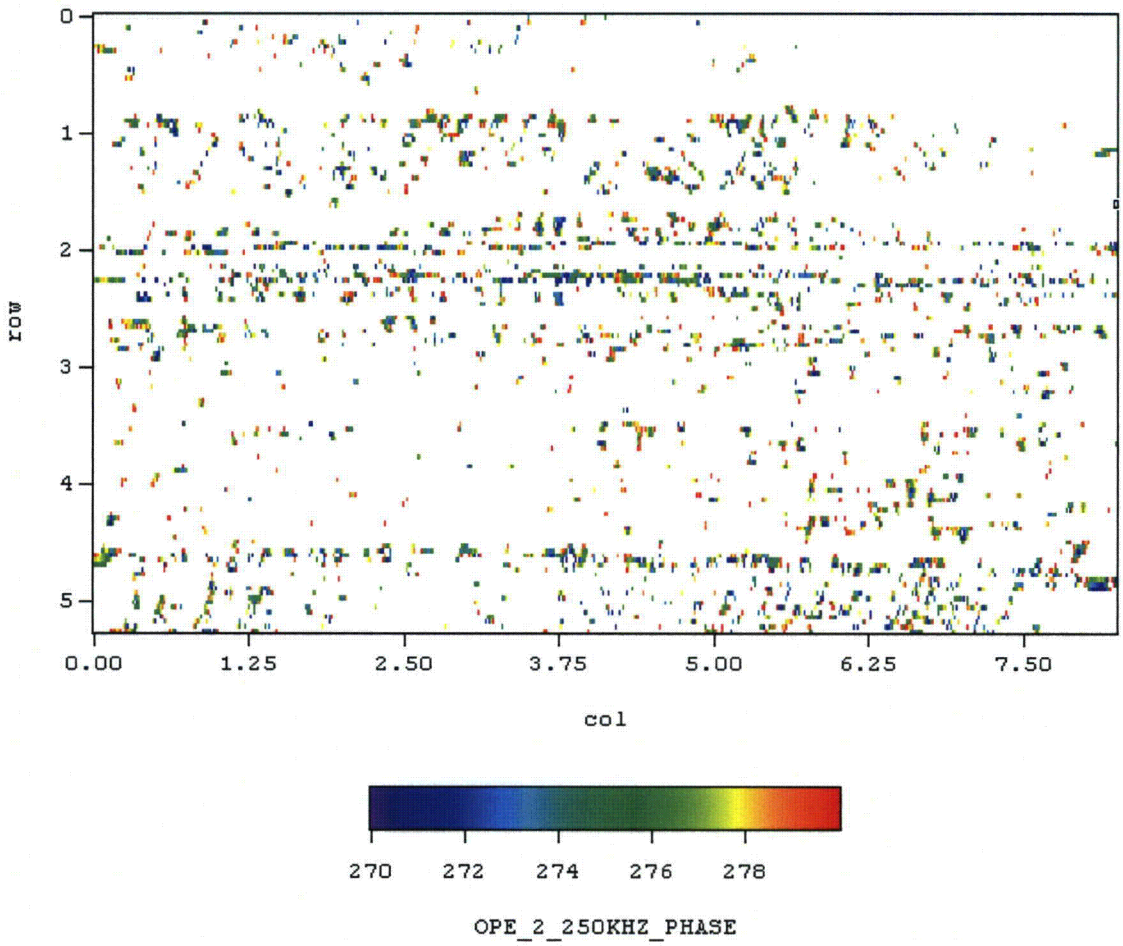

Figure C.12 Phase Response Plot of WOG Specimen OPE-2

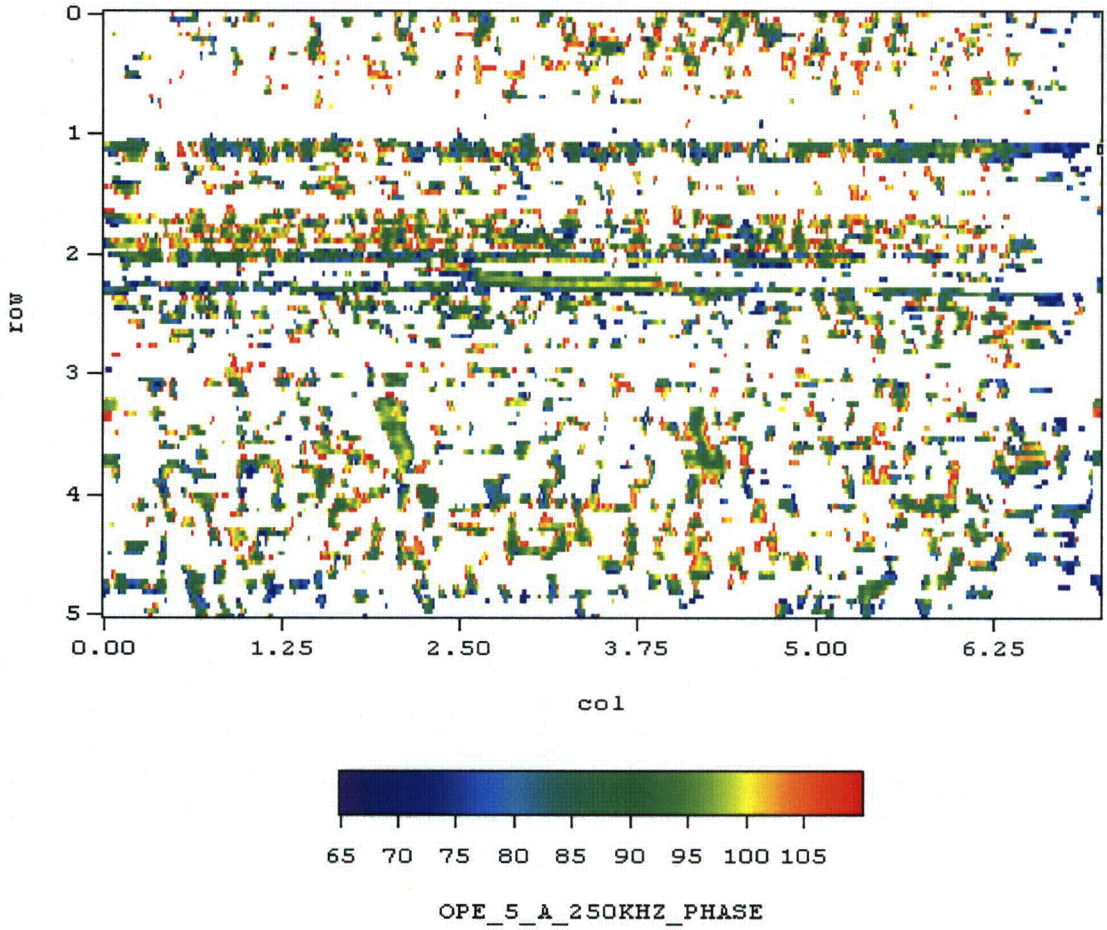

Figure C.13 Phase Response Plot of WOG Specimen OPE-5-A

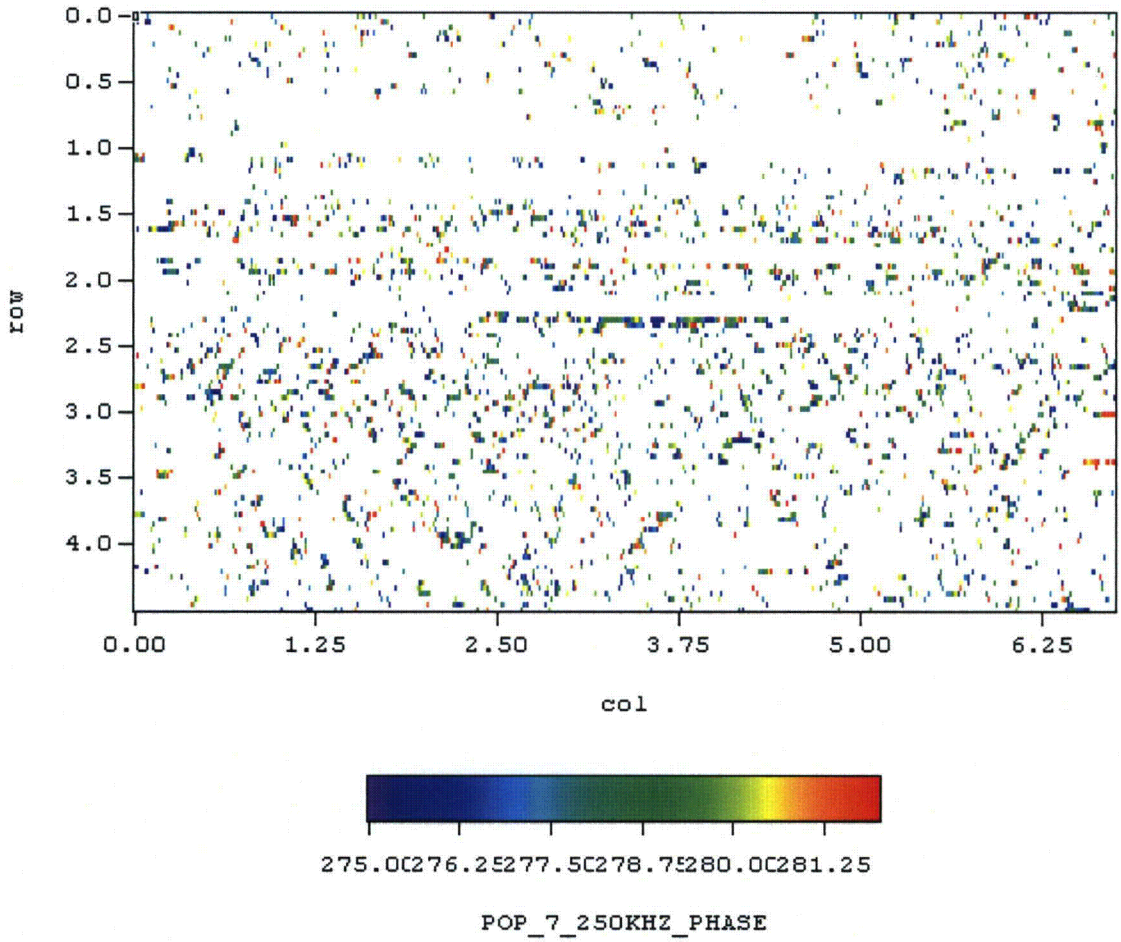

Figure C.14 Phase Response Plot of WOG Specimen POP-7

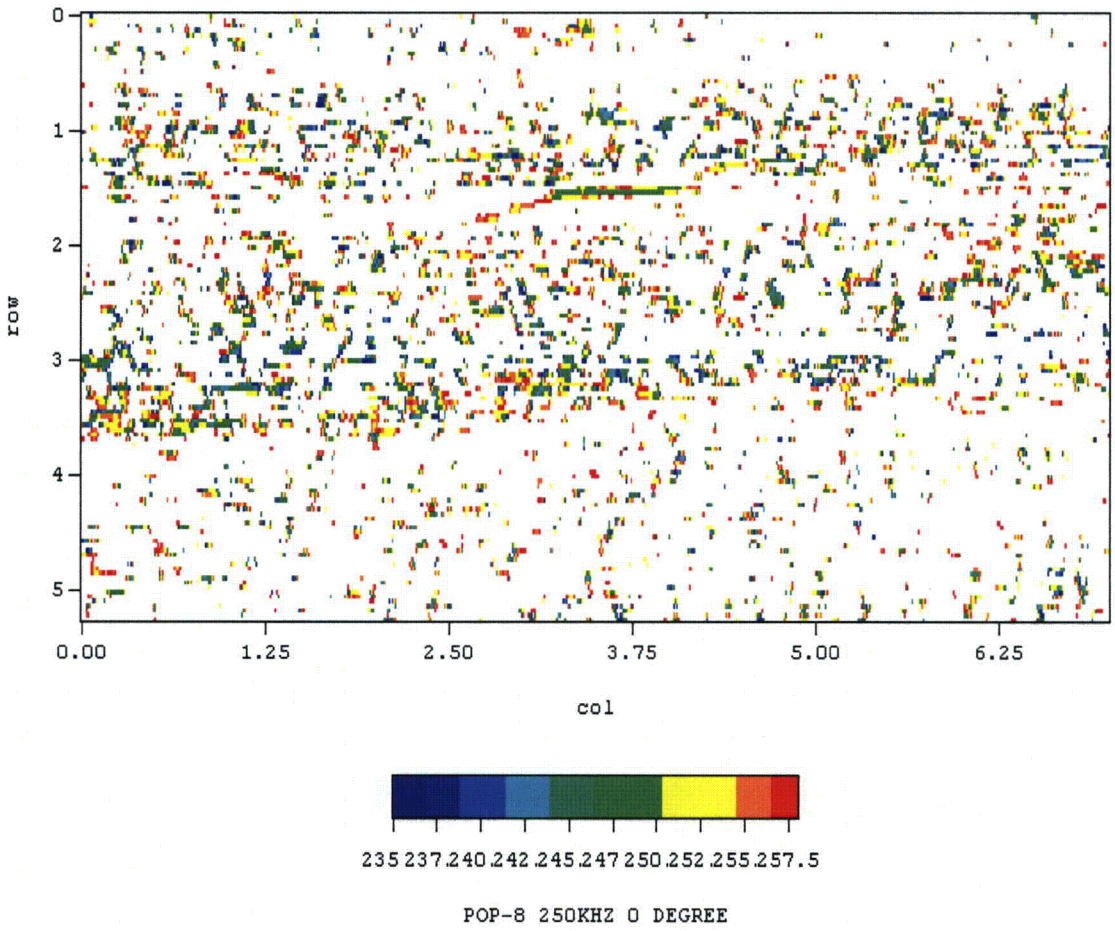

Figure C.15 Phase Response Plot of WOG Specimen POP-8

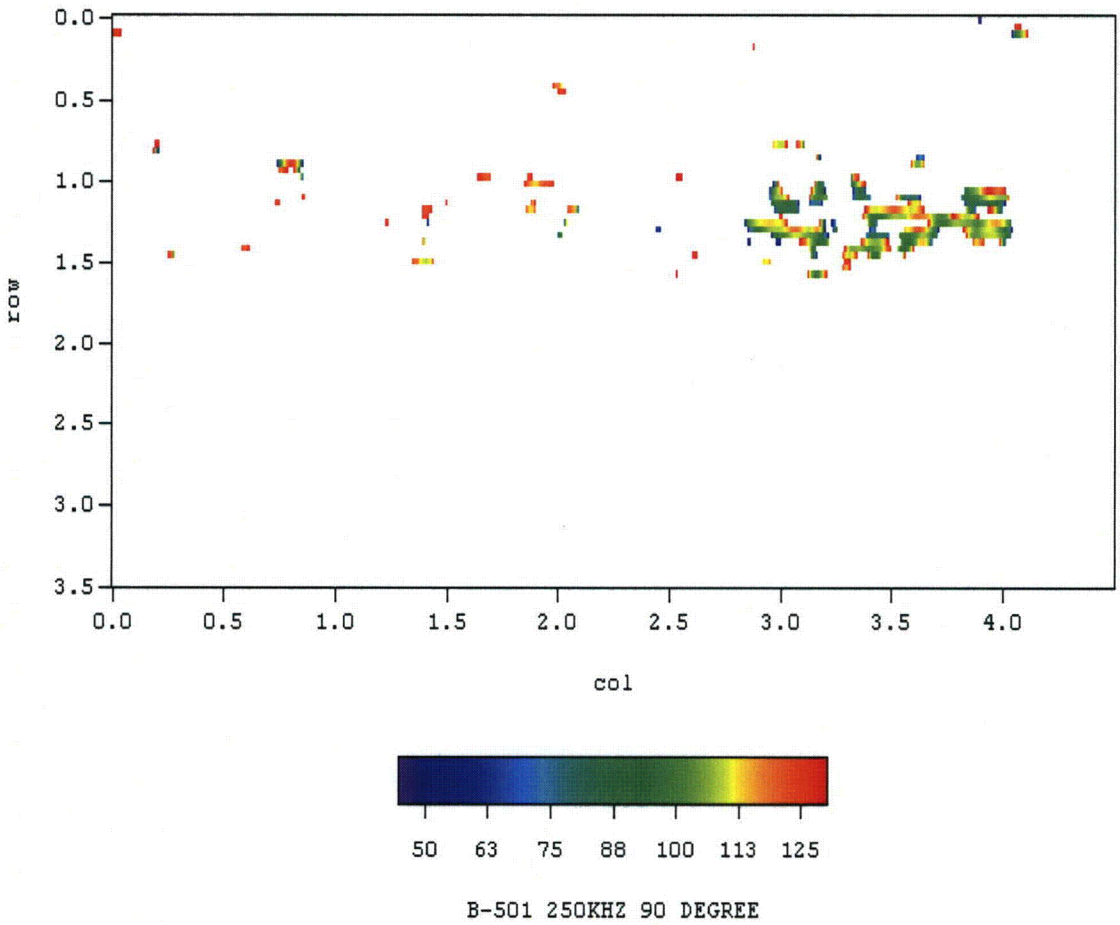

Figure C.16 Phase Response Plot of PNNL Specimen B-501

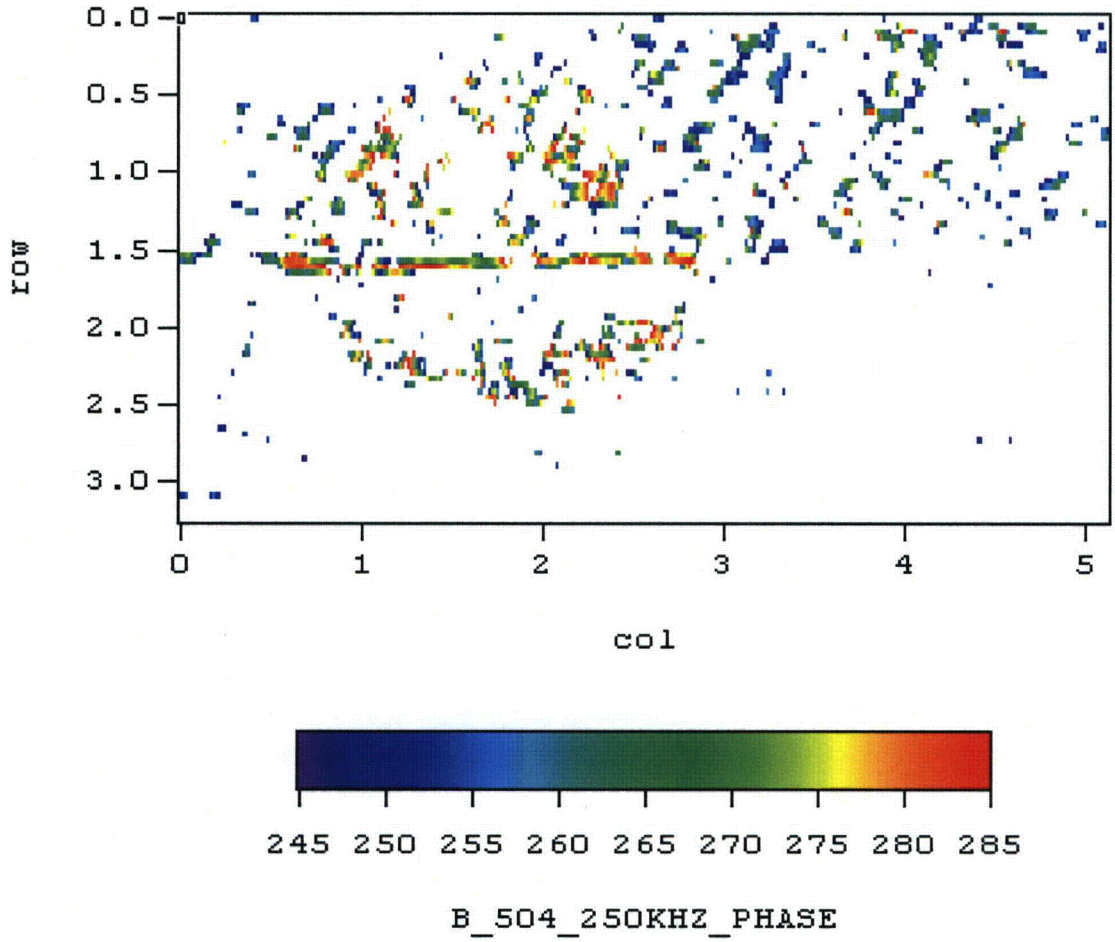

Figure C.17 Phase Response Plot of PNNL Specimen B-504

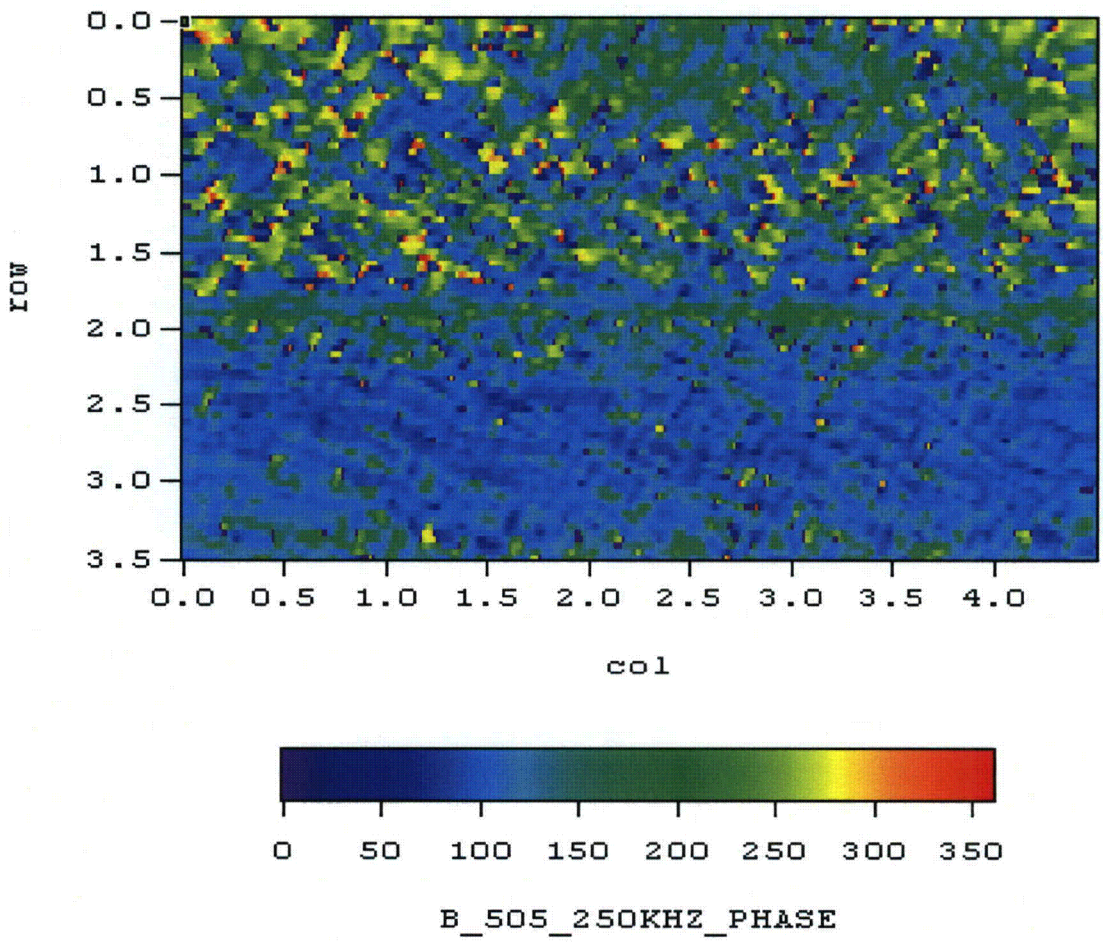

Figure C.18 Phase Response Plot of PNNL Specimen B

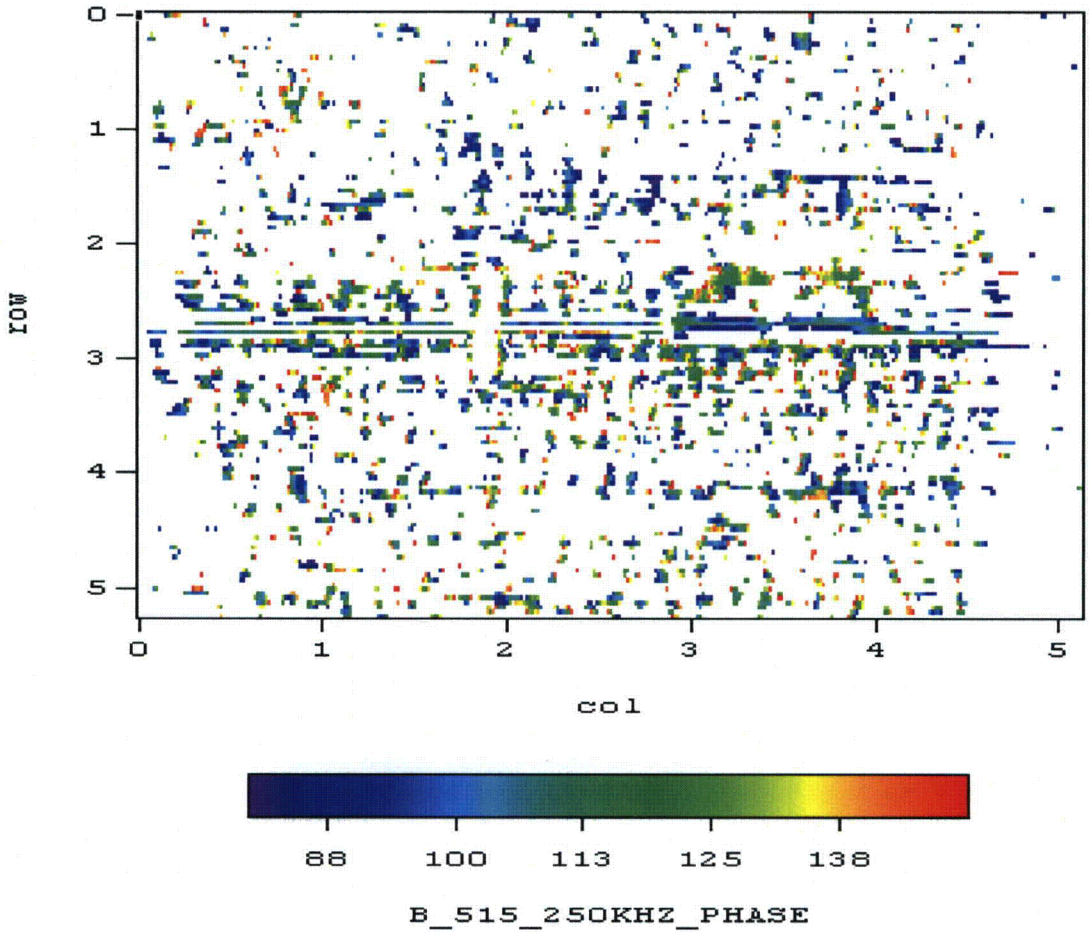

Figure C.19 Phase Response Plot of PNNL Specimen B-515

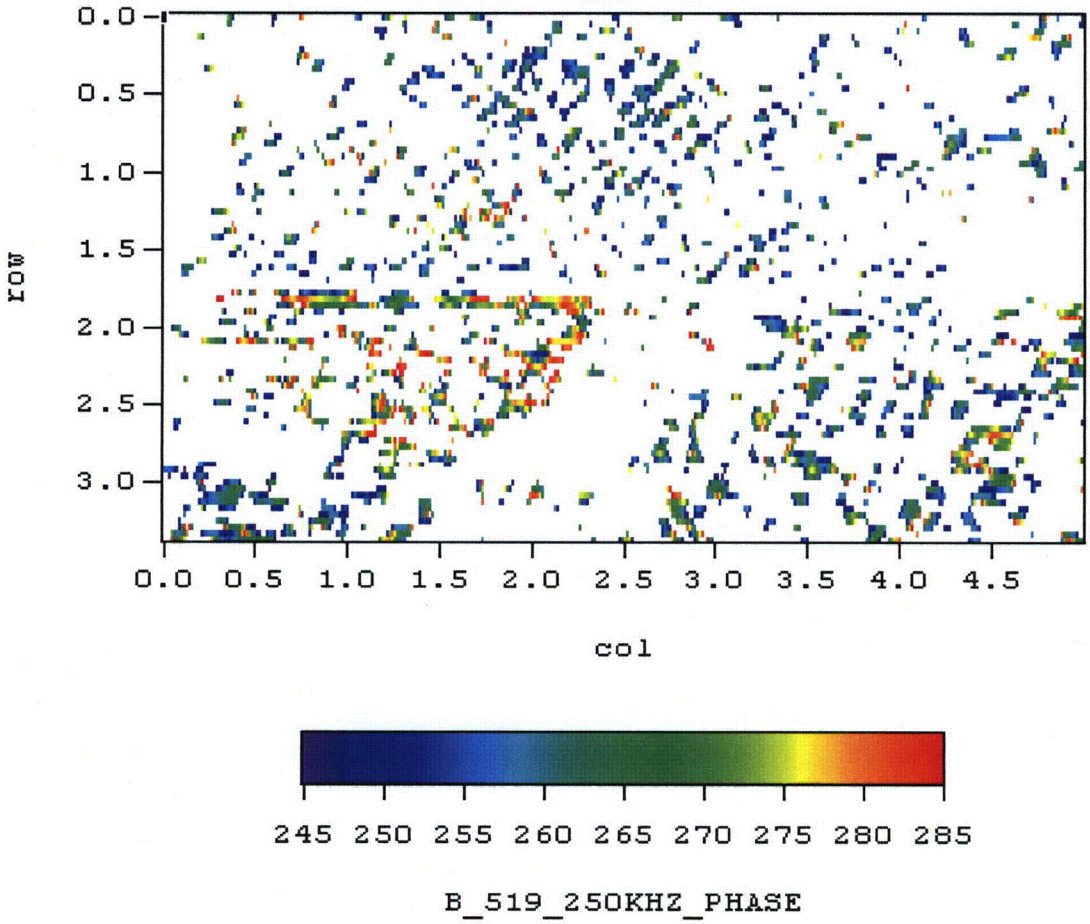

Figure C.20 Phase Response Plot of PNNL Specimen B-519

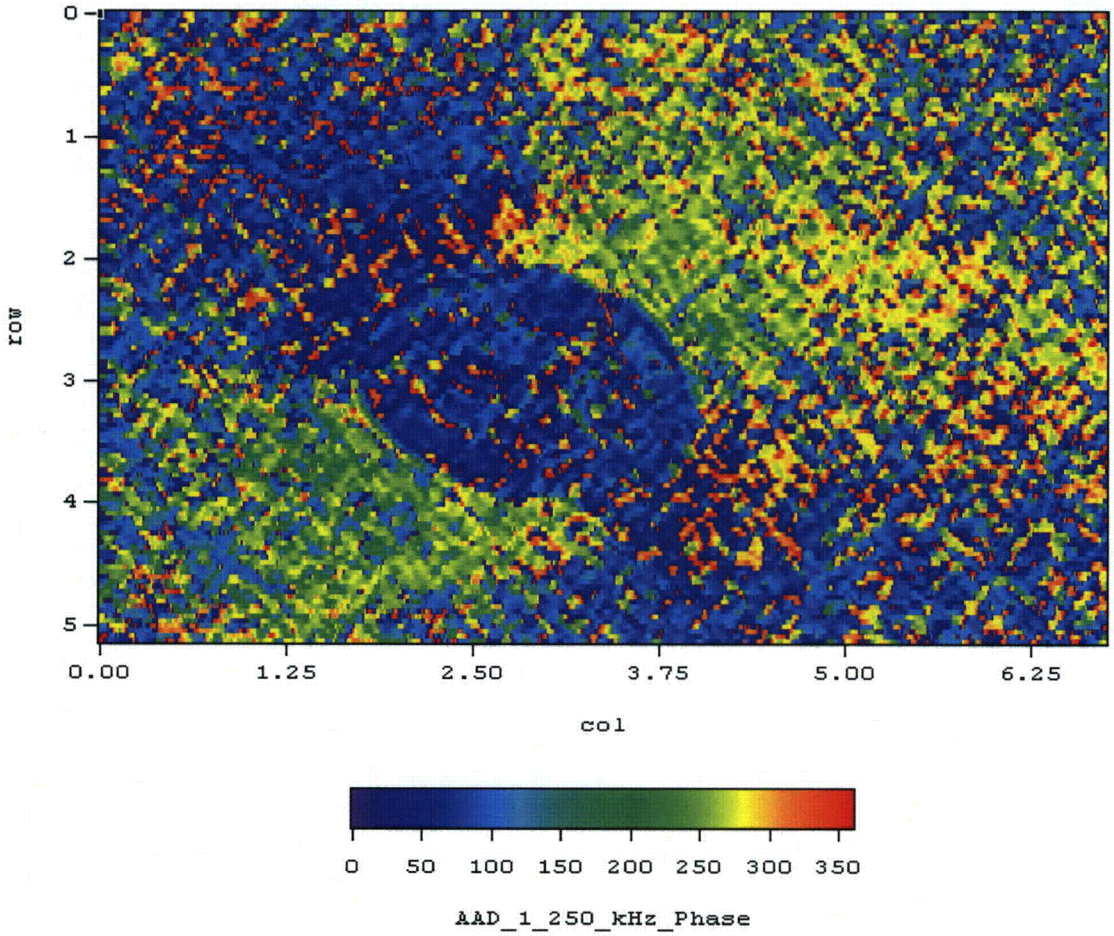

Figure C.21 Phase Response Plot of Southwest Research Institute Specimen AAD

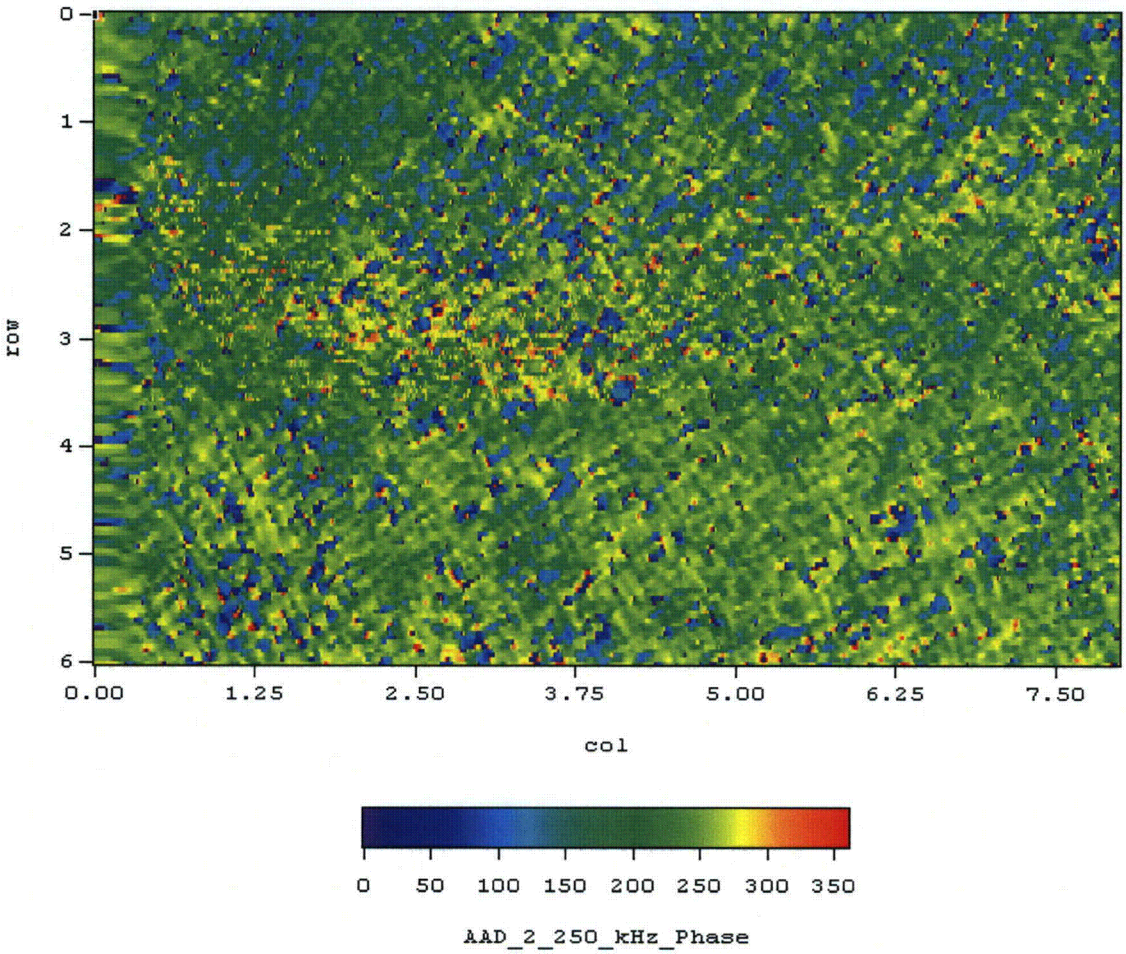

Figure C.22 Phase Response Plot of Southwest Research Institute Specimen AAD-2

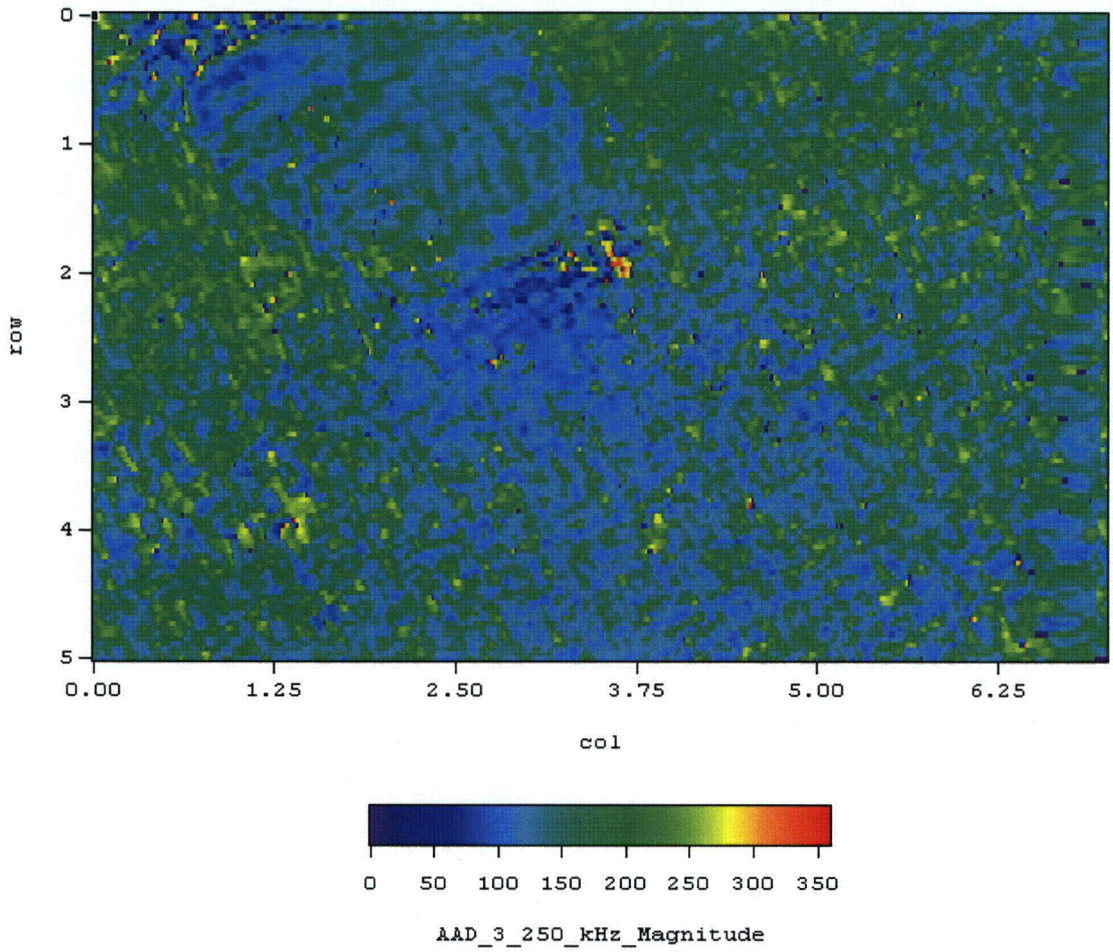

Figure C.23 Phase Response Plot of Southwest Research Institute Specimen AAD-3

Appendix D

Line Plots from Eddy Current Data

Appendix D

Line Plots from Eddy Current Data

All plots in Appendix D have horizontal axes that are in units of inches (2.54 mm).

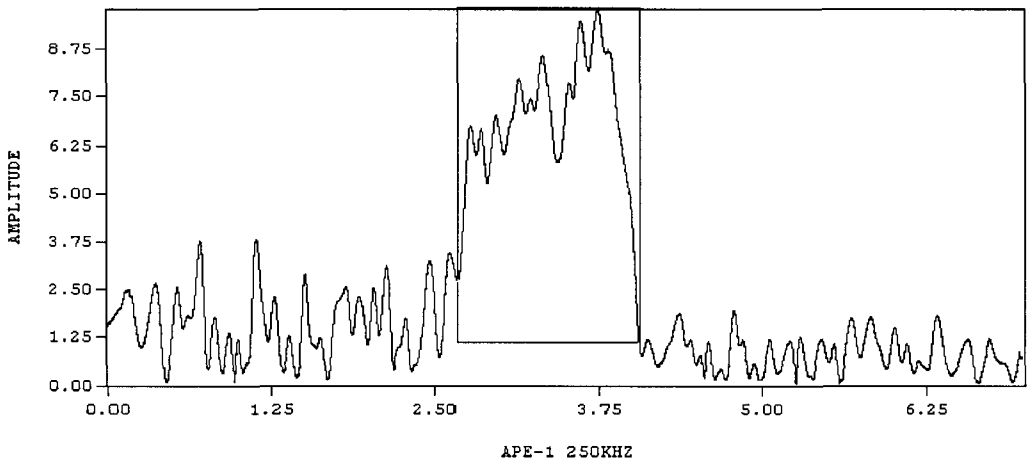

Figure D.1 Line Plot Representation of Magnitude for WOG Specimen APE-1

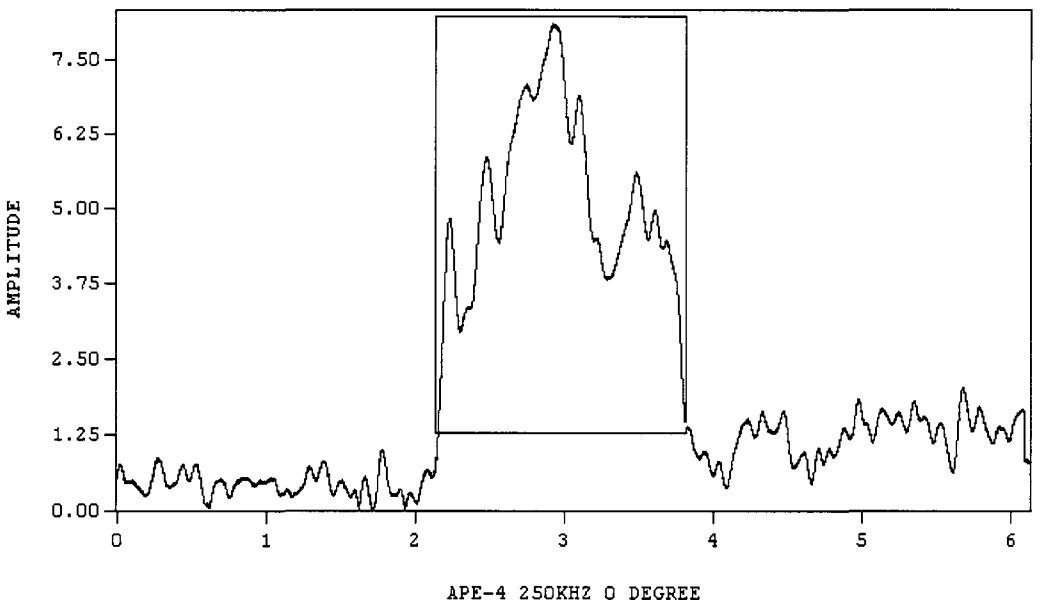

Figure D.2 Line Plot Representation of Magnitude for WOG Specimen APE-4

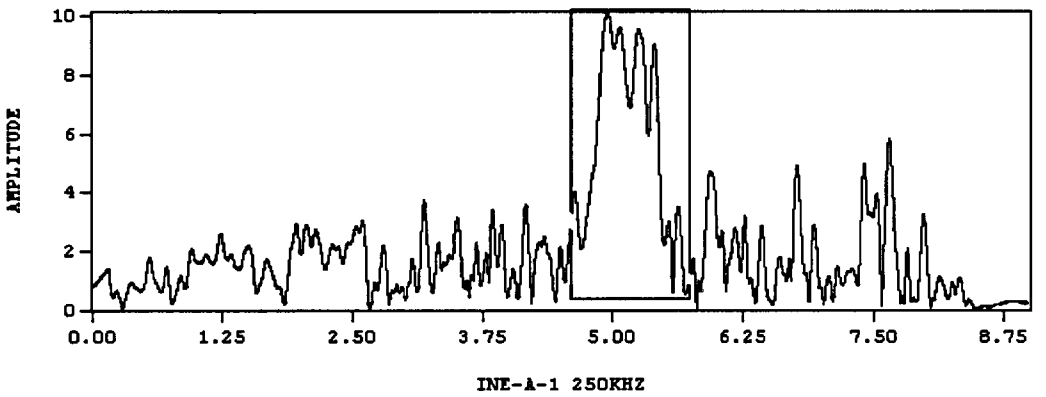

Figure D.3 Line Plot Representation of Magnitude for WOG Specimen INE-A-1

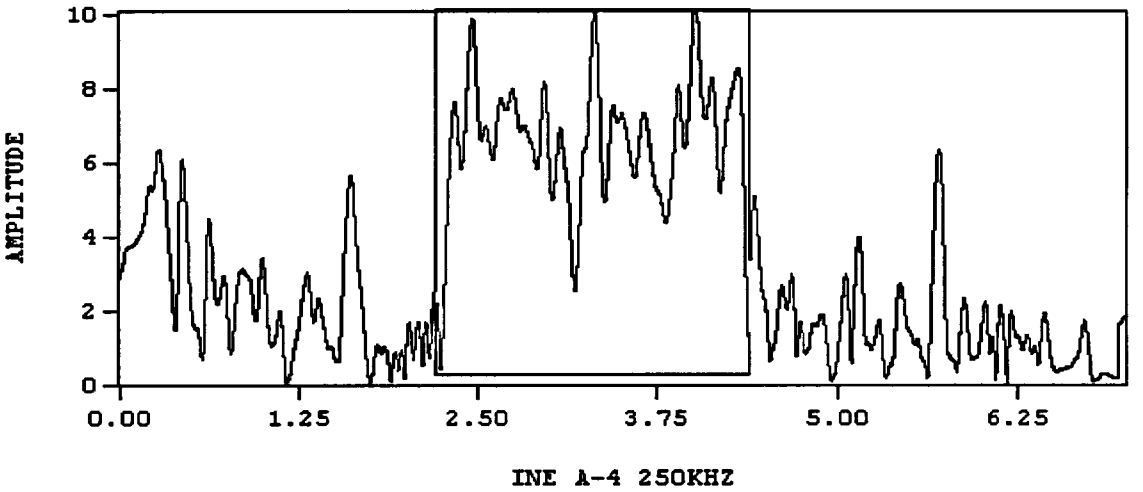

Figure D.4 Line Plot Representation of Magnitude for WOG Specimen INE-A-4

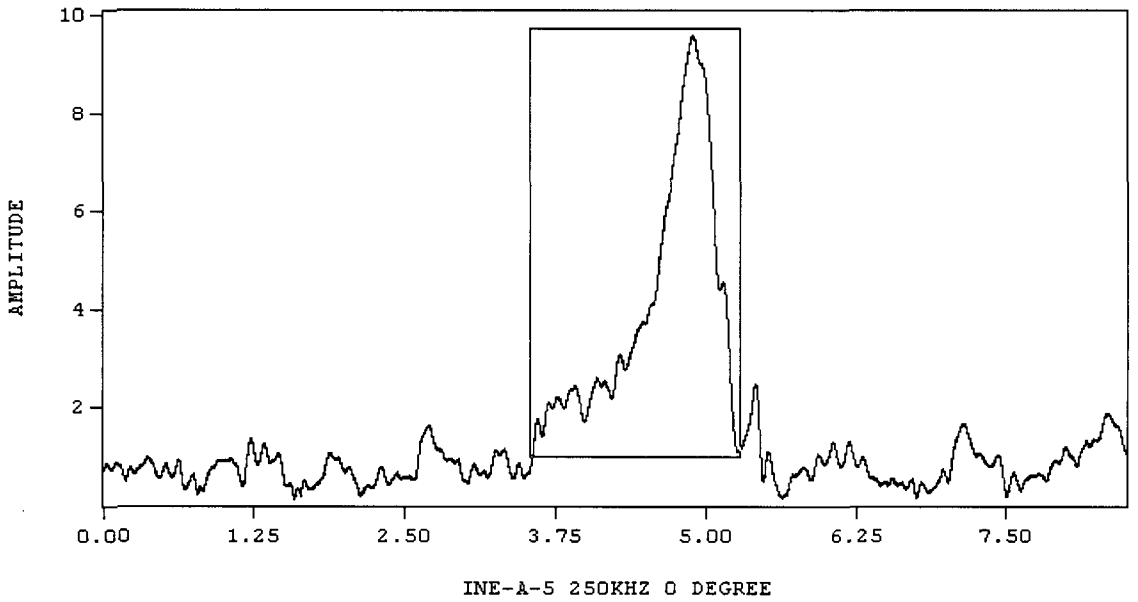

Figure D.5 Line Plot Representation of Magnitude for WOG Specimen INE-A-5

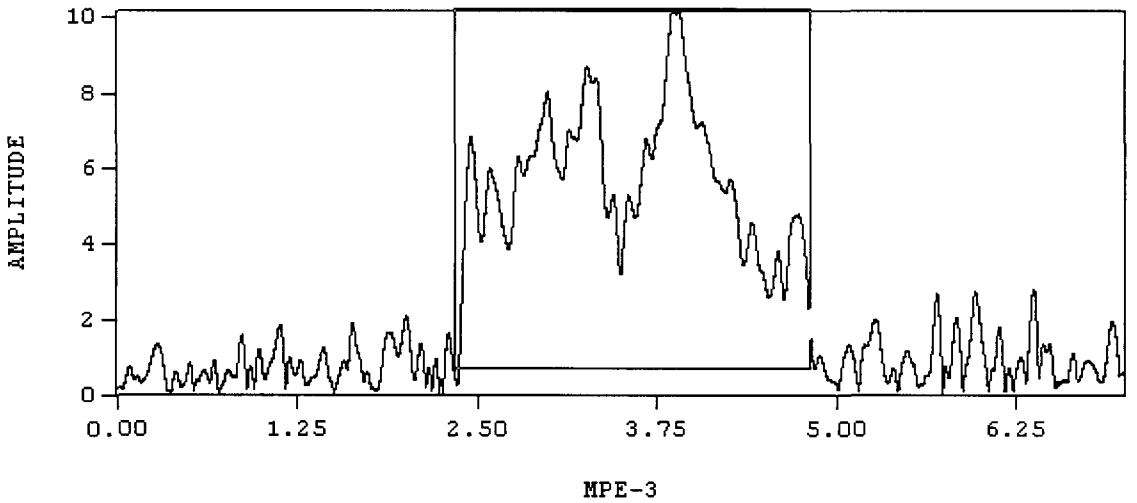

Figure D.6 Line Plot Representation of Magnitude for WOG Specimen MPE-3

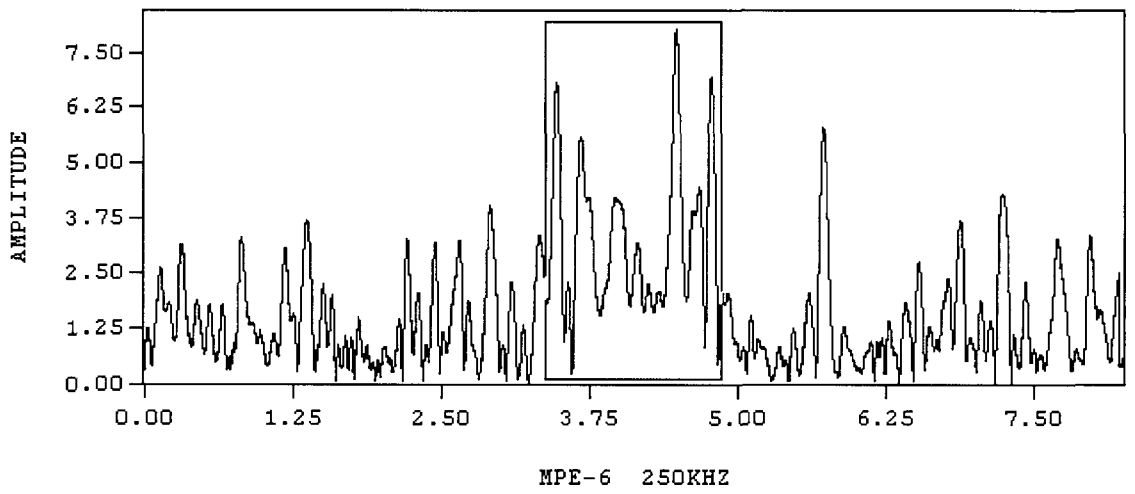

Figure D.7 Line Plot Representation of Magnitude for WOG Specimen MPE-6

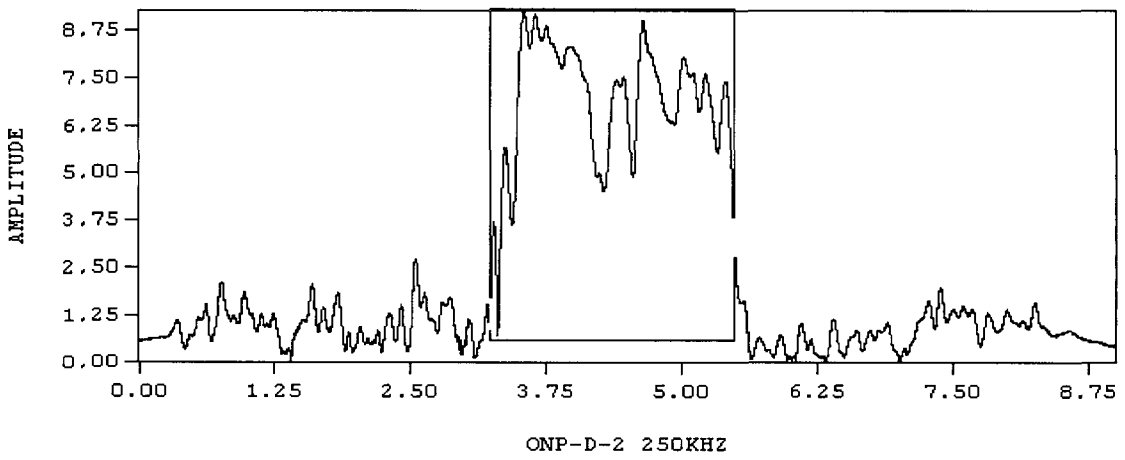

Figure D.8 Line Plot Representation of Magnitude for WOG Specimen ONP-D-2

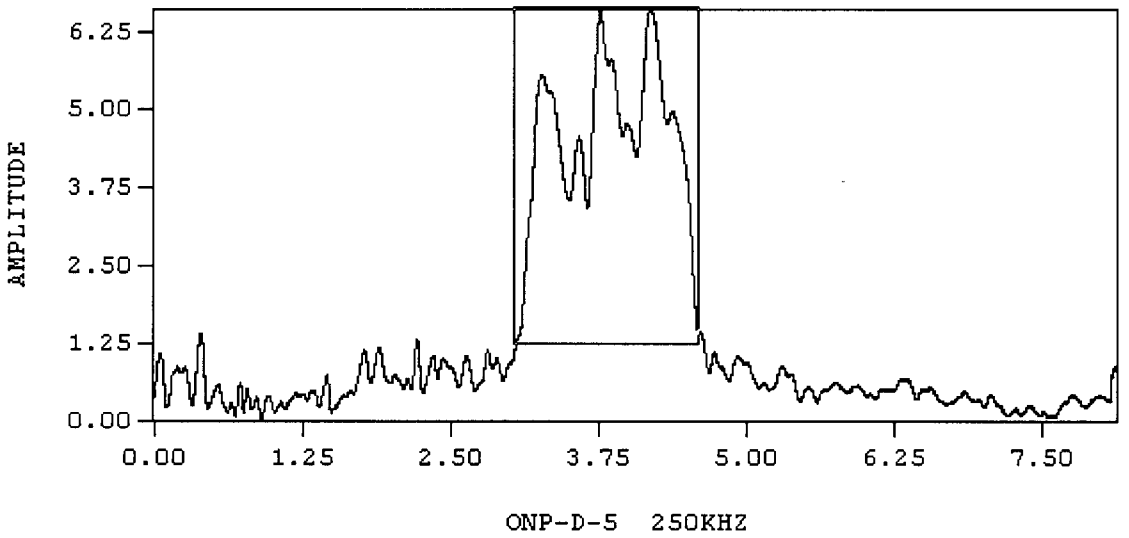

Figure D.9 Line Plot Representation of Magnitude for WOG Specimen ONP-D-5

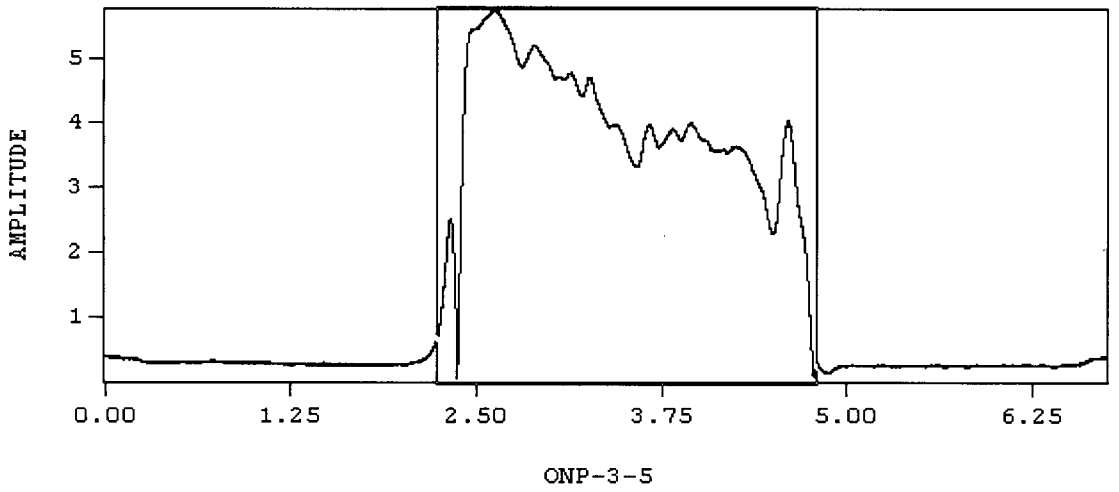

Figure D.10 Line Plot Representation of Magnitude for WOG Specimen ONP-3-5

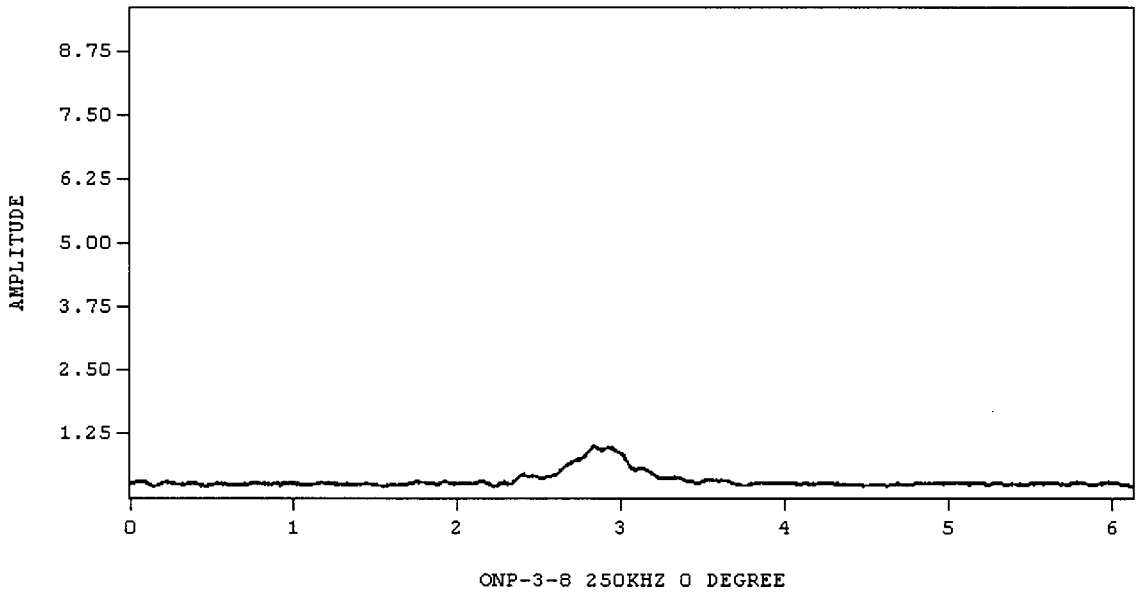

Figure D.11 Line Plot Representation of Magnitude for WOG Specimen ONP-3-8

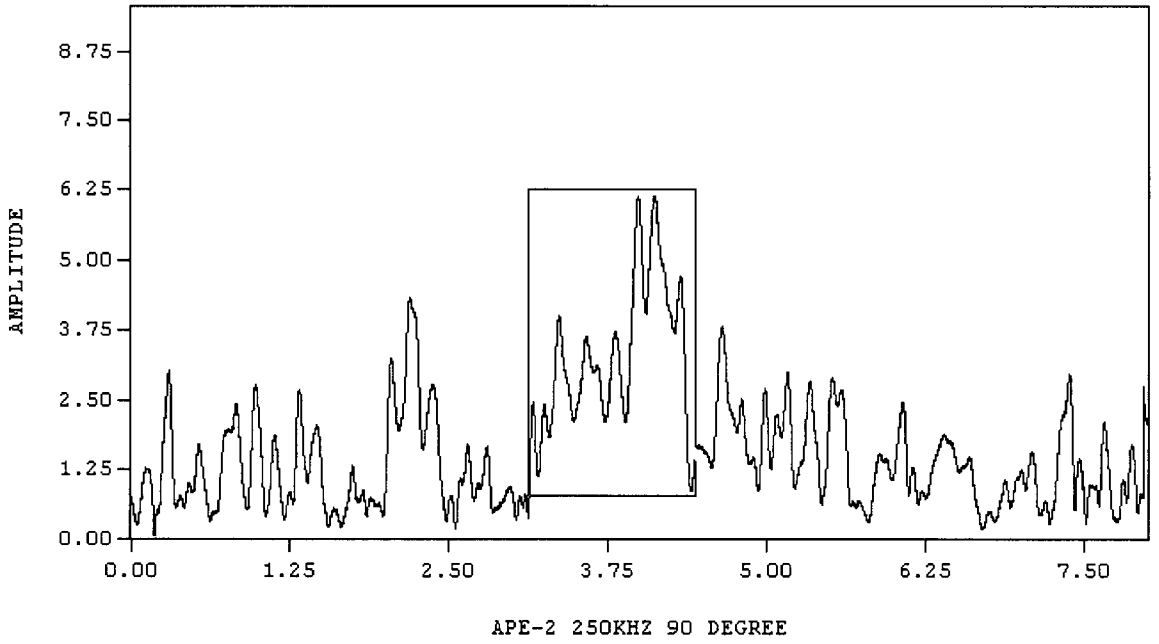

Figure D.12 Line Plot Representation of Magnitude for WOG Specimen OPE-2

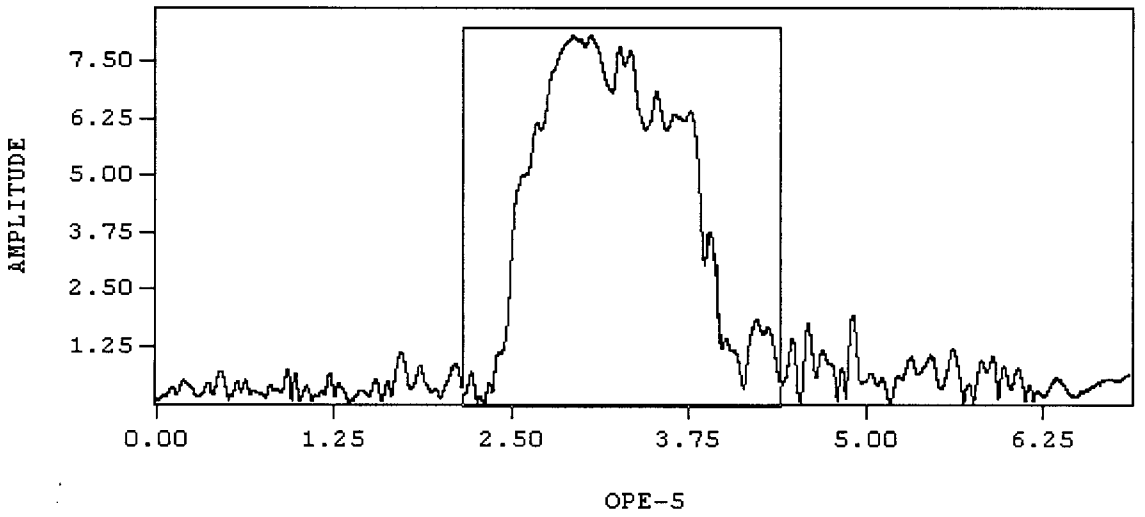

Figure D.13 Line Plot Representation of Magnitude for WOG Specimen OPE-5

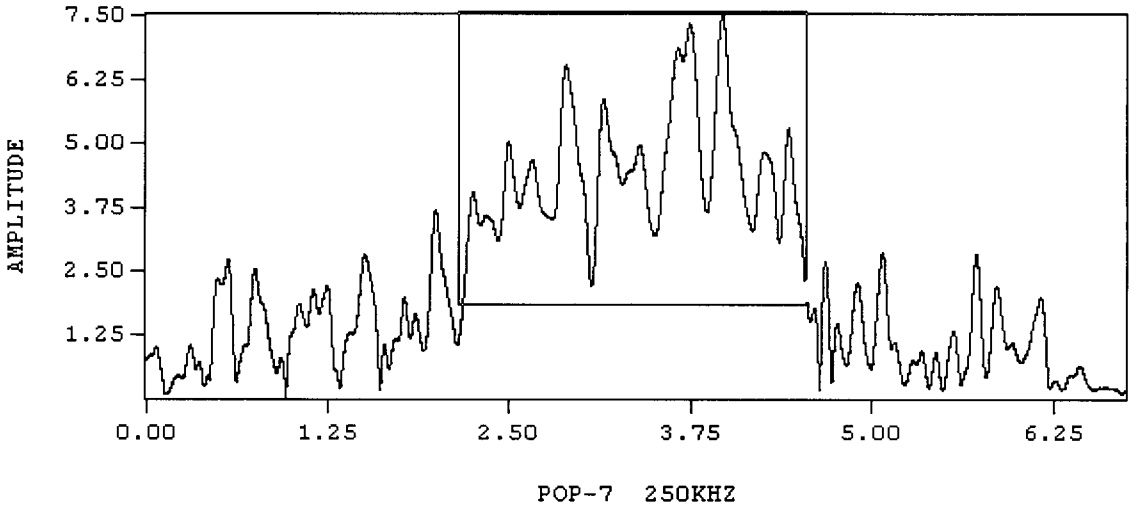

Figure D.14 Line Plot Representation of Magnitude for WOG Specimen POP-7

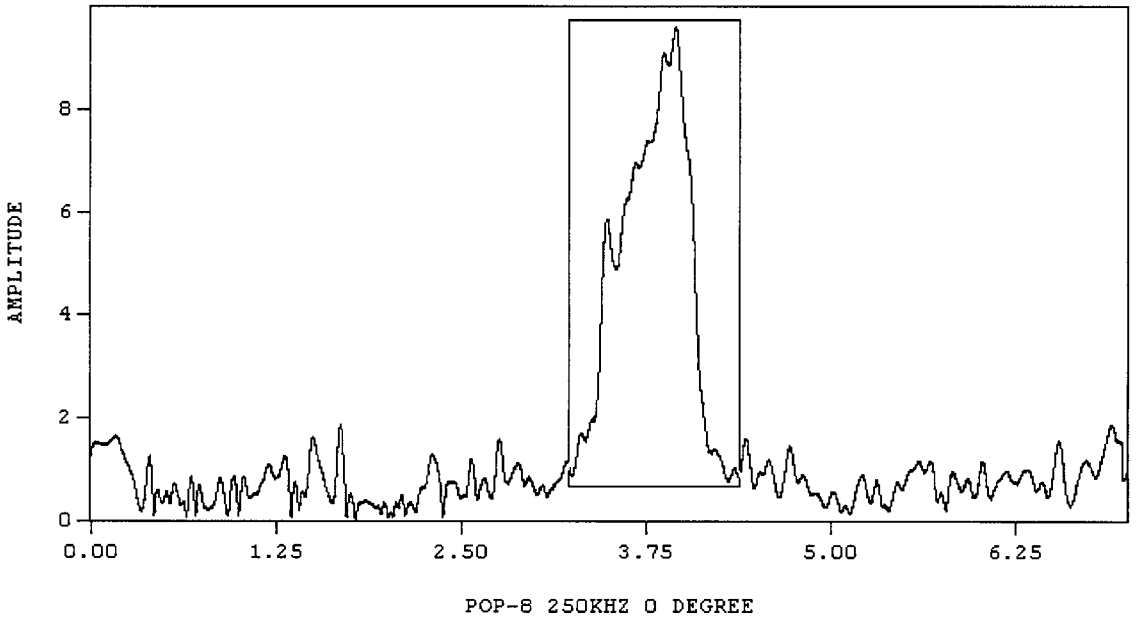

Figure D.15 Line Plot Representation of Magnitude for WOG Specimen POP-8

NRC FORM 335
(9-2004)
NRCMD 3.7

U.S. NUCLEAR REGULATORY COMMISSION

BIBLIOGRAPHIC DATA SHEET

(See instructions on the reverse)

1. REPORT NUMBER
(Assigned by NRC, Add Vol., Supp., Rev., and Addendum Numbers, if any.)

NUREG/CR-6929

2. TITLE AND SUBTITLE

Assessment of Eddy Current Testing for the Detection of Cracks in Cast Stainless Steel Reactor Piping Components

3. DATE REPORT PUBLISHED

MONTH	YEAR
February	2007

4. FIN OR GRANT NUMBER

Y6604

5. AUTHOR(S)

A. A. Diaz, R. A. Mathews, J. Hixon, S. R. Doctor

6. TYPE OF REPORT

Technical

7. PERIOD COVERED *(Inclusive Dates)*

8. PERFORMING ORGANIZATION - NAME AND ADDRESS *(If NRC, provide Division, Office or Region, U.S. Nuclear Regulatory Commission, and mailing address; if contractor, provide name and mailing address.)*

Pacific Northwest National Laboratory
P.O. Box 999
Richland, Washington 99352

9. SPONSORING ORGANIZATION - NAME AND ADDRESS *(If NRC, type "Same as above"; if contractor, provide NRC Division, Office or Region, U.S. Nuclear Regulatory Commission, and mailing address.)*

Division of Fuel, Engineering and Radiological Research
Office of Nuclear Regulatory Research
U.S. Nuclear Regulatory Commission
Washington, DC 20555-0001

10. SUPPLEMENTARY NOTES

11. ABSTRACT *(200 words or less)*

Studies conducted at the Pacific Northwest National Laboratory have focused on assessing the effectiveness and reliability of novel approaches to nondestructive examination (NDE) for inspecting coarse-grained, cast stainless steel reactor components. The primary objective of this work is to provide information to the U.S. Nuclear Regulatory Commission on the utility, effectiveness, and reliability of advanced NDE methods as related to the inservice inspection of primary piping components in pressurized water reactors. This report describes progress, recent developments, and results from the assessment of eddy current testing (ET) for detection of surface-breaking cracks in cast stainless steel (CSS) reactor piping components from the inside surface of the pipe wall.

In assessing the ET inspection technique, PNNL used a range of piping component specimens from four different sources. Eddy current studies were conducted on the inner-diameter surface of piping using a Zetec MIZ-27SI eddy current instrument and a Zetec C Z0000857-1 plus-point spot probe with an operating frequency of 250 kHz. To reduce noise effects, a subset of the CSS specimens was degaussed, resulting in noticeable improvements.

In this report, results from laboratory studies for assessing detection, localization, and length sizing effectiveness are provided, and issues and anticipated future work are discussed.

12. KEY WORDS/DESCRIPTORS *(List words or phrases that will assist researchers in locating the report.)*

eddy current testing
inservice inspection
crack detection
surface-breaking cracks
cast stainless steel
nuclear reactor piping components
pressurized water reactors

13. AVAILABILITY STATEMENT

unlimited

14. SECURITY CLASSIFICATION

(This Page)

unclassified

(This Report)

unclassified

15. NUMBER OF PAGES

16. PRICE

PRINTED ON RECYCLED PAPER

Printed
on recycled
paper

Federal Recycling Program